Title
Bias Adjustment of Satellite-Based Precipitation Estimation Using Limited Gauge Measurements and Its Implementation on Hydrologic Modeling

Author
Alharbi, Raied

Publication Date
2019

UNIVERSITY OF CALIFORNIA,
IRVINE

Bias Adjustment of Satellite-Based Precipitation Estimation Using Limited Gauge Measurements and Its Implementation on Hydrologic Modeling

DISSERTATION

submitted in partial satisfaction of the requirements
for the degree of

DOCTOR OF PHILOSOPHY

in Civil and Environmental Engineering

by

Raied Saad Alharbi

Dissertation Committee:
Professor Kuo-Lin Hsu, Chair
Distinguished Professor Soroosh Sorooshian
Associate Professor Amir AghaKouchak

2019

DEDICATION

To

My parents, Saad and Moody,

my wonderful and supportive wife, Eman,

my uncle, Mohammad,

my lovely sons, Yusuf and Musab,

my brother and my sisters.

Without your supports, encouragement, and beliefs, this dissertation would have never been possible

TABLE OF CONTENTS

Page

LIST OF FIGURES

LIST OF TABLES

Page

ACKNOWLEDGMENTS

As I was writing the acknowledgments page, I began to think about the lovely and wonderful people who help, advise and believe in me, and without their endless support would never reach to this point in my life. Many thanks and appreciations go to them.

First and foremost, I would like to honestly thank my advisor Professor Kuolin Hsu and Distinguished Professor Soroosh Sorooshian for giving me the opportunity to join and study in the Center for Hydrometeorology and Remote Sensing “CHRS” at the University of California, Irvine (UCI). Without their advice and support, this dissertation would not have been possible. They have helped to shape my thinking that I hope I can take with me for my future, and I have considered them as my teachers during my during Ph.D. journey.

I would like to extend my sincere appreciations and thanks to Professor Amir AghaKouchak for his advice, suggestions, and comments in my qualifying exam as well as my dissertation. My special thanks go to Professor Phu Nguyen for his advice and comments on my research.

Special thanks to my friends and colleagues at UCI and CHRS who support and encourage me especially Ata, Pan, Hoang, Matin, Pooya, and Mojtaba, and I would extend my honest thanks to Mohammed for his friendship.

My deepest gratitude goes to my family who provides me with love, support and endless encouragement. To my parents, Saad and Moody, thank you for everything that you have offered to me. I love you with all my heart and I wish this dissertation can serve as a gift that represents your worth in my life. I would like to extend my love to my brother, Ryan, and my sisters.

I will not find words that can show my thanks, appreciation, and gratitude to my lovely wife who stands beside me and never complains. You own my heart and thank you for everting. To my sons, Yusuf and Musab, you are part of my heart and soul, and you have my ultimate love. To Yusuf, you are the best gift that I have got in my life. To Musab, you are the most enjoyable part of my life.

Financial support of this research effort is made available through Saudi Arabia Culture Mission “SACM”, and King Saud University “KSU”. Without this support, this work would not have been possible.

CURRICULUM VITAE

RAIED ALHARBI

Department of Civil and Environmental Engineering
University of California, Irvine
Irvine, Ca 926797

EDUCATION

Ph.D.,	Civil and Environmental Engineering (Hydrology and Water Resources)	University of California, Irvine, USA, 2019
M.Sc.,	Civil and Environmental Engineering (Water Resources Planning and Management Engineering)	Colorado State University, Fort Collins, Co, USA, 2015
B.S.,	Civil Engineering	King Saud University, Riyadh, Saudi Arabia, 2011

RESEARCH INTEREST

- Hydrology and Climatology
- Remote Sensing
- Hydrological Rainfall-Runoff Modeling
- Water Resources Planning and Management
- GIS-based modeling of watershed scale processes

PEER-REVIEWED JOURNAL PAPERS

Alharbi, R., Hsu, K., & Sorooshian, S. (2018). Bias adjustment of satellite-based precipitation estimation using artificial neural networks-cloud classification system over Saudi Arabia. Arabian Journal of Geosciences, 11(17), 1–17. https://doi.org/10.1007/s12517-018-3860-4.

Alharbi, R., Hsu, K. (2019). Bias Correction of Satellite-based Precipitation Estimation Using Limited Gauge Measurements over Saudi Arabia. Arabian Journal of Geosciences, Manuscript submitted for publication.

Alharbi, R., Hsu, K. (2019). Assessing the Efficacy of Bias Corrected Satellite-based Precipitation Estimation over Three Watersheds in Saudi Arabia. Arabian Journal of Geosciences, Manuscript in preparation.

CONFERENCE POSTER PRESENTATIONS

Alharbi, R., Hsu, K., & Sorooshian, S. (2019). Merging Satellite-Based Precipitation Estimates and Rain Gauge Measurements over Saudi Arabia. American Meteorological Society, 18th Annual Student Conference, Phoenix, Arizona.

Alharbi, R., Hsu, K., & Sorooshian, S. (2018). Precipitation Estimation over Saudi Arabia by Merging Satellite and Gauge Measurements. AGU Fall Meeting 2018, Washington D.C.

Alharbi, R., Hsu, K., Sorooshian, S., & Braithwaite, D. (2018). The Effectiveness of Using Limited Gauge Measurements for Bias Adjustment of Satellite-Based Precipitation Estimation over Saudi Arabia. American Meteorological Society, 17th Annual Student Conference, Austin, Texas.

Alharbi, R., Hsu, K., Braithwaite, D., & Sorooshian, S. (2017). Bias adjustment of satellite-based precipitation estimation using limited gauge measurements over Saudi Arabia. *Virtual Poster Showcase, 8* Retrieved from https://dialog.proquest.com/professional/docview/2002204198?accountid=14509

CONFERENCE ORAL PRESENTATIONS

Alharbi, R. (2018, January). The effectiveness of using Limited Gauge Measurements for Bias Adjustment of Satellite-based Precipitation Estimation over Saudi Arabia, NASA JPL scientists visited the Center for Hydrometeorology and Remote Sensing, Irvine, Ca.

Alharbi, R. (2017, May). Bias Adjustment of PERSIANN-CCS Precipitation Estimates over Saudi Arabia using Quantile Mapping and Inverse weighted Distance, the Center for Hydrometeorology and Remote Sensing, Irvine, Ca.

HONORS & AWARDS

- Recipient of Saudi Arabian Cultural Mission Scholarship (SACM) Award for Studying Doctor of Philosophy — 2015-2019
- Travel award for 17th Annual AMS Student Conference, Austin, Texas. — 2018
- Recipient of Saudi Arabian Cultural Mission Scholarship (SACM) Award for Studying Master's Degree — 2013-2015
- Travel award for 17th No-Dig Show, Denver, Colorado. Saudi Arabian Cultural Mission — 2015
- Recipient of Saudi Arabian Cultural Mission Scholarship (SACM) Award for Studying English as Second Language — 2012-2013
- Scientific Excellence Award King Saud University, Civil Engineering Department — 2009

PROFESSIONAL EXPERIENCES

- Reviewer, Peer-Reviewed Journals *Arabian Journal of Geosciences* — 2018 - 2019
- Teaching Assistant, Dept. Civil and Environmental Engineering, King Saud University — June 2011 – Sept. 2015
- Lecturer, Dept. Civil and Environmental Engineering, King Saud University — Sept. 2016 – Sept. 2019

- King Abdullah Financial District — Sept. 2010 – Nov. 2010

PROFESSIONAL AFFILIATIONS

- American Geophysical Union (AGU) — 2015 - 2019
- American Meteorological Society (AMS) — 2015 - 2019
- Saudi Engineer Council — 2011- 2019

ABSTRACT OF THE DISSERTATION

Bias Adjustment of Satellite-Based Precipitation Estimation Using Limited Gauge Measurements and Its Implementation on Hydrology Modeling

By

Raied Saad Alharbi

Doctor of Philosophy in Civil and Environmental Engineering

University of California, Irvine, 2019

Professor Kuo-Lin Hsu, Chair

Precipitation is a crucial input variable for hydrological and climate studies. Rain gauges can provide reliable precipitation measurements at a point of observations. However, the uncertainty of rain measurements increases when a rain gauge network is sparse. Satellite-based precipitation estimations “SPEs” appear to be an alternative source of measurements for regions with limited rain gauges. However, the systematic bias from satellite precipitation estimation should be estimated and adjusted. In this dissertation, a method of removing the bias from the precipitation estimation from remotely sensed information using artificial neural networks cloud classification system (PERSIANN-CCS) over a region where the rain gauge is sparse is investigated, and the method consists of three major parts.

The first part investigates the calculation of monthly empirical quantile mapping of gauge and satellite measurements over several climate zones as well as inverse weighted distance for the

interpolation of gauge measurements. Seven years (2010–2016) of daily precipitation estimation from PERSIANN-CCS was used to test and adjust the bias of estimate over Saudi Arabia. The first six years (2010–2015) are used for calibration, while one year (2016) is used for validation. The results show that the mean yearly bias is reduced by 90%, and the annual root mean square error is reduced by 68% during the validation year. The experimental results confirm that the proposed method can effectively adjust the bias of satellite-based precipitation estimations.

The second part is to provide a merged product by using the interpolated gauge estimates and the bias-corrected PERSIANN-CCS (0.04°×0.04°) estimates. Interpolated gauge estimates are calculated by the inverse weighted distance to the existing gauge points. The merged product is calculated based on the uncertainty of SPE and gauge estimation. Results show both the annual mean bias and root mean square error are reduced by 98% and 83% respectively. Statistical analysis of the merged product over different temporal scales and climate regions are discussed.

The third part of this dissertation is to examine the effectiveness of the bias-corrected approach that is based on quantile mapping and climatic zones in hydrological modeling. Three watersheds, which are Bisha, Byash, and Hail watersheds are chosen over Saudi Arabia. The evaluation is carried between 2011 and 2016 where the monthly and yearly runoff volumes are available. To model, the monthly and annual runoff volumes, Soil Conservation Service (SCS) model is implemented. Three evaluation statistics include correlation coefficient, mean bias, and root mean square error. The results show that the proposed method is effective for removing the bias from the SEPs, and for improving hydrological modeling.

CHAPTER 1: Introduction

1.1 Introduction

Water is vital to life on earth and it can be found in various forms. One of the most important forms is precipitation which is the primary source of water on land (Oki & Shinjiro, 2006; Ramanathan, Crutzen, Kiehl, & Rosenfeld, 2001). More than the half of global annual precipitation on earth falls on land which can contribute to supporting forests and livestock products, and the rest of the yearly global precipitation can add to water resources (International Water Management Institute, 2007; IWMI, 2007; Molden, 2013). The effectiveness of water resources management is highly influenced by precipitation since it is linked to food, health, security, and poverty (Cook & Bakker, 2012; WWAP (World Water Assessment Programme), 2012; Zeitoun, 2011; Zimmerman, Mihelcic, & Smith, 2008). For example, one of the most significant water consumption in the world is the agriculture sector, which is estimated to be around 90% of total water consumption, and 80% of the sector demands are met by precipitation (FAO, 2014; Mancosu, Snyder, Kyriakakis, & Spano, 2015; Shiklomanov, 1998; WWAP (United Nations World Water Assessment Programme), 2015). On the other hands, the world population has risen from 2.5 billion to 7.7 billion today since 1950, and agricultural demands are enormously enlarged to follow the needs of the population (Schmidhuber & Tubiello, 2007; Singh, 2012).

As projected in many scientific papers, the population will exponentially grow, and meeting population needs to secure the food and water will be critical (Boserup, 2013; Food and Agriculture Organization, 2002, 2009; Schmidhuber & Tubiello, 2007). More than 1.8 billions people are expected to face water shortages by 2025, and two-thirds of the world population is likely to live in countries suffering from water stress (UN Water, 2007). As known in the scientific community, climate change influences the world water (Nigel W. Arnell, 1999; Haddeland et al., 2014; Vörösmarty, Green, Salisbury, & Lammers, 2000). The Intergovernmental Panel on Climate Change attempted to summarize the impacts of climate change on water resources (Intergovernmental Panel on Climate Change (IPCC), 2014). With long warmer and few colder days and nights, some part of snowfall will convert into rainfall, and the snow melting seasons will be earlier, which influences regions where the water supply depends upon the snow. With more warmer days, the amount of evaporated water increases when moist air moves to the land or to oceans in then may become a storm which produces intense precipitation. Floods, soil erosion, sedimentations, and injuries are associated with extreme precipitation events (Program, 2018; Rosenzweig, Tubiello, Goldberg, Mills, & Bloomfield, 2002; Simpson, 2011; Wahl, Jain, Bender, Meyers, & Luther, 2015).

The Centre for Research on the Epidemiology of Disasters (CRED), CRED's Emergency Events Database, and The United Nations Office for Disaster Risk Reduction provide an analysis of weather-related disasters worldwide in both developed and developing countries in the last twenty years. Report provided by the agencies concludes floods and tropical storms account for more than 71% of the total global disaster that hits the world (CRED & UNISDR, 2015). In the last two decades, floods are considered to be the most common natural disaster since as they account for more than 40% of global natural disaster since 1995. In the last decade (2005 – 2014), the average number of floods per year was estimated to be more than 170 events per year, while the average amount of floods per year for the decade of (1995 – 2004) was calculated to be around 127 events per year. The number of people who have been affected by floods is estimated to be more than two billion floods are responsible for killing more than 150,000 persons in the last twenty years. In the previous twenty years (1995 – 2015), the deadliest natural disasters were the tropical storms, and it is responsible for killing more than 240,000 persons. Regarding the economy, the floods and the storms are responsible for more than $1.600 trillion ineconomic damage.

The United Nations Office for Disaster Risk Reduction estimated the annual economic loss due to weather-related disasters to be between $250 and $300 billion, which is a main challenge for developing countries (CRED & UNISDR, 2015). Also, Germanwatch Climate Risk Index, which lists the world countries based on the severity of weather-related disasters reports that the top ten countries are developing countries (Kreft & Eckstein, 2014).

One part of the world that is very vulnerable to climate change is the Middle East and North Africa region, where the summer temperatures in this region are expected to rise twice as fast as the global temperature (Lelieveld et al., 2016; Waha et al., 2017). Also, coupling the climate change with the exponential population growth in this region influences water resources (Alpert, Krichak, Shafir, Haim, & Osetinsky, 2008; Gao & Giorgi, 2008; Milly, Dunne, & Vecchia, 2005; Sowers, Vengosh, & Weinthal, 2011). North Africa and the Middle East are in the most water stressed region in the world where the total renewable water resources are less than 500 m3 (Creel & Souza, 2002).

The country level, Saudi Arabia, which is the largest country in North Africa and the Middle East, is facing one of the most significant problems which is the lake of renewable water resources (Al-Zahrani & Baig, 2011; Hussain, Alquwaizany, & Al-Zarah, 2010). There is no a perennial river, and the country has the lowest runoff rates in the world. However, the country has very limited surface water located in the southwest of the country (fao, 2008; Sagga, 1998). As a result of littlie available and feasible water sources, Saudi Arabia is forced to invest in desalination, on- renewable option (Abderrahman, 2005; Ouda, 2014). Currently, Saudi Arabia has spent around SAR 100 billion ($25 billion) for 80 years on desalination, and 50% of Saudi Arabia's oil production is consumed by the production of desalinated water (Hepbasli & Alsuhaibani, 2011). Moreover, the population growth in the country is estimated to be 2.2%, which is twice the global population growth. The annual increase in water demands, and the impacts of climate change have significant influences in the water resources availability in Saudi Arabia (DeNicola, Aburizaiza, Siddique, Khwaja, & Carpenter, 2015; Sowers et al., 2011). In recent years, floods have become common natural disasters (de Vries et al., 2016). In 2018, the significant events of flash floods hit Saudi Arabia where more than 30 people were confirmed dead, and more than 4000 people were affected (DTE, 2018). The deadliest flash floods in Saudi Arabia occurred in Jeddah city, which suffered from two deadly flash floods that took place on November 25th, 2009, and January 25th, 2011. They were responsible for more than 100 deaths, and the economic losses were estimated to be more than $900 million (Almazroui, 2011; de Vries et al., 2016).

To overcome the challenges and to have sustainable manage climate change, the need to observe and measure precipitation is undoubtedly critical. Precipitation has been observed and measured through direct and indirect instruments, rain gauge, radar, and satellite (Reddy, 2005; A. Sharma & Mehrotra, 2010). The simplest way to observe precipitation is by using a rain gauge, which provides the most accurate precipitation measurements at a point of observation (Maliva & Missimer, 2012; Rosenzweig et al., 2002; A. Sharma & Mehrotra, 2010; Willems, Arnbjerg-Nielsen, Olsson, & Nguyen, 2012). However, accuracy of the rain gauge observations is highly influenced by many factors such as wind effects, evaporation, human error, and surrendering objects that limit the rain gauge accuracy (Habib, Krajewski, & Kruger, 2001; Villarini, Mandapaka, Krajewski, & Moore, 2008). Furthermore, when rain gauge observations are extended to cover more spatial coverage rather than a singular point, the degree of uncertainty becomes notable since the extension is done by one of the well-known interpolation tools such as Thiessen Polygon, Inver Weighted Distance, and Kriging (Cheng, Lin, & Liou, 2008; Morrissey, Maliekal, Greene, & Wang, 1995; Moulin, Gaume, & Obled, 2009; Villarini et al., 2008). The accuracy of those methods highly depends on rain gauge locations and density (Mishra, 2013). In fact, the number of operated rain gauges in many regions of the world is decreasing. It has been reported the number of rain gauges across Europe, South America, and Africa, are severally declines by more than 50% (Overeem, Leijnse, & Uijlenhoet, 2013).

Satellite-based precipitation estimates (SPEs) seem to be a suitable source to overcome the dilemma of obtaining reliable spatial precipitation measurements when ground observations are limited or unavailable. SPEs are able to observe and provide global measurements at fine spatial and temporal resolutions. Various SPE products have been developed since the 1990s, which successfully provide valuable information used in hydrological and climatic studies(Adler et al., 2003; Al, Joyce, Janowiak, Arkin, & Xie, 2004; Ashouri et al., 2015; Hong, Hsu, Sorooshian, & Gao, 2004; K. Hsu, Gao, Sorooshian, & Gupta, 1997; K. L. Hsu, Gupta, Gao, & Sorooshian, 1999; G J Huffman et al., 2018; George J. Huffman, Adler, Bolvin, & Nelkin, 2010; George J. Huffman et al., 2007; Sorooshian et al., 2000). Although SPEs provide reliable measurements, several researches have confirmed that they are influenced by bias (Aghakouchak, Behrangi, Sorooshian, Hsu, & Amitai, 2011; Moazami, Golian, Kavianpour, & Hong, 2013; Qin, Chen, Shen, Zhang, & Shi, 2014). The bias may relate to the fact that satellites estimate the rainfall rate indirectly through visible, infrared (IR), and microwave (MW) cloud properties (Pereira Filho et al., 2010). The presenting of the bias on SPEs leads to overestimations or underestimations of the rainfall rate that affects the results of hydrological and climatic studies, so removing the bias of SPEs is a crucial step before implementing SPEs on the hydrologic and climatic studies (J. Chen, St-Denis, Brissette, & Lucas-Picher, 2016; Gebregiorgis, Tian, Peters-Lidard, & Hossain, 2012).

Various bias correction approaches are proposed to remove the systematic bias of SPEs and improve the outcomes of SPEs (Tesfagiorgis, Mahani, Krakauer, & Khanbilvardi, 2011). Some bias correction approaches include linear scaling, local intensity scaling, and histogram equalization (Gudmundsson, Bremnes, Haugen, & Engen-Skaugen, 2012; Lenderink, Buishand,

& Van Deursen, 2007). Linear scaling is a linear method that aims to correct the mean of SPEs to match the mean of ground observations and is done by an additive or multiplicative factor. The linear scaling method only corrects the mean of SPEs without correcting variance on precipitation (Teutschbein & Seibert, 2012a). On the other hand, the local intensity method is proposed by (Schmidli, Frei, & Vidale, 2006) to overcome the scaling limitation. The local intensity method aims to match wet-day and dry-day frequencies and intensities of SPEs and ground observations. The correction is done in two steps. The first step finds a threshold where the intensity of SPEs wet-day is adjusted to match the wet-day of ground observations. The second step is finding the factor that adjusts the mean of SPEs to match the mean of ground observations. However, this method does not make any corrections on daily precipitation occurrences (J. Chen, Brissette, Chaumont, & Braun, 2013). Histogram equalization is known by several names such as probability mapping, and quantile mapping (QM) (Block, Souza Filho, Sun, & Kwon, 2009; J. Chen et al., 2013). QM will be used to represent histogram equalization in this dissertation. QM is a distribution-based approach, and the purpose of QM is to match between probability density functions (PDF) of SPEs and ground observations. The matching between PDFs is done by a transfer function, and the type of QM depends on the type of function. Non-parametric QM was found to perform better than parametric QM in removing the bias due to the fact that the function does not need to pre-define the type of PDF which gives more flexibility (Ajaaj, Mishra, & Khan, 2016; Grillakis, Koutroulis, & Tsanis, 2013; Jakob Themeßl, Gobiet, & Leuprecht, 2011; Piani, Haerter, & Coppola, 2010; Thiemig, Rojas, Zambrano-Bigiarini, & De Roo, 2013). Studies conclude that QM effectively removes the SPEs bias in comparison to other bias correction approaches (Piani et al., 2010).

1.2 Motivations

Precipitation is highly influential as it touches many aspects of human life. On one hand, lack of water can affect human daily water consumption. On the other hand, an excess of water in the form of the precipitation can lead to natural disasters, such as a flood. Therefore, the need to observe and study precipitation patterns is critical. The accuracy of precipitation measurements is considered to be challenging. To have the accuracy precipitation measurements are a function of rain gauge density. Although the rain gauges should be dense, this is not the case for most countries around the world.

From my prospective, SPEs can be the source for reliable precipitation estimations with consideration of the bias that exists of their estimations. Overcoming this limitation makes SPEs become a consistent source of precipitation measurements.

One of my personal motivations is that I am living in a country where the account of each drop of water is essential for present and future generations in Saudi Arabia. The country is facing water shortages, and the country has very high population growth and high water demands. To adopt a sustainable water management, there is a need for reliable precipitation management. Because of the lack of reliable measurements, many scientific papers claim that the country will run out of groundwater in the 30 or 50 years, so the county needs to invest more in the desalination sector which is reported consumes up to 50% of the country's oil production to meet the current demands.

1.3 Objectives

The primary objective of this dissertation is to provide a scientific and practical methodology that can help to remove the existence of the bias in SPEs. As mentioned, the QM is the most effective methods in removing the bias, but the effectiveness of the QM is influenced by the sample size that is used to calculate PDFs. When the sample size is insufficient, the uncertainty enlarges, and vise verse. To enlarge the sample size, including the useful sample within a simple Climatic Zone ‘"CZ" that will overcome this limitation. Therefore, the objectives can be divided into three main objectives which are:

- The first objective is to investigate the effectiveness of QM-CZ on removing the systematic bias of SPEs. Where the assumption is that including the climatic zone will help to overcome the sample size limitations in building consistency PDFs.
- The second objective is to examine the effectiveness of merging between the bias-corrected SPEs and rain gauges. The rain gauges provide the most accurate precipitation measurements that can be used to improve the reliability of the bias-corrected product by merging between the rain gauges and the bias-corrected product. The assumption is that the degree of the uncertainty is a function with the distance, while the bias-corrected product that is based on the climatic zone is a function in the precipitation rates.
- The last objective is to test the applications of QM-CZ on hydrology modeling. Finally, the examination of the results of including the climatic zone and incorporation of the rain gauges in hydrological modeling is the final objective of this dissertation.

1.4 Dissertation Outline

This dissertation consists of five main chapters. Chapter 2 presents and discusses the most common bias correction approaches, and the chapter proposes and discusses the bias correction approach that is based on climatic zones. Chapter 3 describes the common merging approaches, introduces and explains the merging approach that addresses the degree of the uncertainty that relates to the distance and precipitation rates. Chapter 4 provides detailed explanations about the hydrological model that is used to examine the proposed bias correction and merging approaches. Chapter 5 summarizes the findings of this study and discusses future extensions of this work.

CHAPTER 2: Bias Adjustment of Satellite-Based Precipitation Estimation Using Limited Gauge Measurements

2.1 Introduction

The existing of bias in satellite-based precipitation estimations (SPEs) can limit the applications of SPEs on hydrological and climatic studies, so implementations of bias corrections are recommended on hydrological and climatic studies (Christensen, Boberg, Christensen, & Lucas-Picher, 2008; Ehret, Zehe, Wulfmeyer, Warrach-Sagi, & Liebert, 2012; Pierce, Cayan, Maurer, Abatzoglou, & Hegewisch, 2015; Terink, Hurkmans, Torfs, & Uijlenhoet, 2010; Teutschbein & Seibert, 2010, 2012a). Bias corrections can be classified as linear, nonlinear, or distribution-based methods.

2.1.1 Linear Bias Correction

When linear bias correction is applied, the bias is removed by using scaling or threshold factors. In the linear scaling that is proposed by (Lenderink et al., 2007), a monthly correction factor is based on the ratio between the estimated day from SPEs and the observed day from ground true observations (Durman, Gregory, Hassell, Jones, & Murphy, 2001). Also, Equation 2.1 represents linear scaling, where P is biased the precipitation rate that is estimated by SPE, P' is the bias corrected rate. $\overline{\mathrm{O}}$ is the monthly mean of the rain gauge observations, and $\overline{\mathrm{P}}$ is the mean monthly biases precipitation rates that are estimated from SPE.

$$\mathrm{P}' = \mathrm{P} * \left(\frac{\overline{\mathrm{O}}}{\overline{\mathrm{P}}}\right) \qquad 2.1$$

The advantages of this method are that it is simple and easy application where the only one normal monthly is required to compute the correction factor (Ajaaj et al., 2016; Hay, Wilby, & Leavesley, 2000; Lafon, Dadson, Buys, & Prudhomme, 2013). However, using the monthly correction factor does not capture the inter-monthly precipitation variation that effects capturing of the probability distribution of daily precipitations (N. W. Arnell, 2003; Diaz-Nieto & Wilby, 2005). To overcome this limitation, (Schmidli et al., 2006) proposed a local intensity scaling (LIS) method that is based on matching between frequencies of wet and dry days of SEPs and ground observations. First, a threshold is calculated such that the number of the wet days of SPEs that exceed the threshold matches the wet days of ground observations. Second, the monthly correction ratio is calculated based on estimations of the differences between the wet days of SPEs and the wet days of ground true observations. In Equation 2.2, $P_{thrshold}$ is the threshold in which the wet days frequency of SPE matches the frequency of the rain gauge observations, and $\overline{\mathrm{O_m}}$ is the mean monthly precipitation rates for wet days. $\overline{\mathrm{P_m}}$ is the mean monthly precipitation rate of wet days of SPE.

$$\mathrm{P}' = \begin{cases} 0 & if\ P < P_{thrshold} \\ & P * \left(\dfrac{\overline{\mathrm{O_m}}}{\overline{\mathrm{P_m}}}\right) \end{cases} \tag{2.2}$$

2.1.2 Non-Linear Bias Correction

The linear bias correction methods work by correcting the bias the mean without correcting the bias on the variance (J. Chen et al., 2013; Fang, Yang, Chen, & Zammit, 2015; Teutschbein & Seibert, 2012a). Therefore, the non-linear bias correction approach that has an exponential form

$$\mathrm{P}' = \mathrm{a.P^b} \tag{2.3}$$

shown by Equation 2.3, is used to correct the various estimated precipitations by SPEs (Leander & Buishand, 2007; Leander, Buishand, van den Hurk, & de Wit, 2008; Shabalova, van Deursen, & Buishand, 2003; Teutschbein & Seibert, 2012a). In Equation 2.3, a and b are scale factors, and P is the bias the precipitation rate that is estimated by SPE. P' is the bias corrected rate. The parameter b can be estimated iteratively by matching monthly coefficient of variations of the bias corrected SPEs with monthly coefficient of variations of the ground observations. Once that b is estimated, it is calculated by matching the monthly mean of the bias corrected SPEs with monthly the mean of observations. Finally, the daily uncorrected estimations of SPEs is corrected by applying Equation 2.1. When the non-linear bias corrected approach is compared to the linear bias corrected approaches, the non-linear bias correction works by matching the mean and the various ground observations (Terink, Hurkmans, Torfs, & Uijlenhoet, 2009).

2.1.3 Distribution-Based Bias Correction.

The aim of the distribution-based methods is to match the distribution function of the biased SPEs to the distribution function of the rain gauge observations. This method is used to correct the mean, standard deviation and quantiles of SPEs to the mean, standard deviation and quantiles of the rain gauge observations (Fang et al., 2015). In order to accomplish this, a transfer function that can shift the distribution function of biased SPEs to the rain gauge distribution is used (Sennikovs & Bethers, 2009). The function can be classified as parametric or non-parametric. Non-parametric has been extensively used because the function does not need a prior assumption about the distribution function type (Piani et al., 2010; Themeßl, Gobiet, & Heinrich, 2012; Wilcke, Mendlik, & Gobiet, 2013; A. W. Wood, Leung, Sridhar, & Lettenmaier,

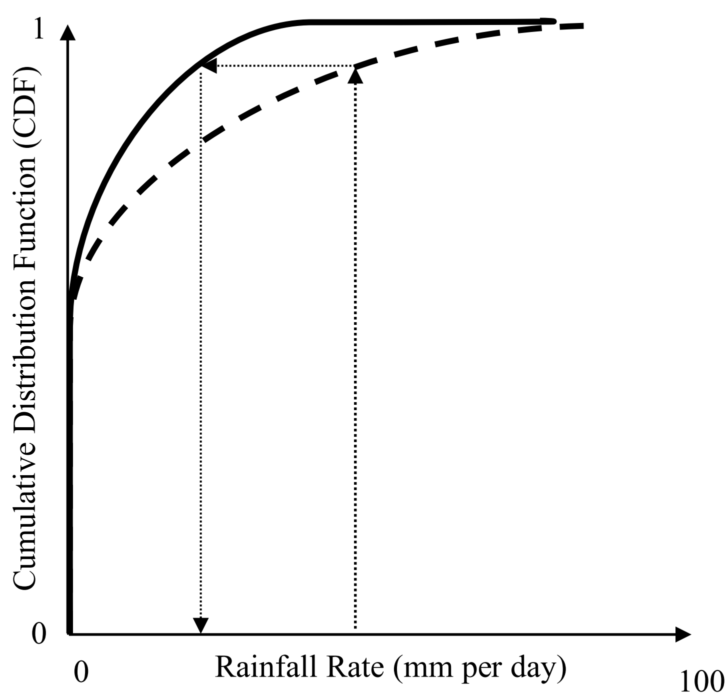

Figure 2.1 Schematic of the empirical distribution correction approach with observed (solid) and simulated

2004; Andrew W. Wood, Maurer, Kumar, & Lettenmaier, 2002). The function, proposed by (Panofsky, Brier, & Best, 1958) known as quintile mapping (QM). To implement the QM method, two empirical CDFs are calculated. One CDF is for biased SPEs and the second is for the rain gauge observations. The value of CDFs at each quantile are replaced by CDF of the rain gauge observations. The description of QM is shown in Figure. 2.1 where dotted lines represent the QM method corrections. The rainfall rates for each quantile are replaced with the observed rainfall rate for the same quantile. Also, QM can be expressed by Equation 2.4 where $\mathrm{P}'_{\mathrm{m,d}}$ is the daily bias corrected precipitation rate, and $\mathrm{ecdf}^{-1}_{\mathrm{obs,m}}$ is the monthly empirical CDF of the rain gauges. $\mathrm{ecdf}_{\mathrm{SPE,m}}$ is the monthly CDF of the SPE, and $\mathrm{P}_{\mathrm{m,d}}$ is the biased monthly precipitation rate.

Several studies have been performed in which QM was implemented to remove the bias.

$$\mathrm{P}'_{\mathrm{m,d}} = \mathrm{ecdf}^{-1}_{\mathrm{obs,m}}(\mathrm{ecdf}_{\mathrm{SPE,m}}(\mathrm{P}_{\mathrm{m,d}})) \qquad 2.4$$

(Bennett, Grose, Post, Corney, & Bindoff, 2011) applied QM to correct the estimations of six regional climate models. The study found that implementing QM improved the spatial correlation between the estimated seasonal and annual rainfalls and the observed rainfalls. Also, the study recommended that QM can be coupled with the regional climate model in hydrological modeling. (Pierce et al., 2013) implemented QM to predict the temperatures and precipitations that were provided by sixteen global general circulation models over California in 2060s. (Reiter, Gutjahr, Schefczyk, Heinemann, & Casper, 2017) used the daily precipitation data of ten regional climate models over Germany provided by the European Union climate change project for the period between 1961 to 2000 to evaluate the performance of QM. QM enhanced the forecasted precipitations that were provided by the models. (Bong, Son, Yoo, & Hwang, 2017) evaluated the capability of QM on removing the bias from HadGEM3- RA a regional climate model by using the 30 years daily precipitation observations (1976 – 2005). The implementation of QM removed the bias, and improved the outcomes of the model by a solid matching between estimated and observed for annual and monthly rainfall. (Ngai, Tangang, & Juneng, 2017) applied the method to remove the bias from daily simulated precipitations that were provided by global and regional models over southeast Asia. The study's showed approved that QM considerably improved the outcomes of the models during the study time of January 1979 to December 2005.

A brief description of the most widely used bias corrections approaches along with their advantages and disadvantages are provided in Table 2.1.

In order to identify which method is most capable of remove bias, (Lafon et al., 2013) compared the performance of the four bias correction methods, which are linear, non-linear, parametric distribution-based, and non-parametric distribution-based (QM), used to remove bias in a regional climate model, HadRM3.0-PPE-UK,. Seven catchments in the United Kingdom have been chosen, and the study time was between 1961 and 2005. The results of the bias correction methods were calibrated and validated with the rain gauge and stream observations. The study found that the non-parametric distribution-based QM had the best performance in removing the bias and matching the stream flow observations. Also, (Fang et al., 2015) evaluated the effectiveness of the bias correction methods in removing the bias in a regional climate model, RegCM, that provided precipitation and temperature estimates over Kaidu River basin in China. The results of the bias correction methods were tested against meteorology and stream observations and showed that QM had best performance in removing the bias in the precipitation estimations. Also, the flow that is simulated by QM

Table 2.1 The Advantages and Disadvantages of the most common Correction Methods

Method	Advantages	Disadvantages	References
Linear Scaling	• It simplest bias correction methods.	• It does not capture the internal monthly variations that affect the probability distribution function (PDF) of the daily precipitation. • The number of the wet-day is larger than observed wet-day.	(Diaz-Nieto & Wilby, 2005; Lenderink et al., 2007; Teutschbein & Seibert, 2012a)
Local intensity scaling	• The frequency of the wet-day is corrected	• It does not made any correction to the daily precipitation occurrence. • It does not capture the differences changing in the frequency of the distribution of precipitations.	(J. Chen et al., 2013; Schmidli et al., 2006)
Mean bias removal technique	• It is a simple. • The correction factor is applied to estimated	• It does not capture the climate pattern.	(Davis, 1976; Kharin & Zwiers, 2002)

	precipitation, and the factor is calculated by matching the mean monthly estimated precipitation with the mean monthly observed for each month.	• It does not remove the bias that is associated with higher precipitation rate.	
Power transformation	• Corrections factors are applied to correct the mean and variation of estimated precipitations	• It is unable to do any adjustments of the temporal in the daily precipitation occurrences	
Quantile mapping based on an gamma distribution (QMG)	• It is distribution-based approach. • The correction is based on a	• The correction highly depends on the estimated precipitations follows the gamma distribution.	(Ines & Hansen, 2006; Piani et al., 2010;

	gamma distribution. • The occurrence of precipitations is corrected by Local Intensity Scaling method	• No adjustments is done for the occurrences of the daily precipitations.	Teutschbein & Seibert, 2012a)
Quantile mapping based on an empirical distribution (QME)	• It is distribution-based approach. • It is most method used for the bias correction. • The cumulative distribution function does not need prior definition. • It corrects the mean, and variability of estimated precipitation by matching all	• It may not capture the occurrences of the daily precipitation.	(Jakob Themeßl et al., 2011)

	quintiles with the observed precipitations.	

matched well in with the curve and peak of stream observations. (Ajaaj et al., 2016) examined the performance of bias correction methods in removing the bias of Global Precipitation Climatology Center (GPCC) between 1980 and 2004 over Iraq. The study found that QM and the bias mean remove were superior compared to other methods. (N'Tcha M'Po, 2016) tested six methods of bias correction in removing the bias of a regional climate model over West Africa. The most effective method in removing the bias from precipitation is QM. Finally, (Luo et al., 2018) implemented five bias correction methods, which are linear scaling, daily translation, variance scaling, distribution mapping, and QM to remove the bias in HadGEM3-RA reginal climate model. The study validated the results of the five bias correction methods with the daily meteorological observations for a period between 1965 and 2004. The study concluded that the distribution-based methods, which are distribution mapping and QM, showed the best performance on removing the bias from temperature and precipitation estimates. Overall, when comparing the QM and other bias correction methods, the QM is superior.

The performance of QM in removing the bias is highly influenced by a simple size that is used to calculate CDF because QM is a distribution-based approach. In other word, when the sample size is insufficient, the result of the mapping is questionable due to the unstable CDF that is based on the sample. In order to overcome this limitation, (Yang et al., 2016) examine the effectiveness of QM in removing the systematic bias of SPEs using rain gauges through a notable method that is based on QM and Gaussian weighted approach where a study area is divided into a number of several 1° by 1° boxes, and CDFs are calculated for each box. Then, QM is applied for each box, and the results of the mapping are interpolated using the Gaussian approach. One of the study recommendations is to implement the method over dense rain gauge areas because using the method over sparse rain gauge reduces the reliability of calculating consistent CDFs. Moreover, implementing the method over sparse rain gauge networks is limited since the method works by dividing the study area into 1° by 1° boxes calculating CDFs over each box with a gauge, and then by filling each box that does not have a gauge with nearest box that has gauge. Therefore, the method is limited to areas where rain gauges are dense, so this method cannot be applied in a region where rain gauges are very sparse because it could to a majority of boxes without rain gauges. This would lead to an unreliable correction of SPE as the nearest box with a rain gauge would be used to fit the rain gauge and SPE of CDFs. However, including climate region should overcome this limitation.

The objective of this chapter is to find a way to identify and remove the systematic bias from one of SPE products over a case study that is identified in the following sections. This chapter proposes a bias correction approach that is based on empirical QM using the climate zone (CZ), and the Inverse Weighted Distance method (IWD), and extends to the ungauged areas.

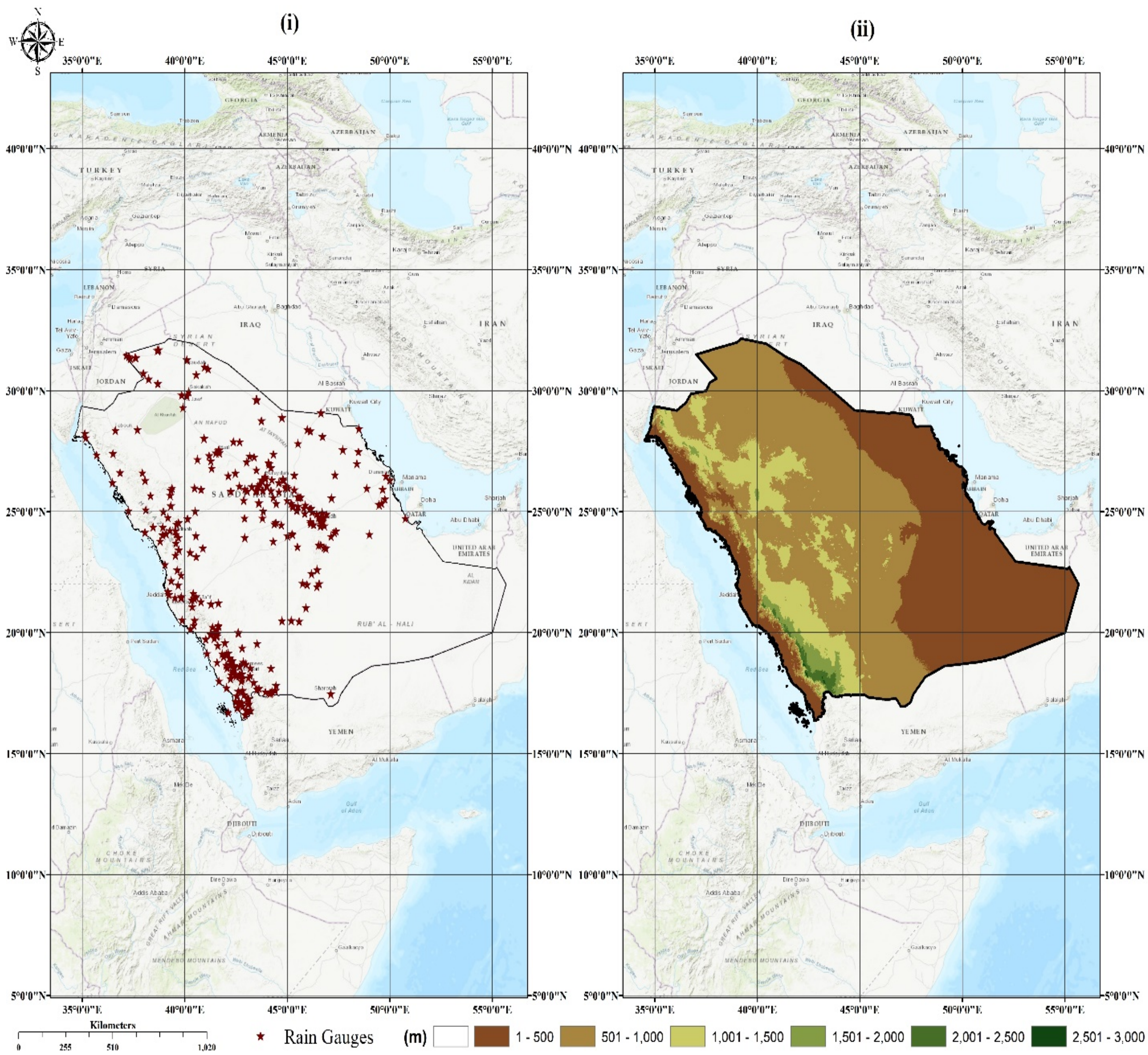

Figure 2.2 Map of Rain Gauge (Left) and Elevation (Right)

2.2 Climate and Precipitation over the Study Area and Data Source

2.2.1 Study Area

Saudi Arabia lies between 15ºN and 30ºN of the equator, and 35º E and 55ºE of Greenwich meridian, and the country covers about 2.25 million km^2 of the Arabian Peninsula, as shown in Figure. 2.2 The country is surrounded by unique boundaries. On the west, it is surrounded by the Red Sea. The Persian Gulf is located on the east side of the country. The seas are the main source of water vapor over Saudi Arabia ((MAW), 1984).

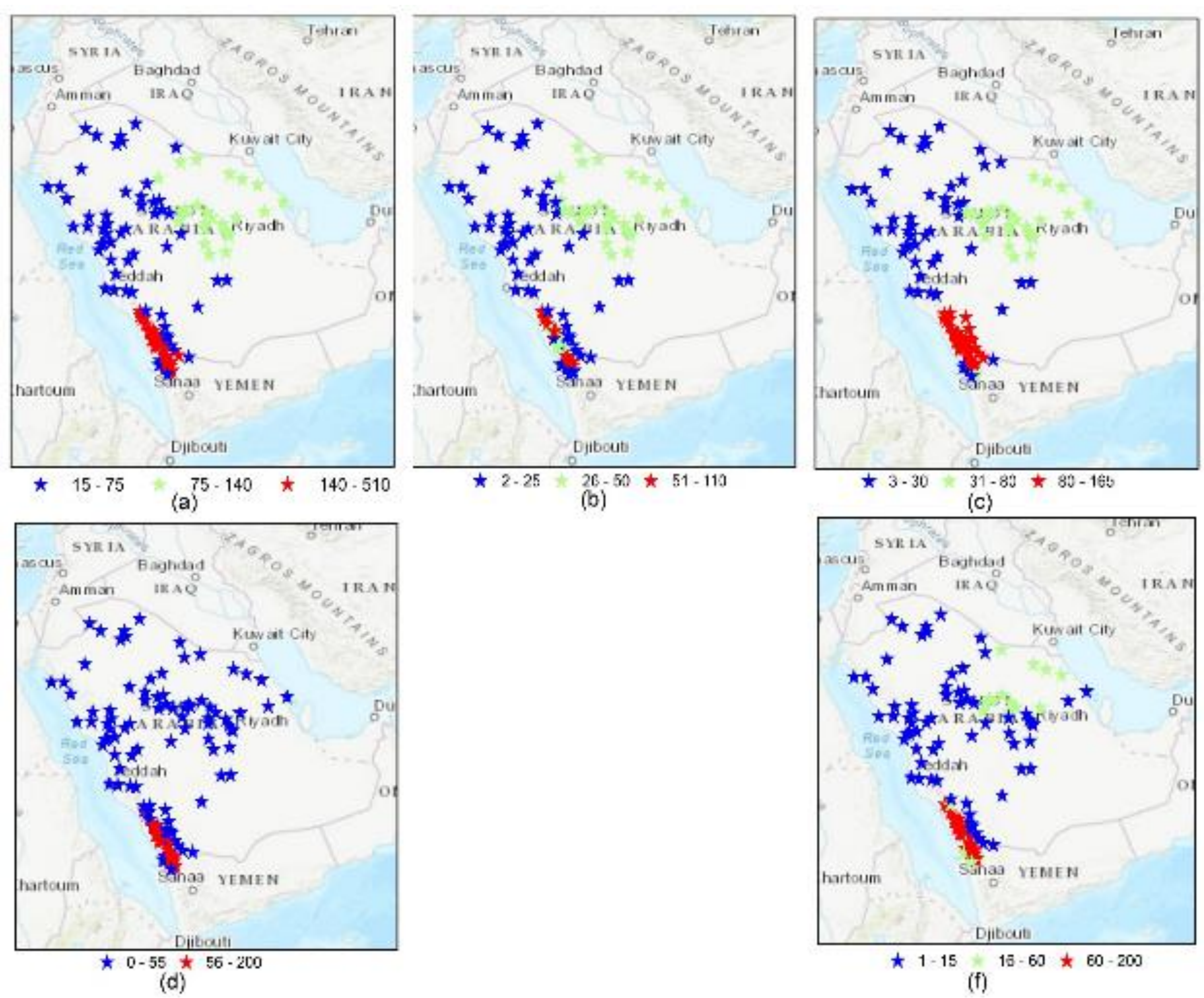

Figure 2.3 (a) Yearly (b) Winter Season (c) Spring Season (d) Summer Season (f) Autumn Season Precipitations in Saudi Arabia

The country has four topographical regions, which includes the coastal plains, the mountainous region, the Najd plateau, and Rub Al-Khali. Coastal plains are extended from the north to the south of the country along the seas. The mountainous areas are over the southwestern of the country, and it is known as Hijaz and Asir. The elevation of the mountains ranges from 2000 m to 3000 m. The slope of the mountains range is steep toward the west, where the Red Sea is located, but uniformly decreases toward the east. Najd plateau occupies most of Saudi Arabia, and the plateau lies the east of the mountains and west of the eastern coastal plain. The plateau's elevation ranges from 800 and 1100 km. The Rub Al-Khali is located in the southeastern part of the country, and the Rub Al-Khali is known as the largest sand desert in the world ((MAW), 1984; Takahashi & Arakawa, 1981).

2.2.2 Climate and Precipitation in Study Area

According to Koppen-Geiger climate classification, the country's climate is classified as hot, sunny and dry during the entire year, and it is coded as BWh. B stands for an arid land, and W stands for low precipitations (Kottek, Grieser, Beck, Rudolf, & Rubel, 2006). The h indicates high temperature. However, the southwest of the country, where Hijaz and Asir mountains are located, has mild to low temperatures and has precipitations during the entire year. It is classified as semi-arid (Abdullah & Al-Mazroui, 1998; Al-Jerash, 1985; A. Subyani, Al-Modayan, & Al-Ahmadi, 2010; A. M. Subyani, 2004). Climate studies by (Ahmed, 1997; Al-Jerash, 1985; Almazroui, Dambul, Islam, & Jones, 2015a) are the latest attempt to regionalize the climate of the country. (Al-Jerash, 1985) Used fifty meteorology stations to identify the climate zone in Saudi Arabia, and the study time was the period between 1970 and 1982. The study identified six climate zones based in twenty years of observations. (Almazroui, Dambul, Islam, & Jones, 2015b) pointed out the subdivisions of climate in the study area, and the study used twenty-seven meteorology stations, and the study used thirty years of observations between 1985 and 2010 (26 years). The study concluded that the country has five climate zones. (Ahmed, 1997) classified the study area to climate zones based on daily observations from fifty-six meteorology stations, and the study time was between 1963 and 1993 (31 years). (World Meteorological Organization, 1989) highly recommended the minimum number of the year that is used for climate studies are 30 years. Therefore, (Al-Jerash, 1985; Almazroui et al., 2015b) did not use the recommended number of years, while (Ahmed, 1997) used the prescribed number of years. Saudi Arabia can be classified into three zones based on annual precipitations. Those three zones are the southwest, center, and the rest, which is presented in Figure. 2.3.

A brief review on moist air mass movements over the country that influence precipitation distributions is described below (Al-Qurashi, 1981; Alyamani, 2001; A. Subyani et al., 2010; Vincent, 2008):

I. Maritime Tropical Air Mass (Monsoon Front) flows during the summer and at the end fall seasons. The air mass carries warm and moist air masses from the Indian Ocean and the Arabian Sea to the south and southwest of Saudi Arabia where Hijaz and Asir mountains are located. Usually, the precipitation is associated with high intensity.

II. Continental Tropical Air Mass, which is warm and moist air masses that comes from the Atlantic Ocean, and prevails during the winter season. It brings low to mild precipitation to the west and center of Saudi Arabia.

III. Maritime Polar Air Mass is formed on the eastern Mediterranean Sea, and it crosses the north and northwest of the country during the winter season. It produces high to mild precipitation.

Precipitations happen mostly in the winter and spring seasons, while the southwest of the county, on the other hand, has precipitations during the entire year ((MAW), 1984). The precipitation amount over the country is less than 100 mm each year, but the southwestern region has more than 350 mm annually (Al-Jerash, 1985; Alyamani, 2001). Precipitations decrease from the south to the north and from the west to the east where the air masses and topography play essential roles in the precipitation process.

Figure. 2.3 shows annual precipitation in the country analyzed from 1966 to 2013. The maximum mean annual precipitation (~500 mm/year) occurs in the southwest of the country. The minimum yearly precipitation (~15 mm/year) occurs in the north and the northwest of the county. For seasonal distribution of precipitations, 37% takes place in the spring season, 22% of precipitations occurs in the winter season. Precipitations during the autumn and the summer accounts for 22%, and 19% of annual precipitation, respectively.

During the winter season, precipitations are cyclonic, and it is formed by maritime polar air masses that come from the Mediterranean Sea, which is cold and moist, and the Atlantic Ocean, which is warm and humid. The highest amount of precipitation is around 100 mm per season and happens in the southwest due to orographic lifting. The second highest precipitation is about 40 mm per season and is located in the northeast of the country because this part of the country is subjected to convection precipitation lifting that is formed by the Mediterranean. The center and southeast of the country have low precipitation, which is 24 mm per season.

During the spring season, the highest precipitation depth is around 160 mm per season and occurs in the southwest due to monsoonal moist air that comes from the Indian Ocean. It crosses the south of the country and is lifted by the mountains. The center of the country still receives the second highest precipitation depth around 60 mm per season, due to the moist monsoonal air. It penetrates the country from the southwest to the east. The north and northwest of is a diest area with a precipitation depth around 20 mm per season.

During the summer season, most of the country does not have precipitation. However, the southwest receives precipitations due to conventional instabilities and the monsoonal air. Most of the storms are thunderstorms, and the amount of precipitation in this part of the country is around 195 mm per season.

During the autumn season, most of the storms are convective and are formed by the meeting of the southeastern air mass that comes from the Arabian Sea and the westerly air mass that comes from the Mediterranean Sea. As expected, the southwest region receives the highest amount of precipitation, which is 180 mm per season, while the driest part is the north and the northwest areas.

2.3 Data Sources

The precipitation data used on this study comes from PERSIANN-CCS (Hong et al., 2004), and historical rain gauges obtained from the Ministry of Environment, Water, and Agriculture (MEWA), and The General Authority of Meteorology and Environmental Protection (GAMEP). PERSIANN-CCS is provided from the Center for Hydrometeorology and Remote Sensing, University of California, Irvine (CHRS, UCI).

2.3.1 Historical Rain Gauges

The rain gauges that are used in this study are provided by MEWA and GAMEP. MEWA provided 290 rain gauges, and they have been recorded manually since 1966. GAMEP provided 28 automatic rain gauges, and they are considered to be the most reliable gauges over Saudi Arabia. Moreover, these gauges are extensively used to study precipitations and the climate in the study area (Abdullah & Al-Mazroui, 1998; Al-Qurashi, 1981; Al-Rashed & Sherif, 2000; Almazroui, 2011; Kheimi & Gutub, 2015).

2.3.2 Satellite-based Precipitataion Estimation

The daily estimation from Precipitation Estimation from Remotely Sensed Information using Artificial Neural Networks - Cloud Classification System (PERSIANN-CCS) is used (Hong et al., 2004). PERSIANN-CCS is developed by the Center for Hydrometeorology and Remote Sensing (CHRS) at the University of California, Irvine (UCI). PERSIANN-CCS estimates the precipitation rate based on utilizing an image processing and pattern reconfigure techniques to categorize a patch-based cloud that is based on the cloud height, areal extent, and variability of texture from satellites imagery. After the patch is identified, the precipitation rate is assigned by the relationship between the precipitation rate and brightness temperatures of the cloud. PERSIANN-CCS provides hourly precipitation estimations at the global scale with the spatial resolution of 0.04º by 0.04º latitude and longitude.

In this study, PERSIANN-CCS estimation was accumulated from hourly estimates to daily estimates since the rain gauge observation were in daily time scale. Also, the daily estimations of PERSIANN-CCS are limited for seven years, which are the period between 2010 and 2016 where the rain gauges record are available.

2.4 Methodology

This study is based on investigating the effectiveness of the QM method by considering CZ. Inverse weighted distance interpolation method (IWD) is used to extend the bias adjusted precipitation estimation to areas where rain gauges are limited or not available. In order to justify the effectivness of the implmentaions of the QM by considering CZ, the comparison between the results of the implmentaions of the QM by considering CZ that is named in this dissertaion as Adjusted PERSIANN-CCS with climate zones (CZ) and the resuls of the implemetiaons of the

QM without considering CZ. That is named in this dissertaion as Adjusted PERSIANN-CCS without claimte zones (CZ). The implementaion of the QM without considering the claimtic zones is followed (Yang et al., 2016).

Seven years, which is 2010 to 2016, of daily rain gauges observations and PERSIANN-CCS estimations are used to evaluate the method. The first six years, which are 2010 to 2015 are used for model calibration, while one year, which is 2016, is the validation year.

QM is implemented to correct the Original PERSIANN–CCS (Org-PERSIANN-CCS)

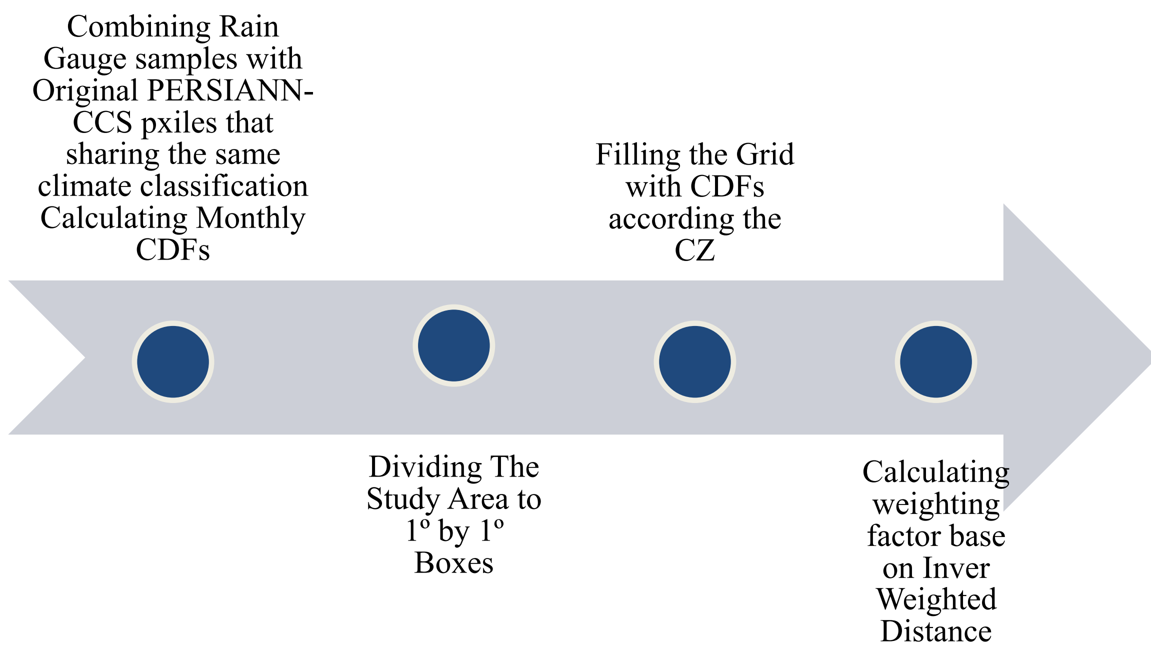

Figure 2.4 Flowchart of QM-CZ

estimations by matching CDF of Org-PERSIANN-CCS to the CDF of rain gauges. The CZs are applied to increase the number of samples for estimating stable CDFs. In addition, IWD is employed to interpolate the results of applying QM to finer resoulation.

2.4.1 Data Quality

MEWA rain gauges observe precipitations manually, while GAMEP gauges are automated. Studies have shown the automated gauges are most consistent and reliable for the precipitation measurements in Saudi Arabia (Abdullah & Al-Mazroui, 1998; Al-Qurashi, 1981; Al-Rashed & Sherif, 2000; Almazroui, 2011; Kheimi & Gutub, 2015). Criteria for choosing a qualified rain

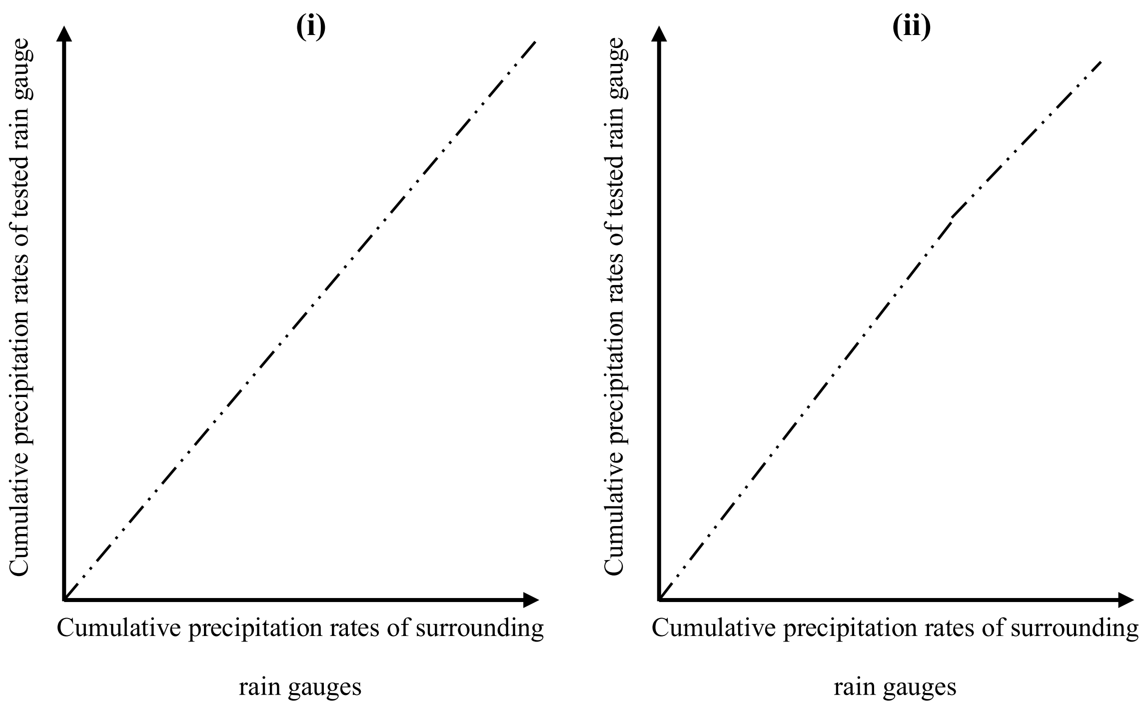

Figure 2.5 Schematic of the double mass curve where (i) the consistent rain gauge, and (ii) the non-consistent rain gauge

gauge are the following:

I. The qualified rain gauge should have been recording for more than five successive years.

II. The qualified is consistent with the nearest gauge using the double mass curve follows (Searcy & Hardison, 1960).

According to (Searcy & Hardison, 1960), a consistent rain gauge should share a similar cumulative precipitation depth with nearest rain gauges, while a non-consistent rain gauge does not have a same depth. Meaning, the cumulative precipitation depth from the tested rain gauges is plotted against the cumulative precipitations of surrounding rain gauges. When the plot is a straight line, the tested rain gauge is consistent with the surroundings rain gauges. In contrast, a break in the slope of the line means the consistency of the tested rain gauge is changed. Figure. 2.5 shows

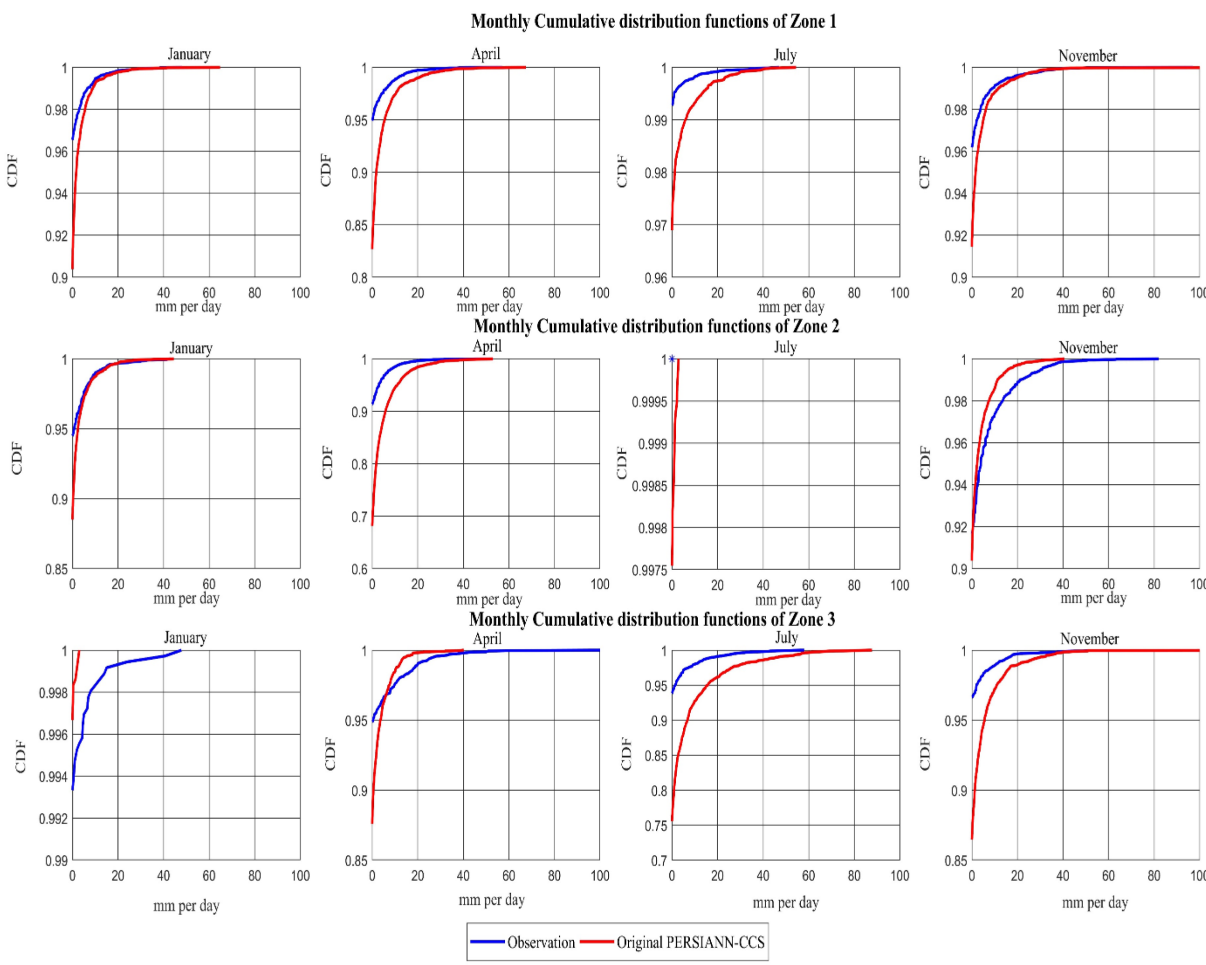

Figure 2.6 January, April, July, and November CDFs for each CZ for each CZ where the zone 1 is the top row, and the second zone is the second row. The third zone is the last row.

the schematic plot of the double mass curve where the consistent rain gauge and the non-consistent rain gauge are displayed.

2.4.2 Localized Quantile Mapping

In order to examine the effectiveness of including the climatic zones (CZ), the implementations of the QM without climatic zones is tested against the including the climatic zones, and it is named as Adjusted PERSIANN-CCS without CZ. The method that are chosen to implement the QM without CZ is proposed by (Yang et al., 2016).

The method is implemented the QM in removing the systematic bias of SPEs using rain gauges through a notable method that is based on QM and Gaussian weighted approach where a study area is divided into a number of several 1° by 1° boxes, and CDFs are calculated for each box. Then, QM is applied for each box, and the results of the mapping are interpolated using the Gaussian approach.

2.4.3 Quantile Mapping and Climate Zone

QM is a distribution-based mapping method, which is sensitive to the sample size used to estimate the CDFs. When the sample is small, the uncertainty of estimation increases. To cover more sample in CDFs, extending the effective sample coverage within a same CZ can be helpful for collecting more samples.

2.4.4 Cumulative Distribution Function of Climate Zones

Non-parametric QM is used to adjust PDF of the daily estimations of Org PERSIANN-CCS to match PDF of daily rain gauge observations for each CZ. It is assumed that CDFs for each month from the rain gauge and PERSIANN-CCS within the same CZ are the same. Therefore, we can calculate the CDFs of the Org-PERSIANN-CCS and gauge observations by collecting co-located the rain gauge observations and Org-PERSIANN-CCS estimations at 0.04° resolution within the same CZ.

The monthly CDFs at each CZ is calculated based on the included gauged pixel of Org-PERSIANN-CCS estimates and the concurrent rain gauge observations, and they are mixed in advance. The method to compute the monthly non-parametric CDFs of rain gauges and Org-PERSIANN-CCS follows (Wilks, 2006) where CDF is like an integral of a histogram with bin width. Meaning, the monthly CDF is calculated by counting the number of days that have precipitation rate less or equal bin width. Notably, the two pairs of CDFs for each zone is calculated. The first CDF is estimated by using the samples from the historical daily rain gauge observations, while the second CDF is determined by the samples of gauged pixels of Org-

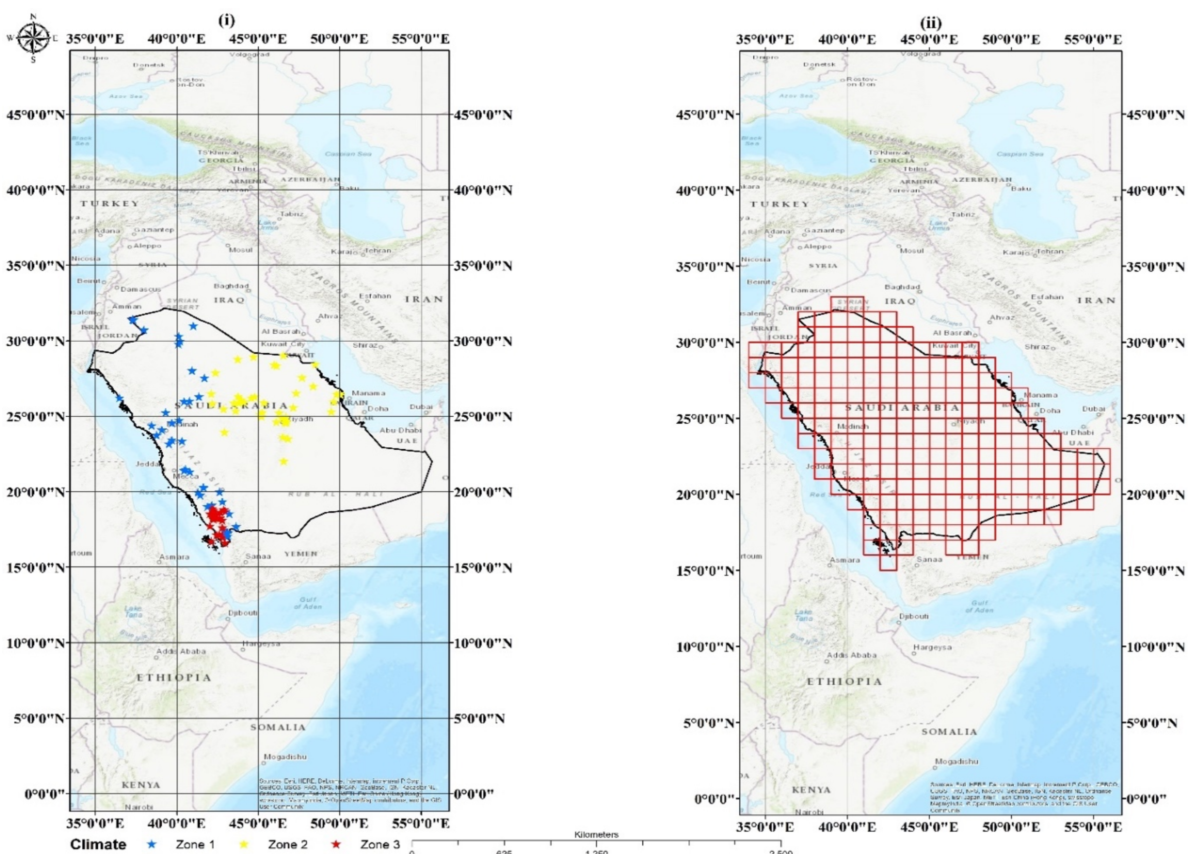

Figure 2.7 1 by 1 boxes with boxes that is highlighted by red boarder are around the country

PERSIANN-CCS. Clearly, for each month, two CDFs are estimated for each CZ as shown by Figure. 2.6.

2.4.5 Bias Adjustment of Satellite Estimation

After the monthly CDFs are calculated for each CZs, the QM is applied. The methodology of QM is explained in the above section. To interpolate the results of QM to fine resolutions which are 0.04° by 0.04° needs to implement an interpolation tool that is based on the concept of inverse weighted distance approach, and it is explained below.

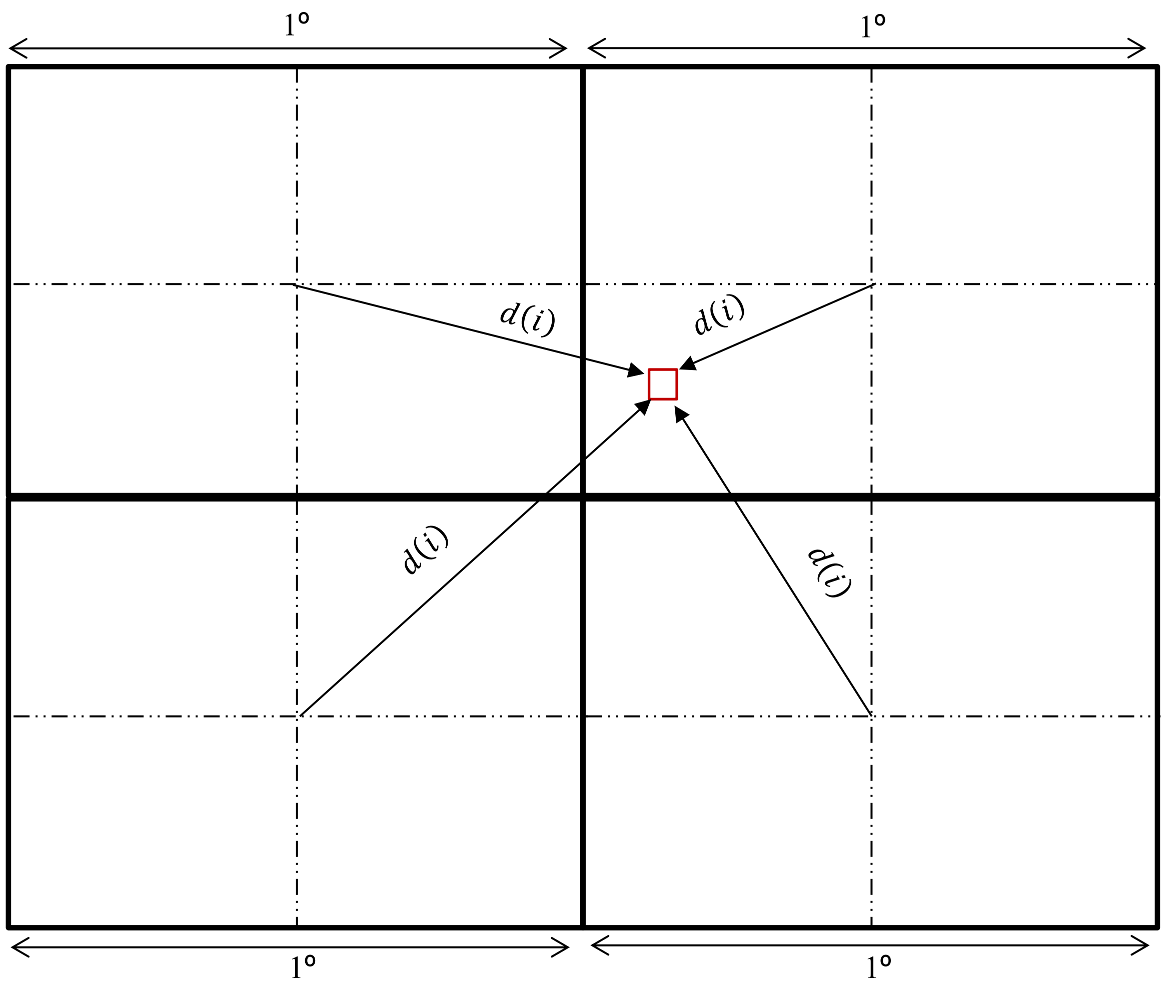

Figure 2.8 Schematic of the interpolation approach where the four boxes are shown and the pixel.

2.4.5.1 Inverse Weighted Distances Approach (IWD)

The approach is done by two steps which are

I. The study area is divided in to number of 1° by 1° boxes. Then the results of QM-CZ are assigned to the box based on CZs as shown by Figure. 2.7.

$$P^{*}(t)_{i} = \sum_{j \to 4}^{j} \omega_{ij} * CDF^{-1}{}_{Gaugue(m)_j} \left(CDF^{-1}{}_{PERSIANN-CCS(m)_j} (P\ (t)_i) \right) \qquad 2.5$$

$$\omega_{ij} = \left(\frac{\frac{1}{d(i)}}{\sum_{j \to 4}^{i} \frac{1}{d(i)}} \right) \qquad 2.6$$

II. The results of QM-CZ are interpolated to fine resolution at 0.04° by 0.04° by using IWD. To interpolate the result of QM-CZ for a pixel, nearest four boxes of 1° by 1 are selected, and the weighted is assigned based on the distance between the pixel and the center of the box. In Equations 2.5 and 2.6.

In Equation 2.5, $P^{*}(t)_i$ is an adjusted PERSIANN-CCS estimation, and it is the bias corrected estimation of the Org PERSIANN-CCS. t is stand for the daily estimations. i is spatial resolution of the PERSIANN-CCS, and it is 0.04° by 0.04°. j is 1° by 1° box. ω_{ij} is weighted that is assigned for pixel (i). $CDF^{-1}{}_{Gaugue(m)_j}$ is monthly CDF of the rain gauges for the box, and m is monthly time scale. $CDF^{-1}{}_{PERSIANN-CCS(m)_j}$ is monthly CDF of the Org PERSIANN-CCS for the same box, and $P(t)_i$ is the daily Org PERSIANN-CCS estimation of the pixel (i).

In Equation 2.6, ω_{ij} is weighted that assigned for the pixel (i) on the box (j). The weighted is estimated base on the inverse distances that is calculated between the center of the four boxes and the pixel as shown on Figure. 2.5 .The calculation of the distance follows Haversian formula (Gellert, Hellwich, Kästner, & Küstner, 2012).

In order to clarify the interpolation approach, a schematic plot is shown in Figure 2.7 where the selected pixel, i, is highlighted by red line border, and four 1° by 1° box are shown by black lines. $d(i)$ is the distance between the pixel, i, the center of the box.

2.4.6 Evaluations

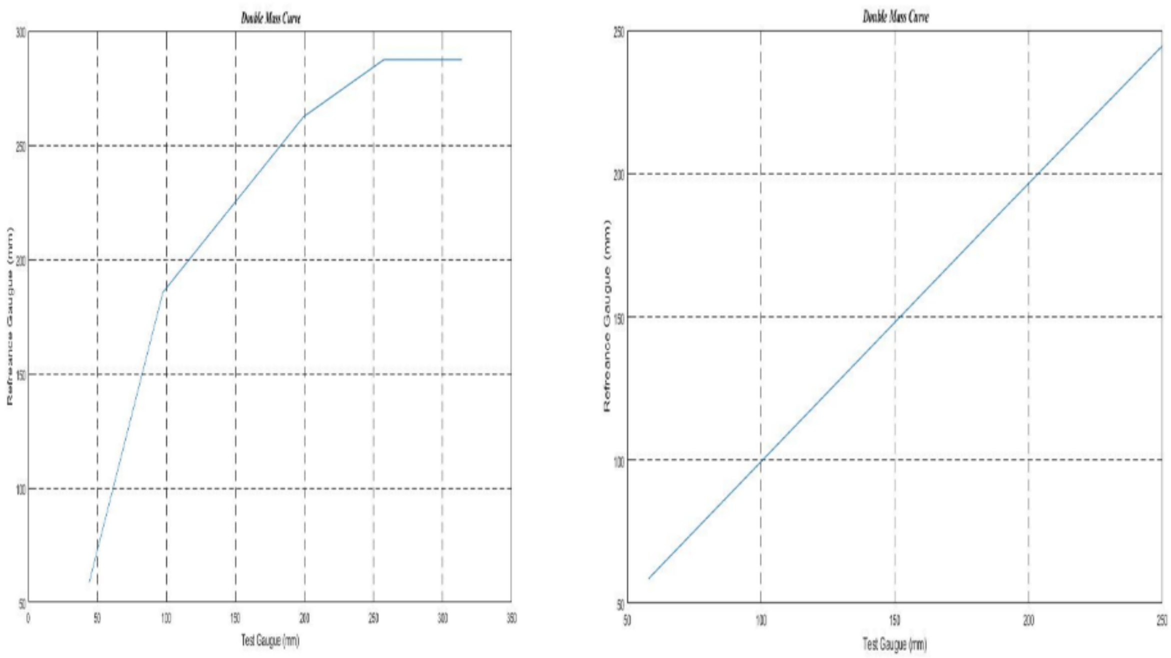

Figure 2.9 An example of the qualified Rain gauge on Right, and the un-qualified gauges on left

The examination of the results of QM-CZ and QM-without CZ during the calibration years and the validation year is done spatially and temporally. Spatial evaluation is studying and interpolating the results of the spatial distribution of the mean annual and monthly precipitation in Saudi Arabia. It is importance to evaluate monthly, and daily precipitation in the country. Correlation Confession (CC), Mean Bias (MB), and Root Mean Square Error (RMSE) are calculated by Equations 2.7 to 2.9 to evaluate the results of the QM with CZ and QM-without CZ spatially and temporally. In Equations (2.7-2.9), G is representations of rain gauges observations,

$$\mathrm{CC} = \frac{\sum_{g=1}^{n}(G_g - \overline{G}) \; * \; \sum_{g=1}^{n}(S_g - \overline{S})}{\sqrt{\sum_{g=1}^{n}(G_g - \overline{G})^2} \; * \; \sqrt{\sum_{g=1}^{n}(S_g - \overline{S})^2}} \qquad 2.7$$

$$\mathrm{MB} \; = \; \frac{\sum_{g=1}^{n}(\; S_g - G_g)}{n} \qquad 2.8$$

$$\mathrm{RMSE} = \sqrt{\frac{\sum_{g=1}^{n}(S_g - G_g)^2}{n}} \qquad 2.9$$

and $\overline{G}$ is mean of rain gauges observations. S is representations of satellite estimations, and $\overline{S}$ is mean of Satellite estimations.

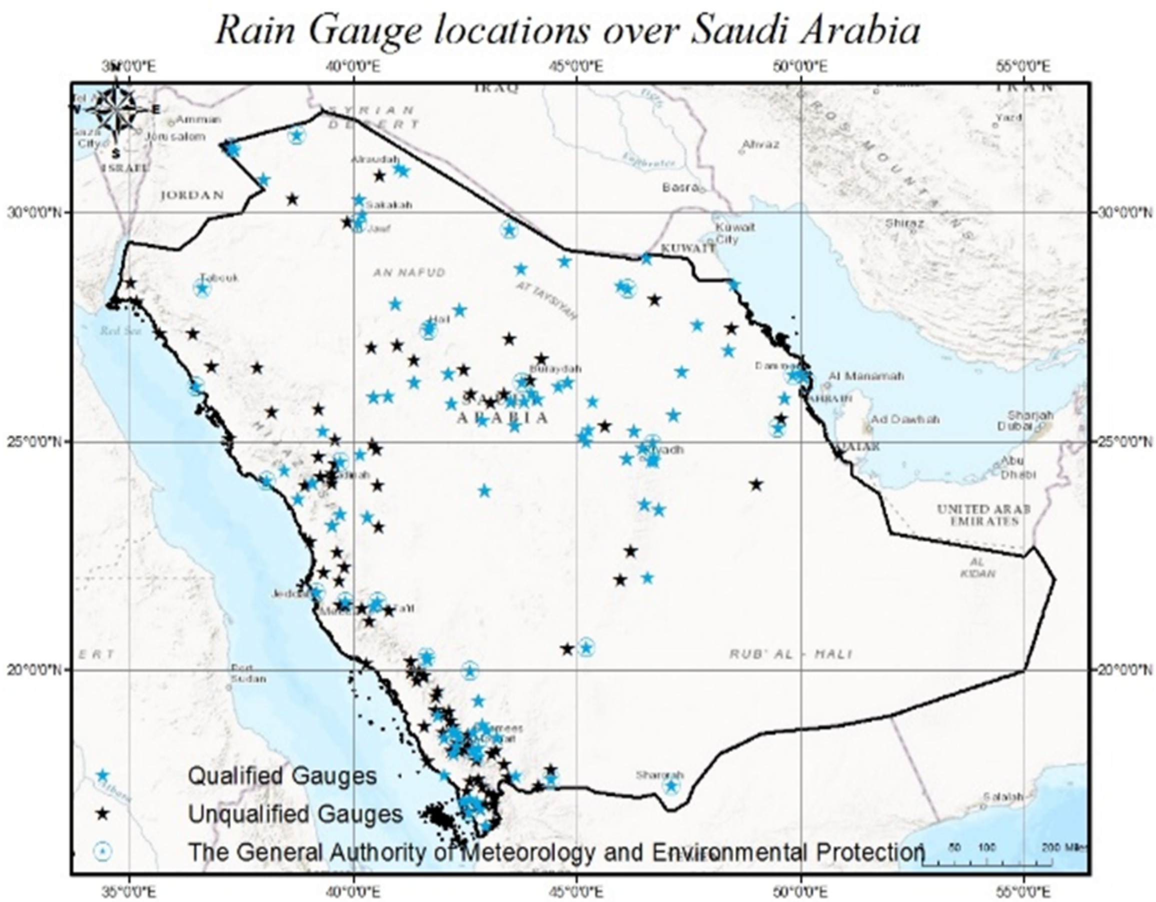

Figure 2.10 Qualified Gauges Representations by Blue Star (qualified gauges), and un-Qualified Gauges Represented by Black Star.

2.5 Results and Discussion

2.5.1 Data Quality

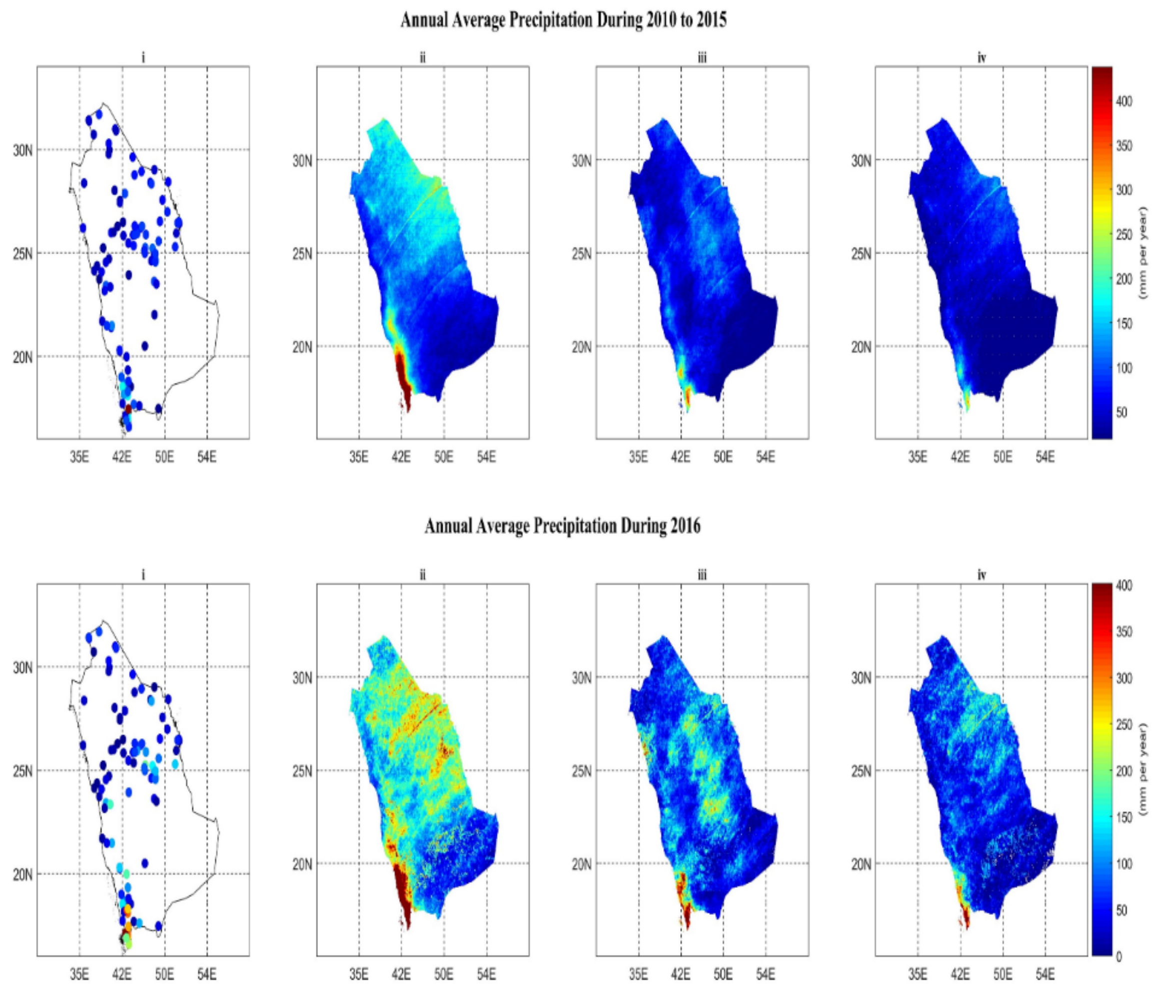

Figure 2.11 Annual Average Precipitation of (i) Rian Gauge, (ii) Original PERSIANN-CCS,(iii) Adjusted PERSIANN-CCS without CZ, (IV) Adjusted PERSIANN-CCS with CZ during Calibration (Top), and Validation (Below)

Because of the implementation of the two criteria selections, 59 % of rain gauges in Saudi Arabia are removed from this study since the gauges are inconsistent, as showing in Figure. 2.10, while 41% of rain gauges are used. 45% of rain gauges have the record for more than five successive years. Also, 41% of the gauges with more than five consecutive years are consistent with the nearest gauges. Also, an example of the consistent and non- consistent gauge is shown in Figure. 2.9.

2.5.2 Spatial Distribution of Precipitation in Saudi Arabia

2.5.2.1 Annual Precipitation

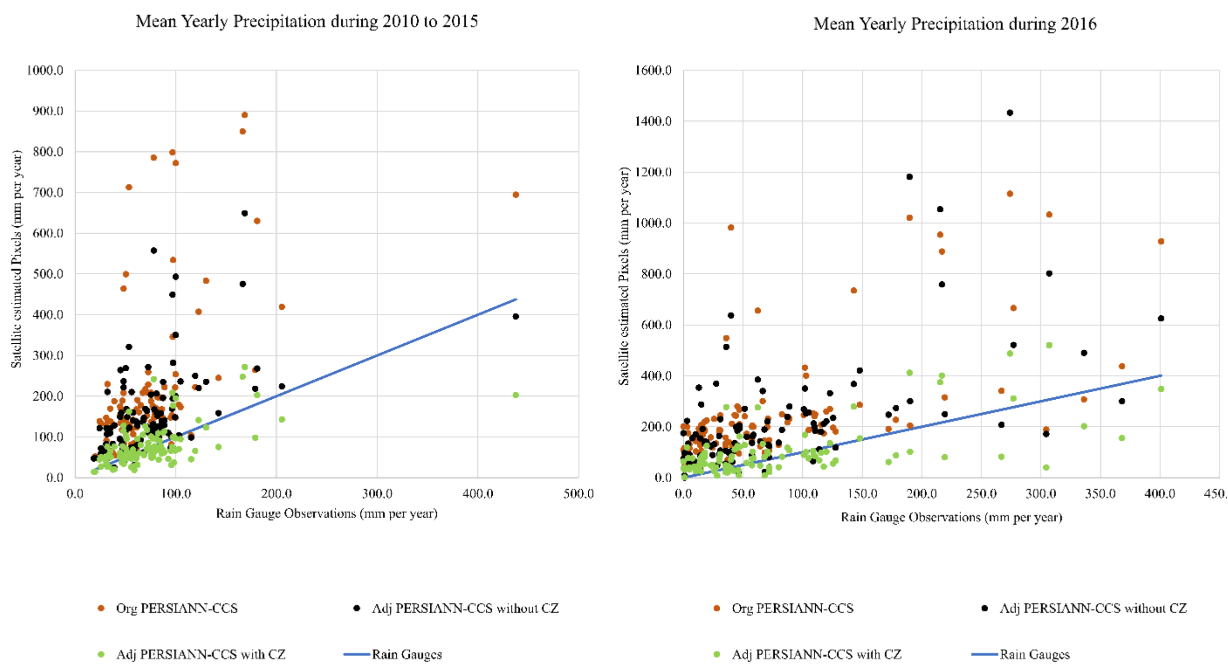

Figure 2.12 Yearly Scatter Plot for Calibration (Left), and Validation (Right)

The results of the annual spatial distribution of precipitation are presented by Figure. 2.11 and 12. The statistical evaluation is presented in Table 2.2 for the calibration years and validation year. Apparently, the Original PERSIANN-CCS overestimates the annual precipitation during the calibration, and the validation as demonstrates by Figure. 2.11, and 2.12 and Table 2.2. As presented in Table 2.2, the original PERSIANN-CCS overestimates the annual precipitation by more than 140 mm per year during the calibration and more than 150 mm per year during the validations. Also, the yearly estimations of Original PERSIANN-CCS have strong correlations with the annual rain gauge observations during the calibration years and validation year, which are calculated to be 0.57 and 0.62, respectively. The annual estimations of the Original PERSIANN-CCS tend to have high yearly RMSE by more than 200 mm per year for both periods, calibration and validation. As shown by Table 2.2, implementing the QM helps to successfully reduce the existence of the systematic bias and overcomes the annual overestimations. In the case of not including the CZs, 99 % of the bias is removed during the calibration, while 96% of the bias is removed during the validation year. Also, not including the CZs help to reduce the annual RMSE by 43.85 mm per year, calibration, and 78 mm per year, validation. However, not including the CZs reduces the annual overestimations by 1.1 mm per year during the calibration years and underestimates the yearly precipitation by 5.56 mm per year in 2016. Implementing QM without CZs reduces the correlation between the annual estimated precipitation by Adjusted PERSIANN-CCS and the annual rain gauges observations in the calibration and the validation periods. In the second case where the CZs are included. We can see that the correlation between the estimated annual precipitation and the rain gauges are improved by more than 17% during the calibration and validation. Including the CZs achieves more reductions in the existence of the bias by 99.98% during the calibration and 99.1% during the validation year. In details, the including CZs makes the annual estimations are reduced by 0.04 mm per year, and 1.54 mm per year in calibration and validation, respectively.

Table 2.2 Statistics Evaluations for Annual Precipitaion

Time	Original PERSIANN-CCS			Adjusted PERSIANN-CCS without CZ			Adjusted PERSIANN-CCS with CZ		
	CC	MB $\frac{mm}{year}$	RMSE $\frac{mm}{year}$	CC	MB $\frac{mm}{year}$	RMSE $\frac{mm}{year}$	CC	MB $\frac{mm}{year}$	RMSE $\frac{mm}{year}$
Year (Calibration)	0.57	140.9	212.9	0.57	1.10	45.53	0.58	-0.04	43.85
Year (Validation)	0.62	155.4	228.0	0.58	-5.65	81.35	0.62	-1.54	77.67

As shown in Figure. 2.11, the Original PERSIANN-CCS overestimates the annual mean precipitation over Saudi Arabia, but the most overestimations are localized in the southwest and the center of the country. The same pattern is shown in the calibration years and the validations year. During the validation year, the Original PERSIANN-CCS estimates most of the total precipitation by around 200 to 350 mm. After the QM is implemented in two cases. First, without including CZ, the highest precipitation is localized to be the low part of the southwest of the country during the calibration and the validation. However, the not including the CZs misleads the pattern of the annual precipitation where the center of the country shows to have the second highest precipitation rate, while it should not have a precipitation rate around 100 to 225 mm per year when it is compared to the annual rain gauges observations. Also, the not including the CZs does not keep the stable spatial variation of the annual precipitation, and it is evident during the validation year. In the center and southeast receive precipitation where both places do not have much precipitation comparing to the rain gauge observations. In the second case where the CZs including, the Adjusted PERSIANN-CCS matches the rain gauge observations during the calibration and the validation periods. The highest precipitation rate is more located to the southwest of the country where most of the precipitation occurs, and the estimated precipitations match the observations in the center of the country

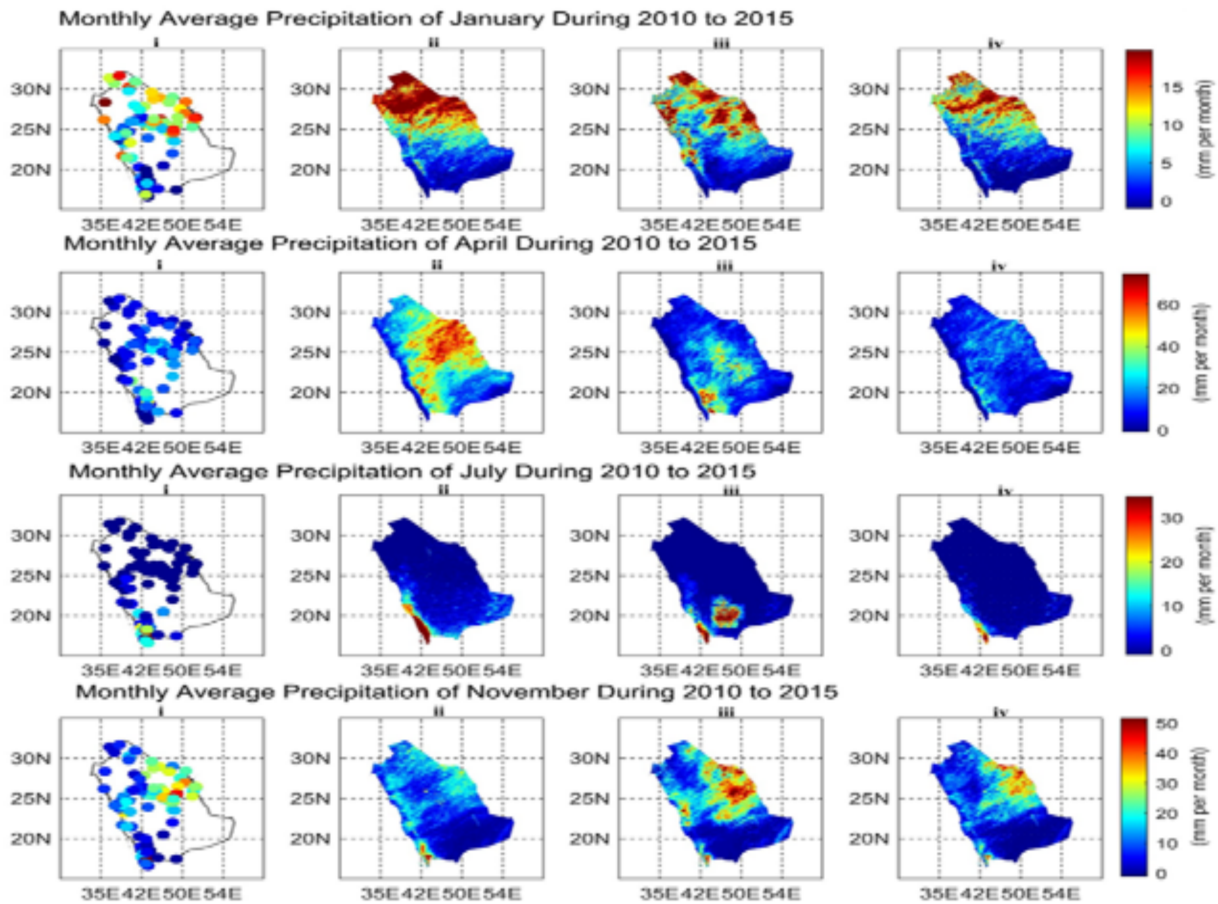

Figure 2.13 Monthly Average Precipitation of (i) Rian Gauge, (ii) Original PERSIANN-CCS,(iii) Adjusted PERSIANN-CCS without CZ, (IV) Adjusted PERSIANN-CCS with CZ during Calibration

When the comparison is made between the annual rain gauge observations and the gauged pixel estimations, the Original PERSIANN-CCS, orange dot, overestimates in the calibration and the validation as shown in Figure. 2.12. Clearly, the performance of QM in removing the bias is different in both cases. First, the Adjusted PERSIANN-CCS without CZ, black dot, still shows the overestimations, while the Adjusted PERSIANN-CCS with CZ, green dot, is different.

2.5.2.2 Monthly Precipitation

The monthly precipitation spatial distributions are shown in Figures. 2.13, 2.14, 2.15 and 2.16 and Tables 2.3 and 2.4. The months that are displayed are January, April, July, and November. Clearly, the same pattern that is shown in the annual pattern is indicated in monthly. According to Table 2.3, the Original PERSIANN-CCS overestimates mean monthly precipitation rates by different values. The highest mean monthly overestimations occur during April by more than 20 mm per month, while the lowest mean monthly overestimation is 2.32 mm per month during November. When the mean monthly estimations of the Original PERSIANN-CCS are evaluated with the observed mean monthly, the Original PERSIANN-CCS has a strong correlation in estimates of mean monthly precipitation over Saudi Arabia especially for January and July where most of the precipitation to occur. However, the Original PERSIANN-CCS does not follow the observed mean monthly during November. When the RMSE is used to evaluate the performance of the Original PERSIANN-CCS, the performance of the Original PERSIANN-CCS during January has the lowest RMSE. When the systematic bias is removed by applying QM with two cases, the performance of the bias-corrected PERSIANN-CCSs shows two different performances during the calibration years. First, the correlation between the Adjusted PERSIANN-CCS without CZs has the same correlation as the Original PERSIANN-CCS where the strong correlations are found for January and July. In the other hand, the mean monthly precipitations that are estimated by the Adjusted PERSIANN-CCS with CZs during July, and April have the highest corrections. In term of MB, the implementing the QM helps to reduce the overestimations in the mean monthly estimations, but the implementing CZs successfully removed the bias on estimating the mean monthly more than 94% for all months. During the validation, the similar results are shows for the

CC, MB, and RMSE where the Adjusted PERSIANN-CCS with CZs removes the most of the bias as shown in Table 2.4 and Figure 2.17.

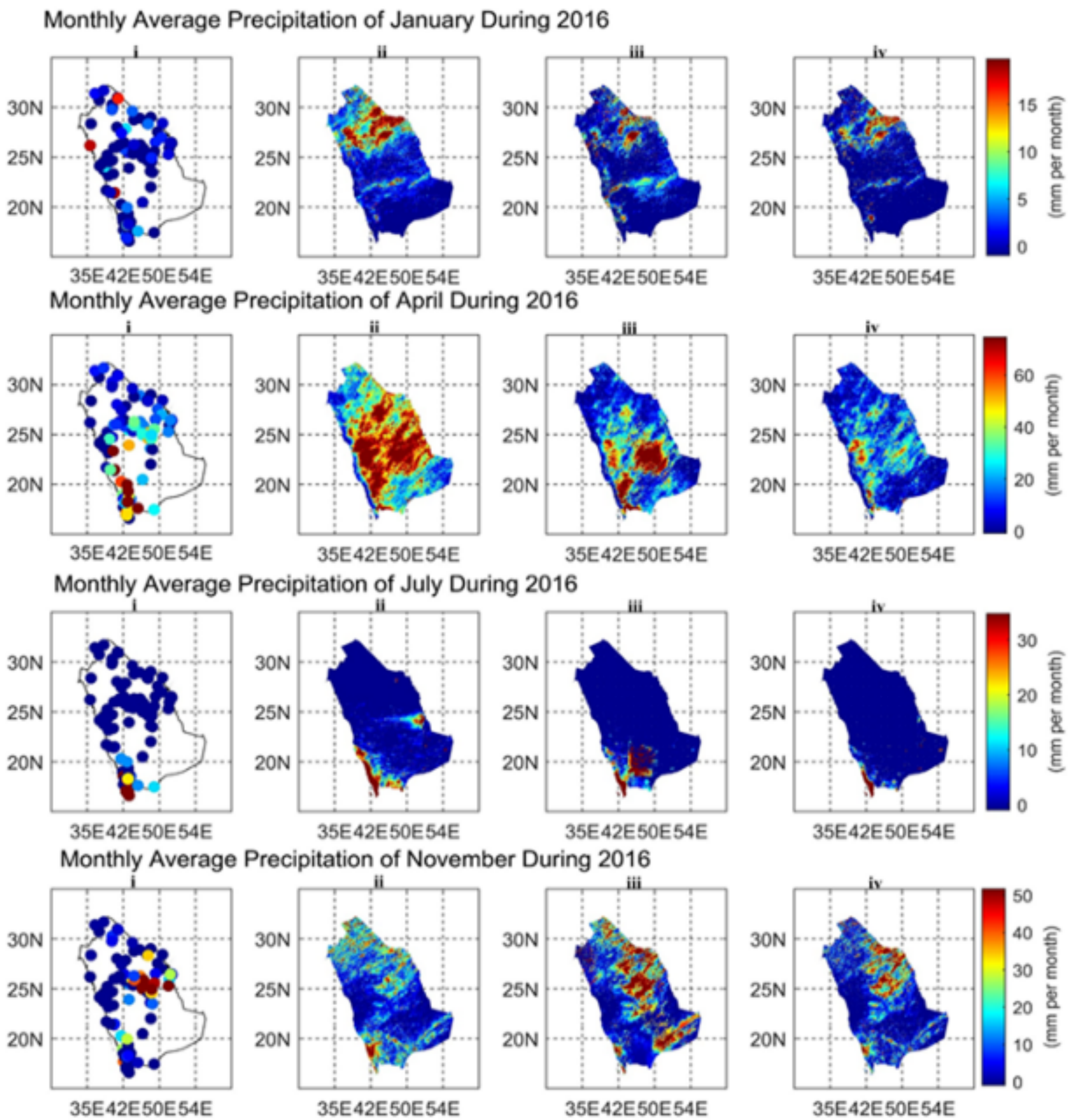

Figure 2.14 Monthly Average Precipitation of (i) Rian Gauge, (ii) Original PERSIANN-CCS,(iii) Adjusted PERSIANN-CCS without CZ, (IV) Adjusted PERSIANN-CCS with CZ during Validation

Table 2.3 Statistics Evaluations for Monthly Analysis during Calibrated Years

Time	Original PERSIANN-CCS			Adjusted PERSIANN-CCS without CZ			Adjusted PERSIANN-CCS with CZ		
	CC	MB $\frac{mm}{month}$	RMSE $\frac{mm}{month}$	CC	MB $\frac{mm}{month}$	RMSE $\frac{mm}{month}$	CC	MB $\frac{mm}{month}$	RMSE $\frac{mm}{month}$
January	0.62	2.51	7.32	0.57	-5.09	6.87	0.58	0.13	5.72
April	0.34	21.08	28.49	0.28	1.26	14.05	0.72	-0.03	9.13
July	0.73	12.59	32.20	0.72	0.33	6.85	0.73	0.22	6.36
November	0.09	2.32	13.31	0.08	1.37	13.87	0.58	0.04	8.93

When the mean monthly precipitation distributions are shown in Figures. 2.13 and 2.14 during the calibration and the validation. Estimated monthly mean precipitations of all months by the Original PERSIANN-CCS shows the overestimations comparing to the rain gauge observations. For example, the highest mean monthly that is observed during January is the north side of the country, and the Original PERSIANN-CCS captures the same spatial pattern, while the value of the mean was more significant than the observed. The same performance is captured for April where most of the precipitation occurs in the center and southwest of the country. On the other hand, the Adjusted PERSIANN-CCS with CZs removes the systematic bias from mean monthly estimations and matches the rain gauges observations in both periods, calibration and validation. Clearly, the Adjusted PERSIANN-CCS with CZs keeps the spatial variability of the precipitations over the country that matches the rain gauges observations. In details, the rain gauges observations during April shows that most of the country, not the center has to mean monthly precipitation less than 20 mm per month that matches the estimations from the Adjusted PERSIANN-CCS with CZs. Also, the country does not revive precipitations during the summer especially in July expect the southwest of the country that is captured by the Original PERSIANN-

CCS and the Adjusted PERSIANN-CCS with CZs. However, not including the CZs leads to miss spatial distribution of mean monthly precipitation. During July, the Adjusted PERSIANN-CCS without CZs shows the highest mean monthly precipitation rate in the Empty Quarter where no precipitation rate falls on that location mainly in summer month. The same performance of miss-locations of the precipitations are found during April, July, and November in the validation year as seen by Figure. 2.14.

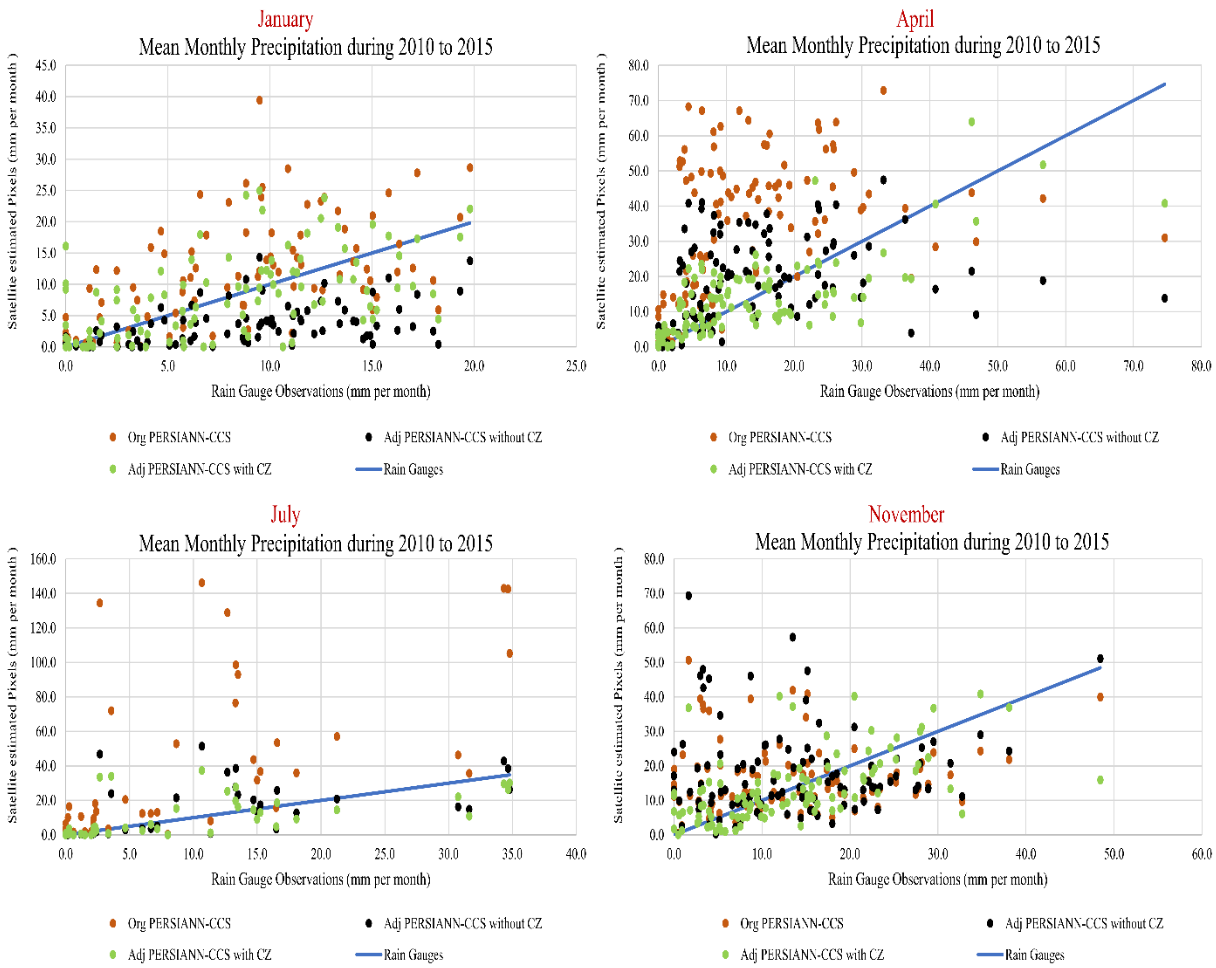

Figure 2.15 Monthly Scatter Plot for Calibration Years.

Table 2.4 Statistics Evaluations for Monthly Analysis during Validation Year

Time	Original PERSIANN-CCS			Adjusted PERSIANN-CCS without CZ			Adjusted PERSIANN-CCS with CZ		
	CC	MB $\frac{mm}{month}$	RMSE $\frac{mm}{month}$	CC	MB $\frac{mm}{month}$	RMSE $\frac{mm}{month}$	CC	MB $\frac{mm}{month}$	RMSE $\frac{mm}{month}$
January	0.066	2.921	9.863	0.053	-0.851	5.704	0.113	1.428	9.648
April	0.450	17.645	44.494	0.421	-8.672	41.835	0.688	-7.462	33.562
July	0.826	24.748	78.966	0.820	5.257	32.335	0.824	2.663	26.239
November	-0.123	11.963	30.030	-0.143	12.845	35.754	0.165	9.053	24.760

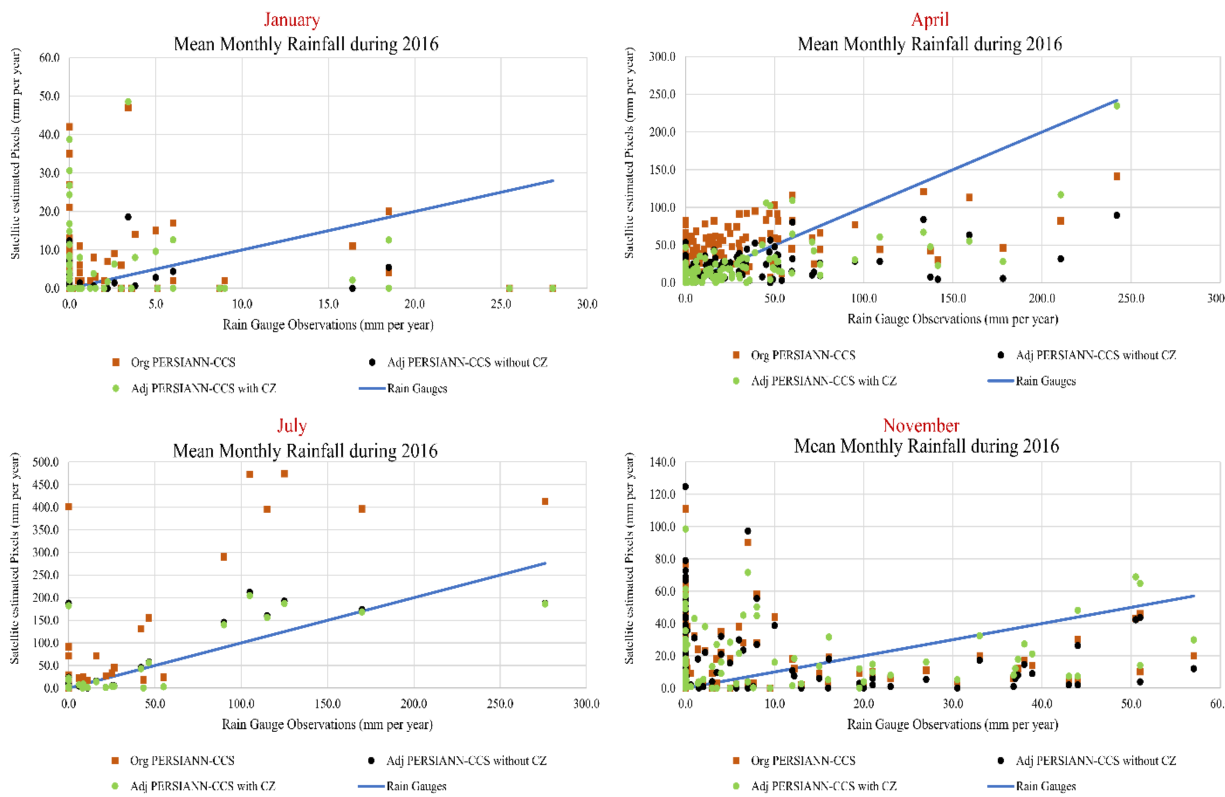

Figure 2.16 Monthly Scatter Plot for Validation Year

2.5.3 Time Series of Precipitations over Saudi Arabia

2.5.3.1 Monthly Time Series

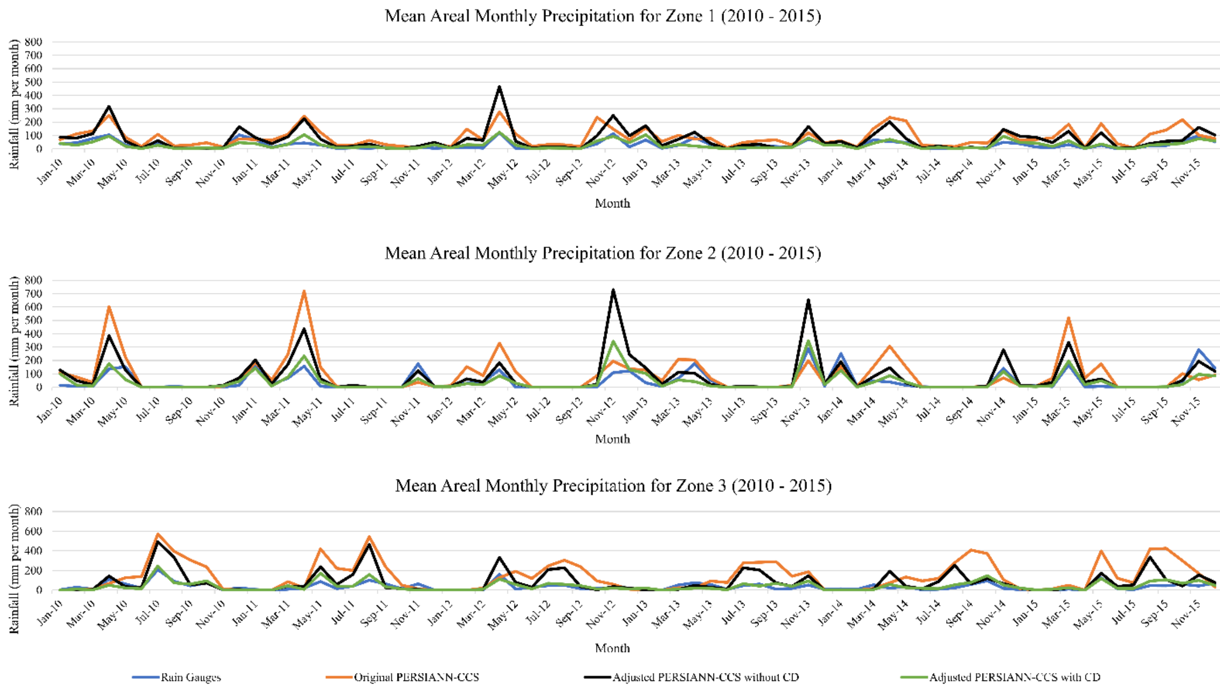

Figure 2.17 Mean Monthly Areal Precipitation for three zones during Calibration

The monthly time series in Saudi Arabia are shown in Figures. 2.17, and 2.18 and Tables 2.5 and 2.6. Figures. Figure. 2.17 and Figure. 2.18 show mean areal monthly for three climatic zones during the calibration and the validation. In the two figures, the first row is zone 1 where the annual precipitation rate is around 130 mm per year, and the second row represents the second climate zone where the annual precipitation rate is above 300 mm per year. The last row is third climate zone, and the annual precipitation is less than 67 mm per year. In the calibration years, the Original PERSIANN-CCS overestimates the mean areal monthly for each CZ by 54.57 mm per month, 45.85 mm per month, and 103.76 mm per month for zone 1, zone 2 and zone 3, respectively. Also, the Original PERSIANN-CCS has moderate to strong correlations with the observed mean areal monthly precipitation where it ranges between 0.56 to 0.65. Finally, the zone

3 has the highest monthly RMSE with 164.20 mm per month, and the second highest RMSE is zone 2 with around 120 mm per month.

Table 2.5 Statistical Evaluation of Monthly Time Series during Calibration

Zones	**Original PERSIANN-CCS**			**Adjusted PERSIANN-CCS without CZ**			**Adjusted PERSIANN-CCS with CZ**		
	CC	MB $\frac{mm}{month}$	RMSE $\frac{mm}{month}$	CC	MB $\frac{mm}{month}$	RMSE $\frac{mm}{month}$	CC	MB $\frac{mm}{month}$	RMSE $\frac{mm}{month}$
Zone 1	0.65	54.57	76.32	0.74	39.53	69.71	0.79	-0.02	19.61
Zone 2	0.56	45.85	122.93	0.74	37.08	106.27	0.75	-0.66	50.78
Zone 3	0.63	103.76	164.20	0.72	44.94	97.66	0.78	4.69	30.10

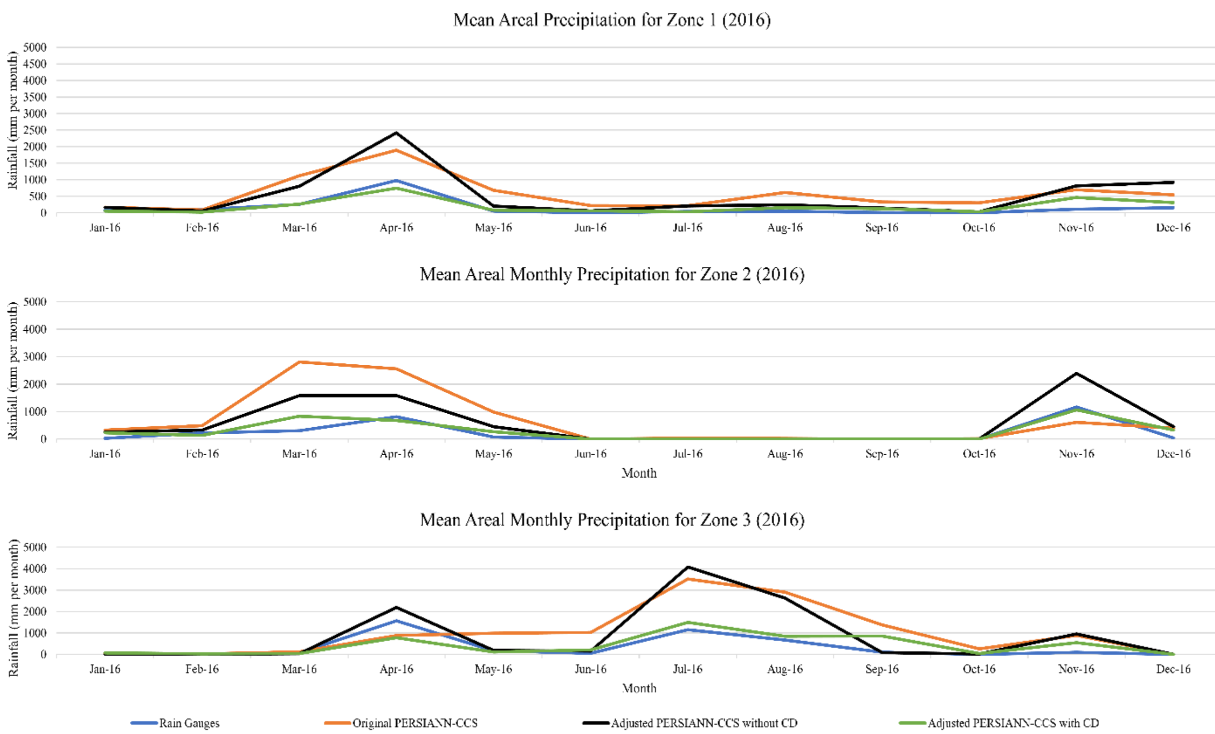

Figure 2.18 Mean Areal Precipitation for three zones during Validation

As expected, when the QM was applied in the two cases, most of the systematic bias was removed. In the first case where the QM is applied without including CZ, the monthly correlation coefficients are enhanced for each climate zone by 14%, 24%, and 14.29%. In term of mean bias, the overestimations are reduced to be less than 44 mm per month for each climate zone, and the significant reduction is for zone 3 where it is calculated to be 57%. On the other hand, incorporation of the CZ with the QM improves all the statistical evaluations. First, the strong correlations are found with the value above 0.75 for all zones, and the improvements are calculated to be 21%, 34%, and 23.8 for zone 1, zone 2, and zone 3, respectively. Second, more than 97% of the bias is removed for all zones, but the Adjusted PERSIANN-CCS with CZ underestimates the mean areal monthly precipitation by marginal values, which are 0.02,0.66, and 4.69 mm per month for zone 1, zone 2, and zone 3, respectively.

As expected for the validation year, the Original PERSIANN-CCS still overestimates the mean areal monthly depth by more than 400 mm, and the same result is founded during the calibration. In term of the correlations between the observed depth and the estimated one, the Original PERSIANN-CCS for zone 1 has the strongest correlation with the value of around 0.89. When the correlation approach, that includes the CZ is applied, the same findings are found. First, the correlations for each zone is improved to be more than 0.75, and the overestimations are reduced to be less than 90 mm during 2016. The highest RMSE is calculated to be 362 mm, which is zone 3.

Table 2.6 Statistical Evaluation of Monthly Time Series during Validation

Zones	Original PERSIANN-CCS			Adjusted PERSIANN-CCS without CZ			Adjusted PERSIANN-CCS with CZ		
	CC	MB $\frac{mm}{month}$	RMSE $\frac{mm}{month}$	CC	MB $\frac{mm}{month}$	RMSE $\frac{mm}{month}$	CC	MB $\frac{mm}{month}$	RMSE $\frac{mm}{month}$
Zone 1	0.89	419.58	505.88	0.85	352.01	545.15	0.85	41.57	141.14
Zone 2	0.50	466.79	946.28	0.83	366.62	585.07	0.87	75.42	200.16
Zone 3	0.59	674.19	1119.57	0.75	533.80	1062.54	0.74	90.35	362.72

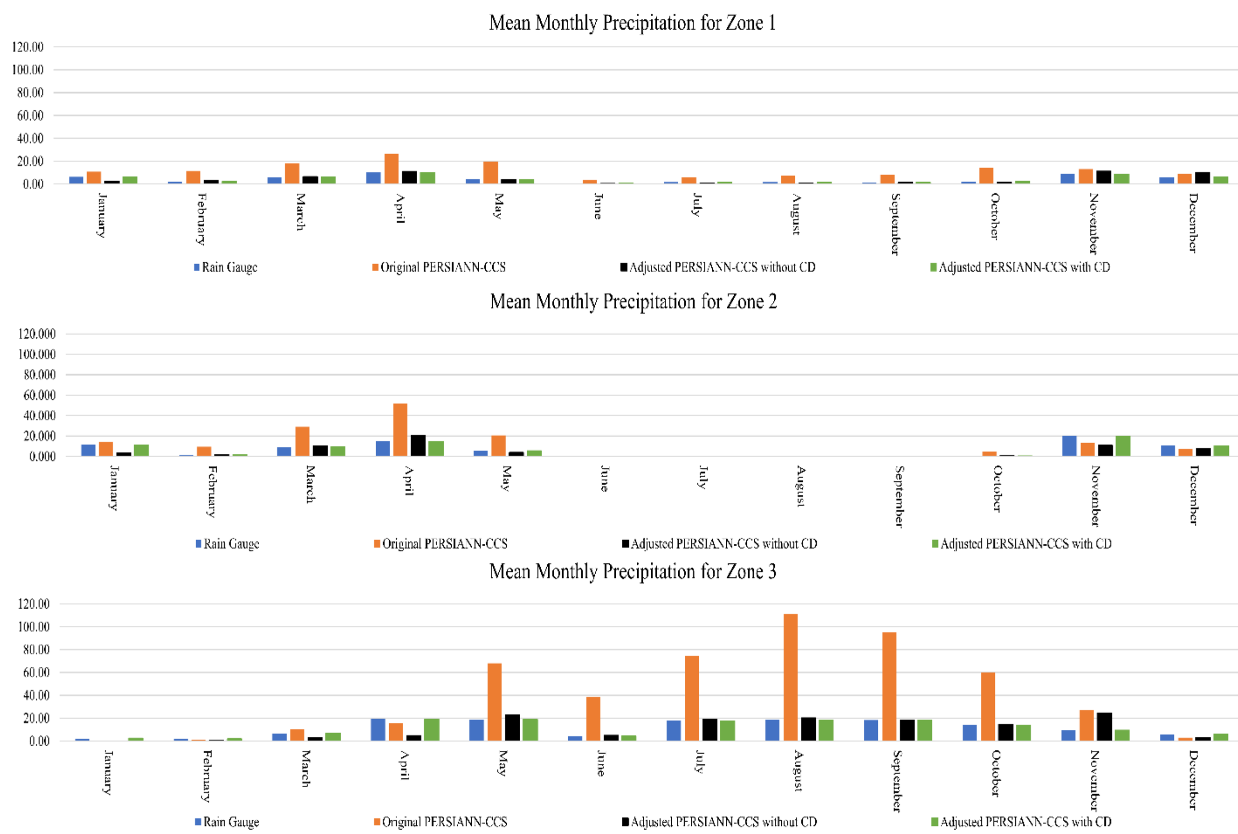

Figure 2.19 Average Monthly Precipitation during Calibration

2.5.3.2 Average Monthly Precipitation

The average monthly precipitations are displayed in Figure. 2.19 and Figure. 2.20, and the statistical results are shown in Table 2.7 and Table 2.8.

According to Figure. 2.19, highest rainy months for zone 1 and zone 3 are April and November with average monthly precipitation that around 15 mm per month. On the other hand, the wet months for zone 2 are April, July, and August with the average monthly precipitations that are around 20 mm per month. As presented in the Figure, the Original PRESIANN-CCS overestimates the average monthly precipitation for all zones. For example, the highest average monthly precipitation for Zone 1 that is estimated by the Original PERSIANN-CCS is April with the rate around 50 mm per month. Also, a similar result is found for zone 3 where the highest rate is more than 25 mm per month. Finally, the highest average monthly is founded to be August with more rate more than 100 mm per month. As expected of applying the QM and incorporating the climate zone, the average monthly precipitation that is estimated by the Adjusted PRESIANN-CCS matches the observed average for all zones. As shown in Table 2.7, the strongest correlations are founded between the observed and estimated averages after the correction is applied.

Table 2.7 Statistical Evaluation of Average Monthly Precipitation during Calibration

Zones	Original PERSIANN-CCS			Adjusted PERSIANN-CCS without CZ			Adjusted PERSIANN-CCS with CZ		
	CC	MB $\frac{mm}{month}$	RMSE $\frac{mm}{month}$	CC	MB $\frac{mm}{month}$	RMSE $\frac{mm}{month}$	CC	MB $\frac{mm}{month}$	RMSE $\frac{mm}{month}$
Zone 1	0.703	0.896	1.000	8.119	0.149	-0.051	9.366	1.867	0.062
Zone 2	0.637	0.817	1.000	6.425	-1.265	-0.054	13.332	4.067	0.072
Zone 3	0.764	0.708	1.000	30.61	-0.174	-0.128	44.44	6.371	0.269

Table 2.8 Statistical Evaluation of Average Monthly Precipitation during Validation

Zones	Original PERSIANN-CCS			Adjusted PERSIANN-CCS without CZ			Adjusted PERSIANN-CCS with CZ		
	CC	MB $\frac{mm}{month}$	RMSE $\frac{mm}{month}$	CC	MB $\frac{mm}{month}$	RMSE $\frac{mm}{month}$	CC	MB $\frac{mm}{month}$	RMSE $\frac{mm}{month}$
Zone 1	0.827	0.711	0.770	8.556	0.174	-0.436	11.361	4.795	4.007
Zone 2	0.55	0.742	0.831	10.22	0.468	1.247	21.337	5.339	4.415
Zone 3	0.62	0.526	0.871	27.86	-3.810	-2.457	49.57	22.982	12.466

As predicted, incorporating the climatic zone helps to enhance reduce the gap between the observed average and the estimated average precipitation as shown in Table 2.8 and Figure. 2.20. For example, the correlations are founded to be more than 0.77 during the validated year. Also, when the comparison between the observed average precipitation for all zones and the estimated

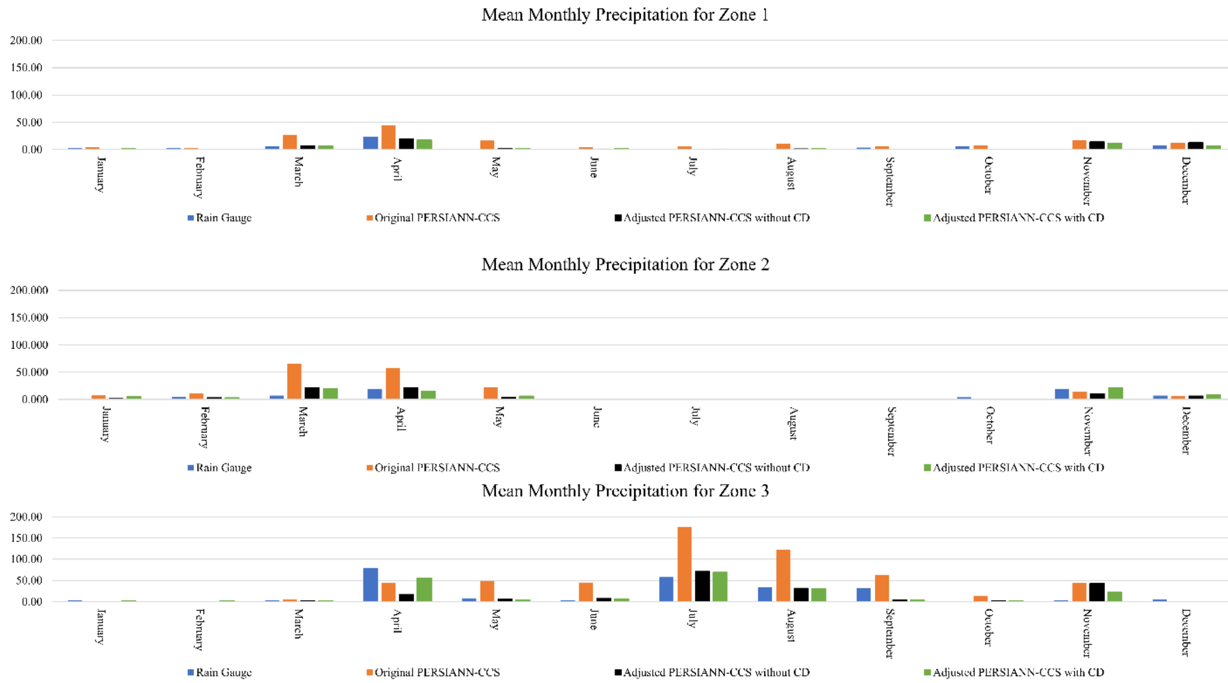

Figure 2.20 Average Monthly Precipitation during Validation

average precipitations for all zones, the great reduction in the systematic bias. On other hand, not including the climatic zone has maximum correlations 0.74 with underestimations of the average monthly precipitation that are around 2.45 mm per month.

2.5.4 Daily Time Series

2.5.4.1 Cumulative Daily Precipitation

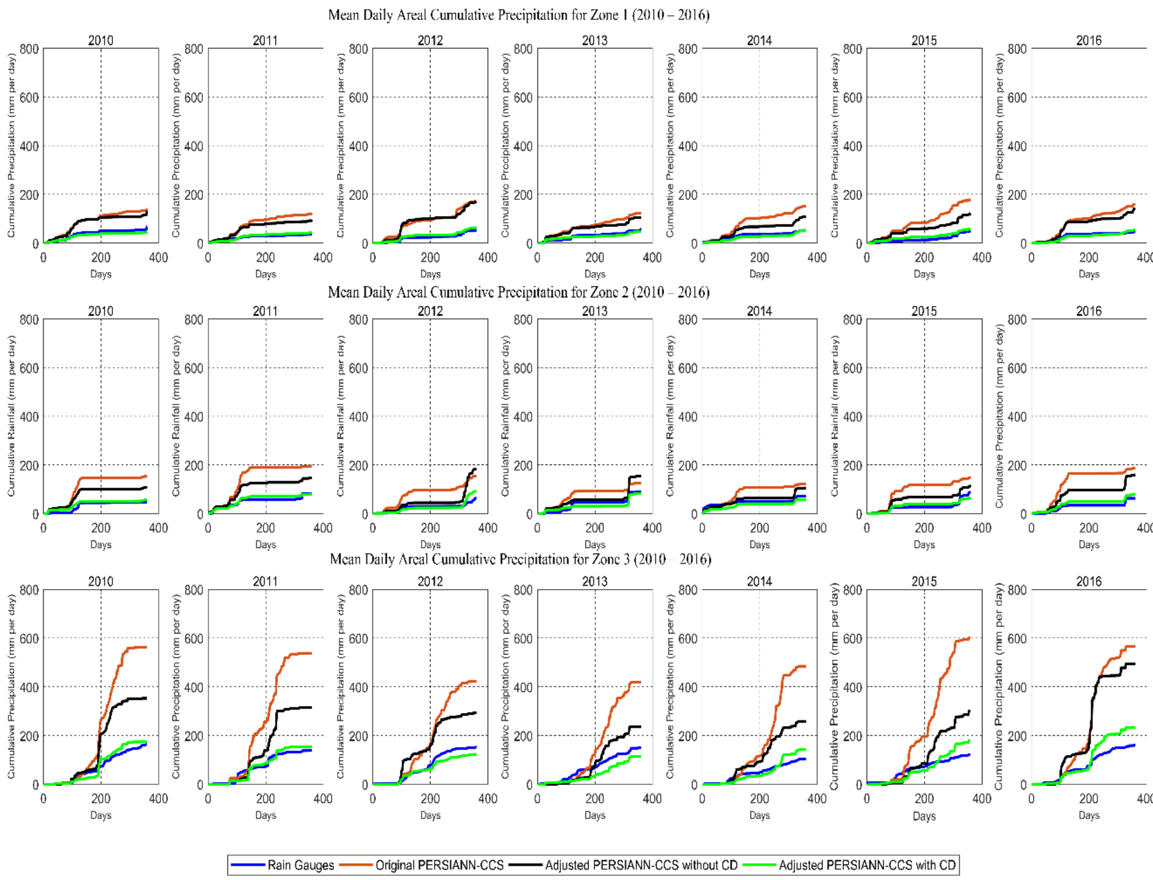

Figure 2.21 Mean Daily Cumulative Precipitation for all zones

The results of the cumulative areal daily precipitation for each year is presented by Figure. 2.21, and the average of the statistical results are show in Table 2.9 where the average of the daily correlation confession, daily mean bias, and daily RMSE are in the Table

Table 2.9 Statistical Evaluation of Mean Daily Cumulative Precipitation

Zones	Original PERSIANN-CCS			Adjusted PERSIANN-CCS without CZ			Adjusted PERSIANN-CCS with CZ		
	CC	MB $\frac{mm}{day}$	RMSE $\frac{mm}{day}$	CC	MB $\frac{mm}{day}$	RMSE $\frac{mm}{day}$	CC	MB $\frac{mm}{day}$	RMSE $\frac{mm}{day}$
Zone 1	0.98	54.56	62.92	0.98	39.95	45.44	0.98	1.24	8.07
Zone 2	0.92	65.79	74.57	0.95	32.08	39.21	0.94	6.92	11.29
Zone 3	0.97	141.69	205.97	0.97	74.63	108.86	0.98	7.15	23.45

According to Figure. 2.21, the Original PERSIANN-CCS overestimates the daily precipitations on all zones. Clearly, the orange line that represents the estimations of the Original PERSIANN-CCS overestimates when the line is compared to rain gauge observations (Blue Line). Table 2.9 shows the mean bias and RMSE of zone 3, which has the highest values compared to the other zones. As not expected, the Adjusted PERSIANN-CCS without CZ overestimates the cumulative daily precipitations for all zones, and it is near the Original PERISNANN-CCS estimations. As shown in Table 2.9, the mean bias and RMSE are reduced by implementing the QM without CZ, but the overestimation is not successfully removed. For example, the daily overestimations of zone 3 are reduced by 47%. On the other hand, the incorporation of the climatic zone into the QM achieves more reduction in the overestimations and helps to matches between the observations and the estimations. Instance, the Adjusted PERSIANN-CCS with CZ overestimates the cumulative daily precipitation for zone 1 by 1.24 mm per day that is 2% of mean bias of Original PERSIANN-CCS. Also, the Adjusted PERSIANN-CCS with CZ overestimates the zone 3 by 7.15 mm per day that equals to 5% of the Original PERSIANN-CCS mean bias. Finally, the Adjusted PERSIANN-CCS with CZ, which is showed by the green line, follows the rain gauge observations (blue line) closely. When the line of the Adjusted PERSIANN-CCS is compared to the other lines, which are the orange line (Original PERSIANN-CCS) and black line (Adjusted PERSIANN-CCS without CZ), the Adjusted PERSIANN-CCS has the lowest gaps.

2.5.4.2 Mean Areal Daily time series

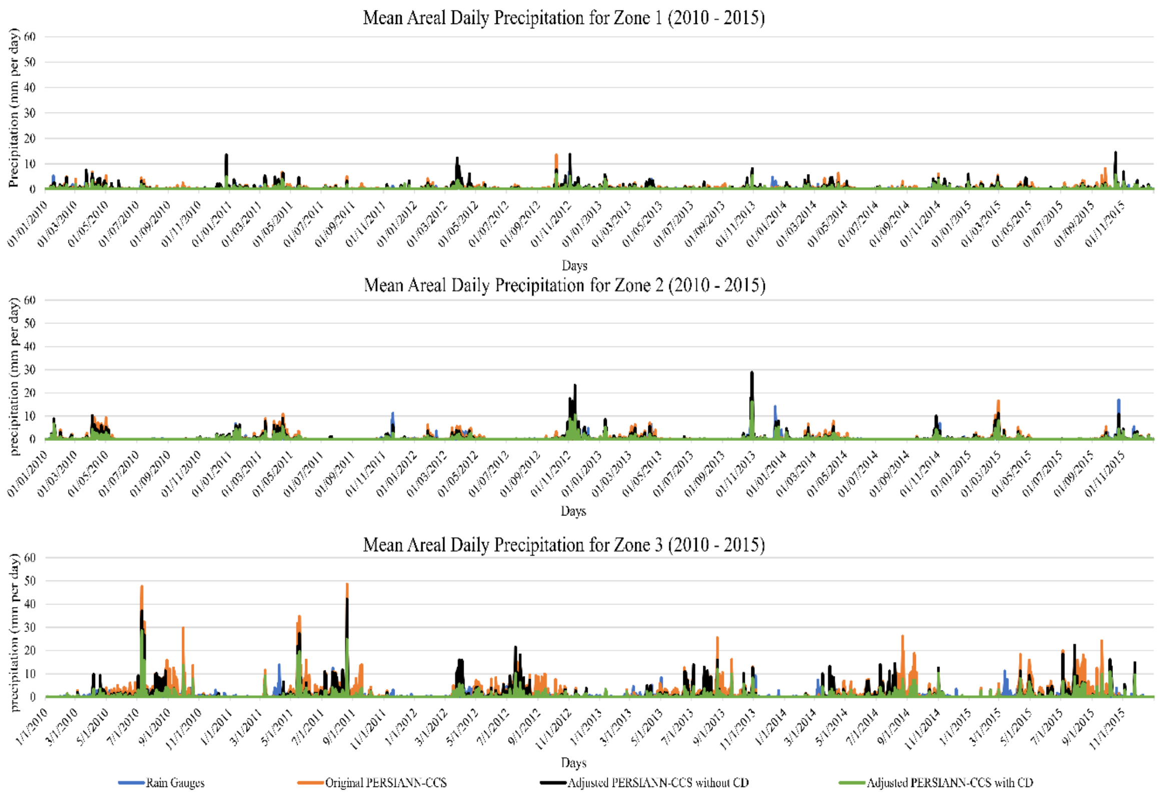

Figure 2.22 Mean Areal Daily Precipitation during Calibration

On order to evaluate the performance of the QM with and without climatic zones in daily scales, correlation coefficient, mean bias, and RMSE are calculated for each zone with values that are displayed in Table 2.10, and Table 2.11. The time series distributions are shown in Figure.2 22 and Figure. 2.23.

As expected, the original PERSIANN-CCS overestimates the daily precipitation by 0.26, 0.21, and 0.15 mm per day during the calibration for zones 1, 2, and 3, respectively. During the validation, the original PERSIANN-CCS overestimates the daily precipitation by 0.34, 0.36, and

1.23 mm per day for zone 1, 2, and 3, respectively. As shown by Table 2.10 and Table 2.11, the daily RMSEs are 0.9, 1.28, and 3.68 mm per day for zones 1, 2, and 3 respectively. During the validated year, the daily RMSEs are 0.85, 1.46, and 4.26 mm per day for zones 1, 2, and 3 respectively.

According to Table 2.10 and Table 2.11, the daily estimations of the adjusted PERSIANN-CCS without CZ are reduced to be 0.19, 0.17, and 0.42 mm per day for zones during the calibration years. Moreover, the adjusted PERSIANN-CCS without CZ still overestimates the daily precipitation in zones 1, 2, and 3 by 0.28, 0.28, and 1.01 mm per day. However, the daily correlation confessions are improved during both calibration years and the validation year for all zones as shown in Table 2.10 and Table 2.11.

Table 2.10 Statistical Evaluation of Daily Time Series during the calibration

Zone	Original PERSIANN-CCS			Adjusted PERSIANN-CCS without CZ			Adjusted PERSIANN-CCS with CZ		
	CC	MB $\frac{\text{mm}}{\text{day}}$	RMSE $\frac{\text{mm}}{\text{day}}$	CC	MB $\frac{\text{mm}}{\text{day}}$	RMSE $\frac{\text{mm}}{\text{day}}$	CC	MB $\frac{\text{mm}}{\text{day}}$	RMSE $\frac{\text{mm}}{\text{day}}$
Zone 1	0.37	0.26	0.90	0.45	0.19	0.96	0.41	0.00	0.55
Zone 2	0.35	0.21	1.28	0.41	0.17	1.42	0.44	0.00	0.93
Zone 3	0.15	1.00	3.68	0.16	0.42	2.81	0.17	0.03	1.74

The adjusted PERSIANN-CCS with CZ effectively remove the systematic bias during the calibration years and the validation year as shown by Table 2.10 and Table 2.11. During the

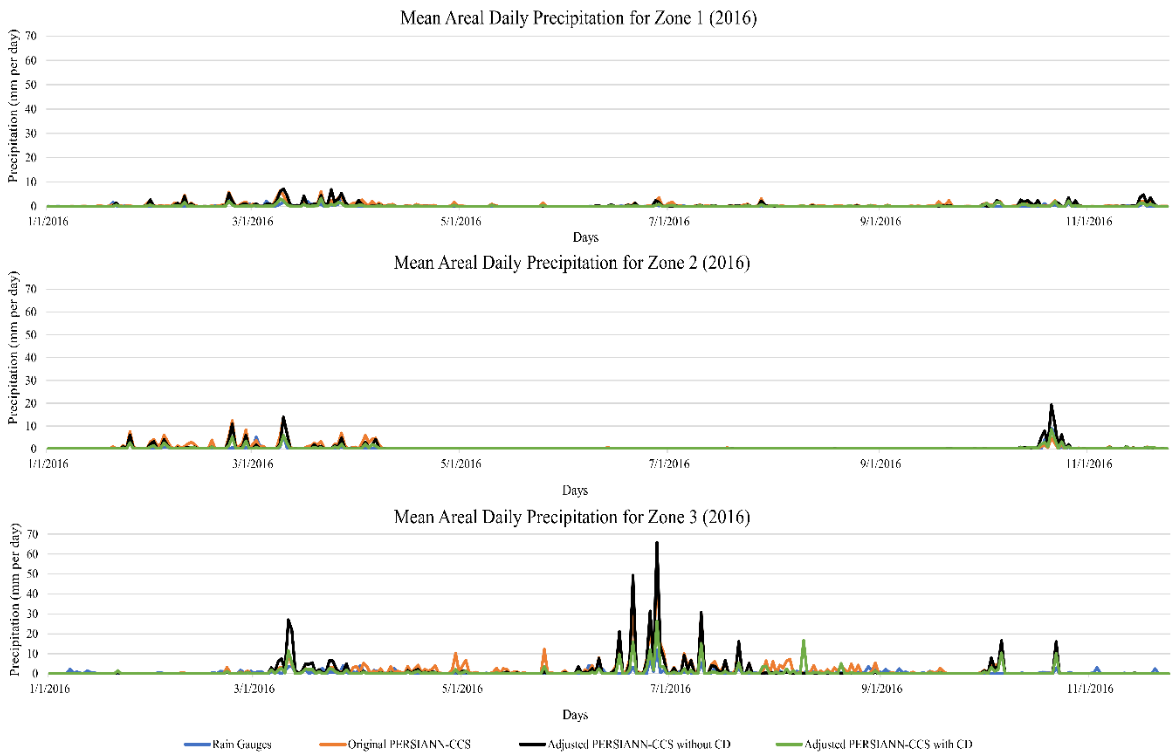

Figure 2.23 Mean Areal Daily Precipitation during Validation

calibration years, the bias is reduced to be less than 0.03 mm per day for zone 3 where most of the precipitation occurs in Saudi Arabia, and zones 1, and 2 have insignificant biases mm per day. Additionally, the daily RMSEs are reduced to 0.55, 0.93, and 1.74 mm per day for zones 1, 2, and 3 respectively. As predictable during the validation, the adjusted PERSIANN-CCS with CZ overestimates the daily precipitation for all zones by 0.03, 0.04, and 0.22 mm per day for zone 1, zone 2, and zone 3 respectively.

Table 2.11 Statistical Evaluation of Daily Time Series during the validation

Zone	Original PERSIANN-CCS			Adjusted PERSIANN-CCS without CZ			Adjusted PERSIANN-CCS with CZ		
	CC	MB $\frac{\text{mm}}{\text{day}}$	RMSE $\frac{\text{mm}}{\text{day}}$	CC	MB $\frac{\text{mm}}{\text{day}}$	RMSE $\frac{\text{mm}}{\text{day}}$	CC	MB $\frac{\text{mm}}{\text{day}}$	RMSE $\frac{\text{mm}}{\text{day}}$
Zone 1	0.57	0.34	0.85	0.62	0.28	0.93	0.63	0.03	0.43
Zone 2	0.47	0.36	1.46	0.71	0.28	1.31	0.73	0.04	0.63
Zone 3	0.67	1.23	4.26	0.59	1.01	5.29	0.72	0.22	2.06

As it clear that the implementation of the QM and incorporation CZ effectively removes the systematic bias the spatial mean yearly and monthly precipitation distribution in Saudi Arabia since the including the CZ helps to stabilize the cumulative distribution functions. Meaning, the QM effectively removes the bias by matching between the two CDFs, which one is related to rain gauge observations and the second one is related to the gauged pixels. The effectiveness of the QM on removing the bias is associated with the reliability of CDFs, which it relates to the number of the sample. Since including the CZ to the QM overcomes the sample size, the effectiveness of the QM in the removing the bias is excellent when it is compared to the QM without CZ. The explanation, according to Table 2.2, the overestimations in yearly scale is calculated to be 0.04 mm per year during (calibration) and 1.54 mm per year (validation) that is best values comparing to the removing of the bias without including CZ. Also, the similar results are found in Table 2.3 and Table 2.4.

Including the CZ into the QM maintains the spatial mean yearly and monthly precipitation distribution in Saudi Arabia since the way to interpolate the results of the QM with CZ helps to maintain the precipitation patters. Meaning, after the result of the QM with CZ is done, the filling the 1° by 1° boxes with the results of the QM with CZ based on location of the box in which climatic zone that helps to keep the precipitation variations. To explain the importance of the interpolation approach, Figure. 2.24 shows the red cycles where the mean yearly and mean monthly precipitations are incorrectly placed for regions by not including CZ.

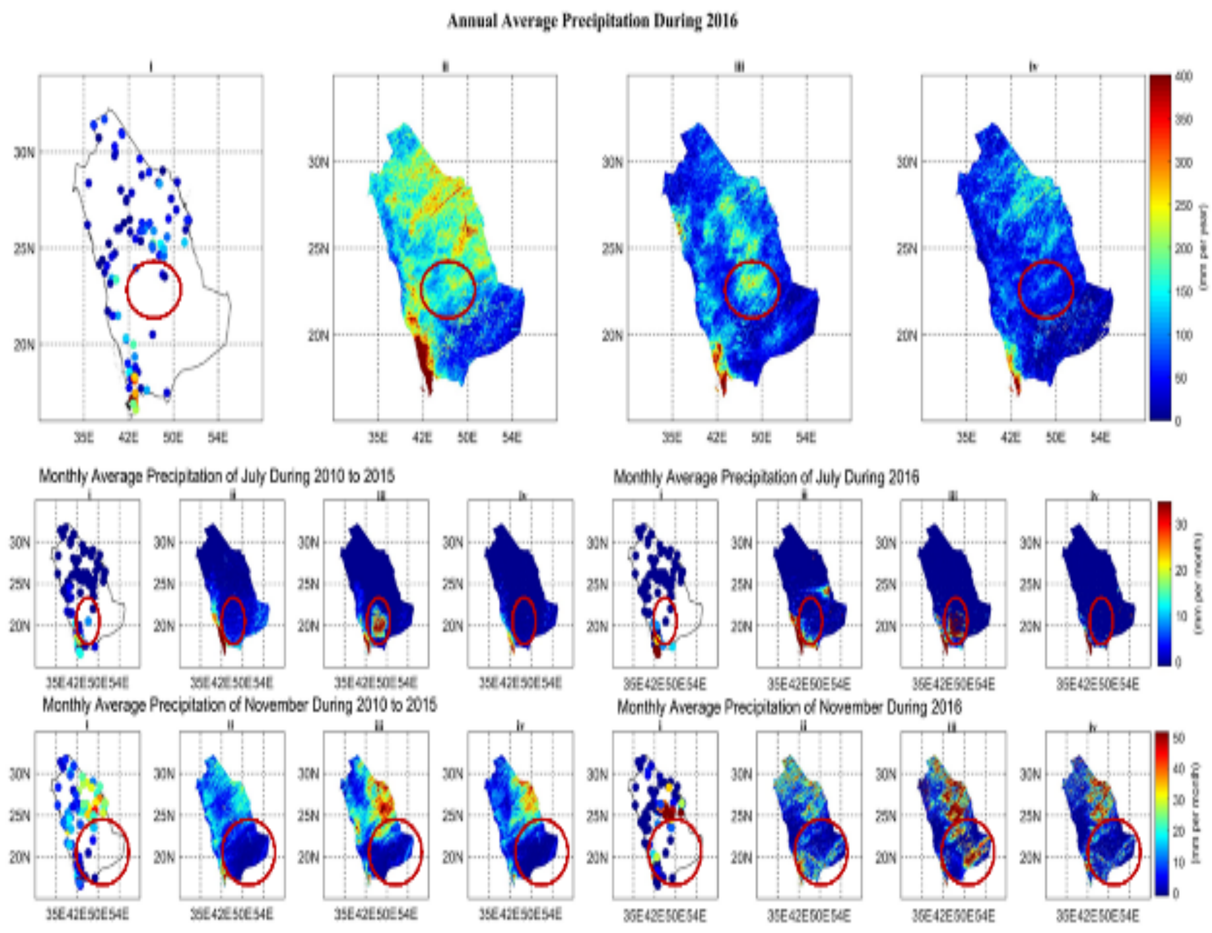

Figure 2.24 An example of including the CZ into the QM helps to maintain precipitation patter.

The major disadvantage of the QM is that the QM does not perform well in the daily scale, which is mentioned in Table 2.1. According to Table 2.10, the daily correction of the bias-corrected PERSIANN-CCSs in each zone has poor correlations with the observed daily precipitation rate. The QM does not any adjustments on the daily estimations since the method works by matching the quintiles of the monthly CDFs.

2.6 conclusion

The study provides a framework that can be used to correct SPEs for a region when the rain gauges are unavailable or limited with using CZs. Saudi Arabia is chosen to verify the effectiveness of the study using the daily estimations of PERSIANN-CCS and the daily observations of the rain gauges over the country between 2010 and 2016. The spatial and temporal results prove that the framework is capable of correcting and improving outcomes of SPEs and including CZs enhances the effectiveness of QM on correcting SPEs outcomes. However, one of the framework's limitation is that correct SPEs day – the day to rain gauges, and we believe that combining the rain gauges and SPEs estimations may help to adjust the random bias and improve the effectiveness of QM and CZ.

CHAPTER 3: Merging Satellite Precipitation Estimates and Rain Gauges over Saudi Arabia

3.1 Introduction

The accuracy of precipitation measurements is critical for hydrological and climatic studies since the quality of the measures of precipitation influence the results of the studies (Cole & Moore, 2008; Fekete, Vörösmarty, Roads, & Willmott, 2004; Moradkhani & Sorooshian, 2008). Directly measured precipitations by rain gauges are considered to be the most reliable measurements at the point of observation. However, studies found that the degree of uncertainty increases when the observations of the rain gauges are extended to cover more spatial coverage, and are associated with the density of rain gauges (Andreassian, Perrin, Michel, Sanchez, & Lavabre, 2001; Faurès, Goodrich, Woolhiser, & Sorooshian, 1995; Huff, 1970; King, Alexander, & Donat, 2013; Tozer, Kiem, & Verdon-Kidd, 2012; Villarini et al., 2008). (Chaplot, Saleh, & Jaynes, 2005; Duncan, Austin, Fabry, & Austin, 1993) examined the impact of the degree density of rain gauges on the runoff observations and found that the degree of density of the rain gauges profoundly impacted the results of the total runoff. On other hand, Satellite-based Precipitation Estimates (SPE) provides the global measurements with high spatial and temporal resolutions, so SPE becomes an alternative source of measurement when the rain gauges are limited (Al et al., 2004; Ashouri et al., 2015; Hong et al., 2004; Hou et al., 2014; K. Hsu et al., 1997; George J. Huffman et al., 1997, 2010, 2007; Kubota et al., 2006; Sorooshian et al., 2000).

The bias of SPEs had been discussed in many publications (Adler, Huffman, Bolvin, Curtis, & Nelkin, 2000; Aghakouchak et al., 2011; Melo et al., 2015; Pereira Filho et al., 2010). The bias influences spes because they measure precipitation indirectly (Moazami et al., 2013; Qin et al., 2014). The existence of the bias can overestimate or underestimate precipitation, which it leads to uncertainty on hydrological and climatic studies (Bitew & Gebremichael, 2011; J. Chen et al., 2018; Gebregiorgis et al., 2012; Teutschbein & Seibert, 2012b). Therefore, removing the bias is an important step prior to the implementation of SPEs on the hydrologic modeling (J. Chen et al., 2016; Gebregiorgis et al., 2012; Liu, Yang, Hsu, Liu, & Sorooshian, 2017; Pierce et al., 2015; Tesfagiorgis et al., 2011).

To remove the bias and improve the outcomes of the SPEs, researchers develop schemes that combine between rain gauge observations and estimations of satellites precipitations, and those approaches can be classified as direct or indirect approaches.

3.1.1 Direct Combinations

The rain gauges observations are directly combined to satellite precipitation estimations by additive and multiplicative schemes. The additive scheme can be defined by Equation 3.1, and the multiplicative is defined by Equation 3.2.

$$\mathrm{R_{Mer}} = \mathrm{R_{sat}} + (\mathrm{R_{gauge}} - \mathrm{R_{sat}}) \qquad 3.1$$

$$\mathrm{R_{Mer}} = \mathrm{R_{sat}} * \left(\frac{\mathrm{R_{gauge}}}{\mathrm{R_{sat}}}\right) \qquad 3.2$$

In Equation 1, $\mathrm{R_{sat}}$ is the satellite precipitation estimations, and $\mathrm{R_{gauge}}$ is the rain gauge observations. $\mathrm{R_{Mer}}$ is the merged product. The bias is addressed by the second part of Equation 3.1 where the bias is differences between the satellite precipitation estimations and the rain gauge observations. In Equation 3.2, the bias is presented by the second part where the bias is ratio between the satellite estimations and the rain gauge observations.

Both schemes have been widely applied to combined between the satellite precipitation estimations and rain gauge observations. For example, (Dinku, Hailemariam, Maidment, Tarnavsky, & Connor, 2014) implemented an additive scheme to combined between satellite estimations and rain gauges to generate high-quality precipitation product, which has 10 km spatial resolution and ten-day temporal resolution of 30 years (1983 – 2014) over Ethiopia. Also, (Vila, de Goncalves, Toll, & Rozante, 2009) combined the additive and multiplicative schemes to merge between the rain gauge observations and TRMM 3B42RT estimations over Continental South America, and this merging approach has been tested against the different degree of the rain gauge network density. The results showed this approach could effectively remove the bias and improve the outcomes of satellite estimations.

3.1.2 Indirect Combinations

Many indirect approaches combine rain gauge estimates to remove the bias of SPEs have been developed to improve SPEs outcome in global and regional scales. In global scale, the Global Precipitation Climatology Project (GPCP) has provided monthly global precipitation measurements at 2.5º by 2.5º latitude-longitude resolution since January 1979 to the present, by combining rain gauges, and low earth orbit, and geostationary satellite estimates (Adler et al., 2003; George J. Huffman et al., 1997). Tropical Precipitation Measuring Mission (TRMM) 3B43 is a global monthly precipitation measurement at 0.25º by 0.25º latitude-longitude spatial resolution. This product combines monthly TRMM 3B42 estimates and the monthly Global Precipitation Climatology Center (GPCC) rain gauge via inverse random-error variance weighting (Condom, Rau, & Espinoza, 2011; George J. Huffman et al., 2010, 2007; Sun et al., 2017). Multi-Source Weighted-Ensemble Precipitation (MSWEP) has 3-hourly temporal resolution and 0.1º by 0.1º latitude-longitude spatial resolution. MSWEP combines rain gauges, satellites, and atmospheric models via the weights for each grid. The gauge weights are assigned based on network density, while the satellites weights are assigned based comparative performance to the surrounding gauges (Beck et al., 2017). Precipitation Estimation from Remotely Sensed Information using Artificial Neural Networks' (PERSAINN) Climate Data Record (CDR) provides the daily precipitation estimations at 0.25° by 0.25° latitude-longitude; GPCP is used to adjust PERSIANN estimations at monthly scale (Ashouri et al., 2015).

For merging SPEs and rain gauges at the regional scale, (Woldemeskel, Sivakumar, & Sharma, 2013) had combined TRMM 3B42 and rain gauges across Australia between January 1998 to December 2007 by combining these two data sets using a linearized weighting procedure. (Teng et al., 2017) uses collocated co-kriging (ColCOK) to merge the daily rain gauge observations and daily TRMM 3B42 estimations across China and recommended that the ColCOK can be a useful tool for merging the rain gauge and SPEs. (Nerini et al., 2015) examines approaches using the mean bias correction and double-kernel smoothing over the Andean watershed in Peru and recommended that the double- kernel smoothing performs better than the mean bias correction approach. (M. Li & Shao, 2010) implement a nonparametric kernel smoothing approach to merge between the rain gauges and TRMM 3B42 over Australia.

Some studies accomplished the merging between the rain gauges and SPEs by removing systematic bias on SPEs before merging the rain gauges. (Pingping Xie & Xiong, 2011) combined rain gauges and CMORPH over China; the study implemented two steps to merge between the rain gauges and the SPE.

First, a matching the probability density function (PDF) is used to remove the systematic bias of the SPE before merging. Then optimal interpolation is used to perform the merging of bias-corrected SPE and gauge observations. The removing of the systematic bias improves the results of merging the two datasets and has been demonstrated in several publications (De Vera & Terra, 2012; Shen, Zhao, Pan, & Yu, 2014; P Xie et al., 2014). (Yang et al., 2016, 2017) merged the rain gauges and PRESIANN- Cloud Classification System (CCS) (Hong et al. 2004) over Chile between 2009 and 2014 using the notable correction approach. (Yang et al., 2016) removed the systematic bias of PERSIANN-CCS by implementing the localized matching between the PDF of the rain gauges and the concurrent pixels that share the same location and time with the rain gauges within 1º by 1º latitude-longitude grids. Then, the Gaussian weights approach was used to interpolate the results of the matching to fine resolutions at 0.04º by 0.04º latitude-longitude. This method can be highly influenced by the degree of rain gauge density over the study area. It had been shown that high uncertainty for estimates over a region where the rain gauges are scattered. (Yang et al., 2017) merged the rain gauges and PERSIANN-CCS over Chile by assigning the weights for each dataset based on precipitation rate and distance. The study assumed that the uncertainty of the bias adjusted of PERSAINN-CCS estimates is a constant for each season. It means that the high-intensity precipitations have the same degree of uncertainty as low-intensity precipitations. However, the uncertainty of the precipitation estimates is changeable based on the intensity of the rate. The high-intensity precipitation estimation usually has a greater degree of uncertainty than the low-intensity precipitation estimation.

In the previous chapter, we implement quantity mapping (QM) and the climatic zones (CZ) approach that aims to remove the systematic bias of PERSIANN- Cloud Classification System (CCS) over Saudi Arabia where rain gauge measurements are limited. The temporal and spatial results of the study show that using QM-CZ effectively removed the bias. However, if the user of QM-CZ does not eliminate random bias, we can merge the bias-corrected estimates with limited rain gauge observations at the end of each day.

The objective of this chapter is to improve the outcomes of the bias-corrected approach that was proposed by merging between the outcomes of QM-CZ that was introduced by the previous chapter, and the rain gauge observations. It is done by assuming that the uncertainty of bias adjusted PERSIANN-CCS is a function of precipitation rate, and distance of a useful rain gauge. A merged product of rain gauges and bias-corrected PERSIANN-CCS estimations are processed in three significant steps: (1) QM-CZ is used to remove the systematic bias; (2) gridding of the rain gauge observations based on climatic zone; and (3) the two datasets are merged based on the distance from rain gauges and error associated with precipitation rate. On following sections, an in-depth explanation of the data sources and methodology are mentioned.

3.2 Study Area and Data Source

3.2.1 Study Area

Saudi Arabia is selected as the study area, and the country is located in the southwest of Asia as shown in Figure. 3.1. Saudi Arabia has a desert climate which is extreme hot during a day and the temperature drops at night with low annual precipitation. However, the southwest of the country where Asir Mountains plays an important role in precipitation occurrences can have annual precipitation rate around 500 mm per day (Kheimi & Gutub, 2015). The comprehensive explanations of the study area climate and the precipitation patter can be found in Chapter 2 section 2.

3.2.2 Data Source

3.2.2.1 Historical Rain Gauges Observations

The daily rain gauge observations are provided by the Ministry of Environment, Water, and Agriculture (MEWA) and the General Authority of Meteorology and Environmental Protection (GAMEP). The daily observations of seven years (2010 – 2016) are available, and the further explanation can be found in Chapter 2 section 3.

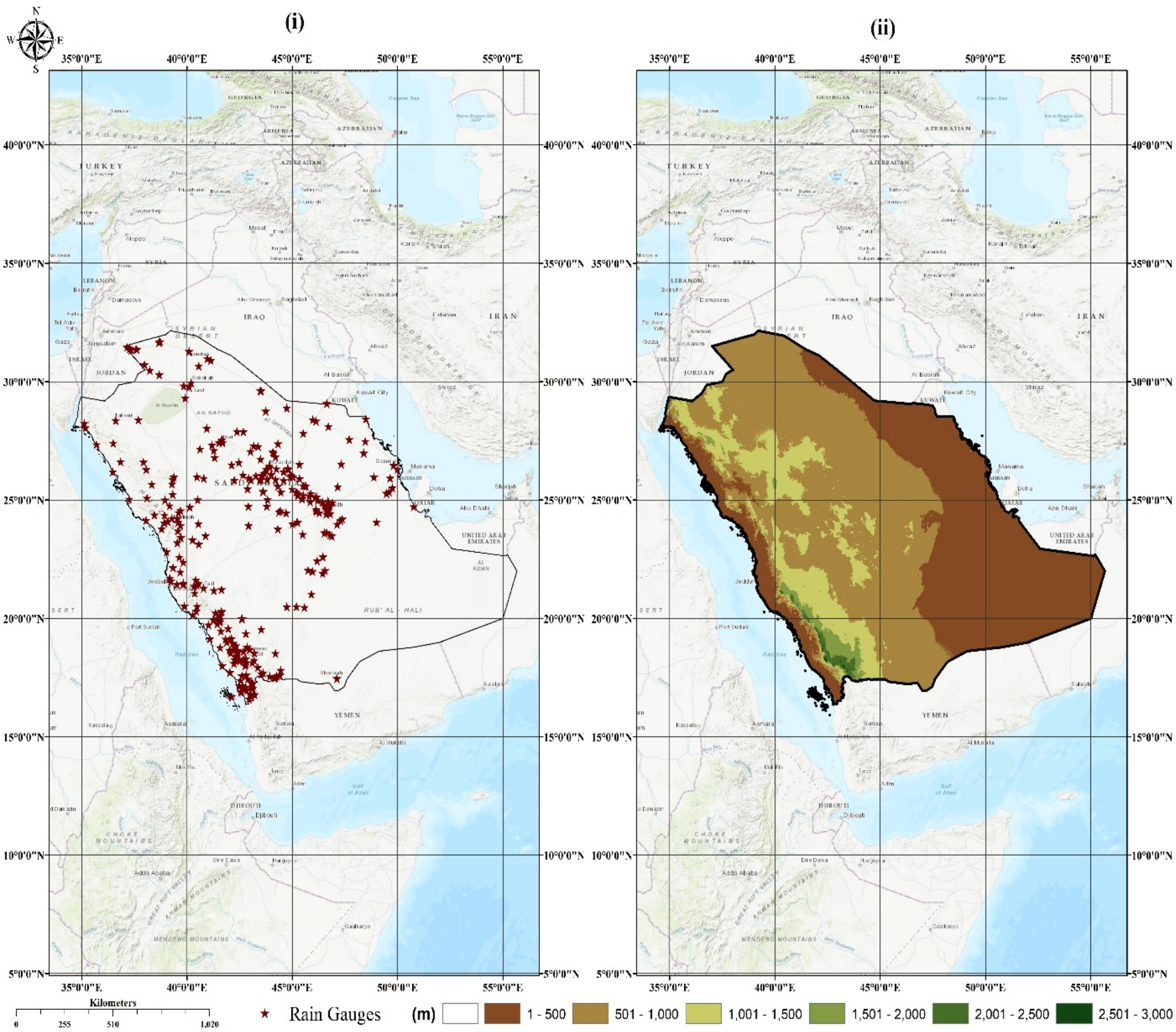

Figure 3.1 Map of Saudi Arabia where (i) is map of Rain gauges, and (ii) is map of the elevation

3.2.2.2 Satellite-based Precipitataion Estimation

The daily estimation from Precipitation Estimation from Remotely Sensed Information using Artificial Neural Networks - Cloud Classification System (PERSIANN-CCS) is used (Hong et al., 2004). PERSIANN-CCS is developed by the Center for Hydrometeorology and Remote Sensing (CHRS) at the University of California, Irvine (UCI). PERSIANN-CCS provides hourly global estimations with 0.04° by 0.04° (latitude by longitude). Further explanation of PERSIANN-CCS can be found in Chapter 2.

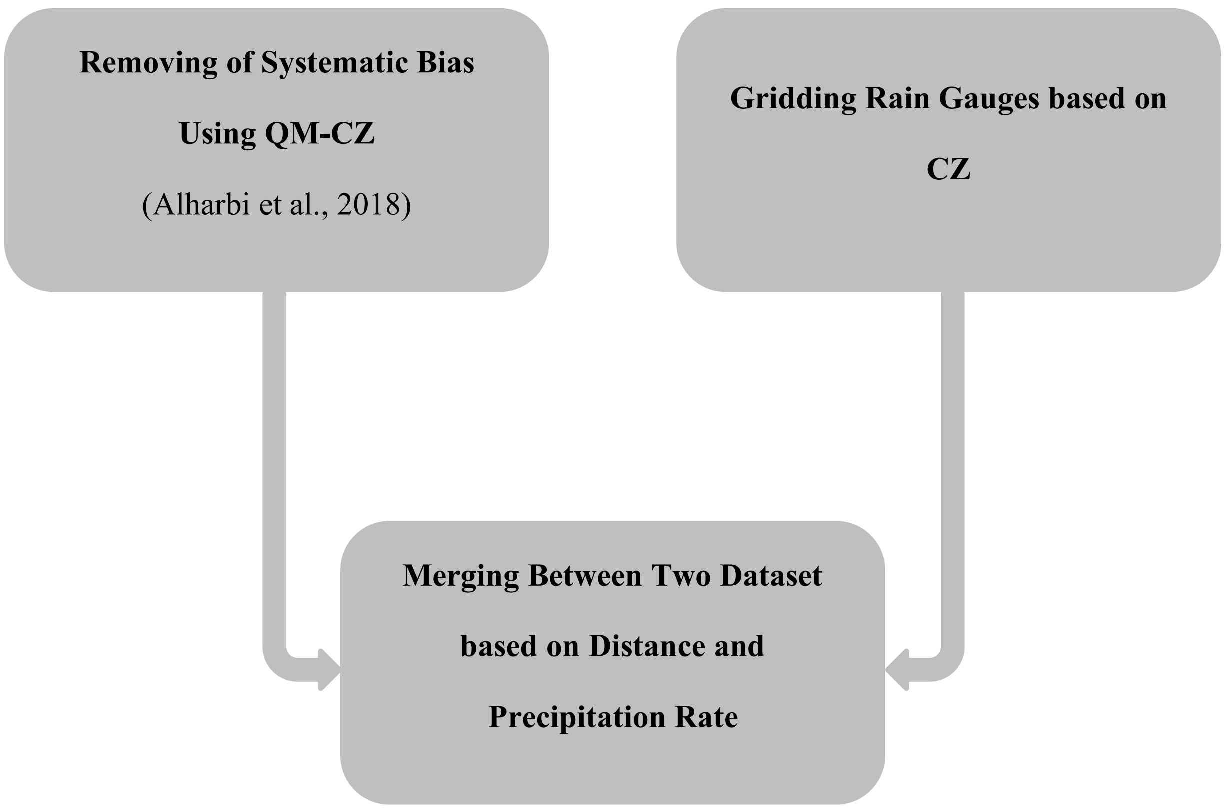

Figure 3.2 Flowchart of the merging of Rain gauges and SPEs

To match between the estimations and the observations, the estimations are accumulated from hourly estimations to daily estimations. Also, the estimations of PERSIANN-CCS are limited to seven years which are the daily observations between 2010 and 2016.

3.3 Methodology

As shown in Figure. 3.2 , the merging of rain gauges and SPEs is proceeded in three major steps: (1) use quantity mapping over the climatic zones to remove systematic bias of SPEs (Alharbi, Hsu, & Sorooshian, 2018); (2) interpolate the rain gauge observations to the same spatial and temporal resolutions of SPEs over the climate zones using Inverse Weighted Distance (IWD); (3) merge the gridded the rain gauges and SPEs by assigned weights that are inverse to the uncertainty (root mean square error, $RMSR^{-1}$) on each data source. Those steps are described below.

3.3.1 The Removing of Systematic Bias

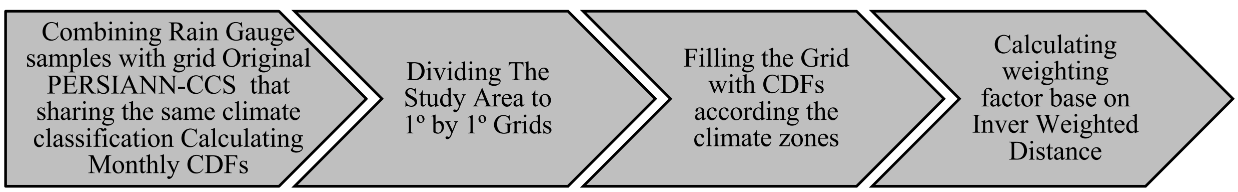

Figure 3.3 Flowchart of the QM-CZ

The systematic bias is removed by the implementation of QM-CZ (Alharbi et al., 2018), and the flowchart of the QM-CZ is shown in Figure. 3.3. Here is a brief description of the method. First, the method relays in the implementation of QM, which is found to be a superior approach when it is compared to other bias correction approach such as scaling linearly, and power transformation (Ajaaj et al., 2016; Jakob Themeßl et al., 2011; Miao, Su, Sun, & Duan, 2016; Piani et al., 2010; Thiemig et al., 2013). QM is a distribution-based approach, and it matches probability density functions (PDF) of SPEs and rain gauges through non-parametric function. Since QM is based on the matching of two PDFs, sufficient samples are needed to calculate PDFs. For getting more samples, we use rain gauges within the same climatic zones to share the same PDF. The correction is done by calculating daily rainfall cumulated distribution functions (CDF) each month for which collocated spatial and temporal samples were collocated from rain gauges and SPEs. We estimate the CDF for each climatic zone. Second, the study area is divided into many four $1^{o}x1^{o}$ latitude and longitude grids and filled with the results of QM based on the grid location. Then, the CDFs of nearby four $1^{o}x1^{o}$ latitude and longitude grids are used to interpolate to high resolution at that match the SPEs' spatial resolution ($0.04^{o}x0.04^{o}$). The QM-CZ is described in detail in Chapter 2, and (Alharbi et al., 2018).

3.3.2 Gridding Rain Gauges

Rain gauges were gridded for merging purpose indirectly. Differences between the rain gauge observations and SPEs at different points of observation are calculated, Differences were spatially interpolated at the same resolutions of SPEs and then were added them to SPEs (Boushaki et al., 2009; Cheema & Bastiaanssen, 2012; Dinku et al., 2014; Duan & Bastiaanssen, 2013; Jongjin, Jongmin, Dongryeol, & Minha, 2016; Vila et al., 2009). However, in this study, the daily rain gauges observations are gridded to the same spatial resolution of SPEs by using inverse weighted distance (IWD) and climatic zones (CZ). IWD is a deterministic interpolation method that estimates the precipitation rate for an unknown point based on the inverse distance. IWD is extensively used to grid the daily precipitation because of the simplicity of the method (Basistha, Arya, & Goel, 2008; M. Chen, Xie, Janowiak, & Arkin, 2002; Dirks, Hay, Stow, & Harris, 1998; Ly, Charles, & Degré, 2013; Vila et al., 2009; Yatagai, Xie, & Alpert, 2007). Based on those studies, the IWD is found to be the superior interpolation method compared to the other spatial interpolation methods on a daily scale. In this study, IWD is used to grid the daily rain gauges observation, and IWD is modified to include the climatic zones. The IWD estimates the precipitation for a gridded pixel based on Equation 3.3

$$G_i = \frac{\sum_{i=1}^{nj} \frac{r_{g_j}}{d_{ij}^p}}{\sum_{i=1}^{n} \frac{1}{d_{ij}^p}} \qquad 3.3$$

In Equation 3.3, G is the gridded rain gauge observations at pixel i, n is the number of rain gauges within the climatic zone. j is the climatic zone, and d is the distance between the pixel and each rain gauge. p is the power in which distance is raised.

As shown by Equation 3.3, IWD has two unknown parameters- the number of rain gauges, n, that are selected for interpolation, and the power parameter, p. The two parameters of each climatic zone are optimized by using leave-one out cross-validation that follows (Cressie, 1994), where the two parameters minimize daily root mean square error (RMSE).

In fact, the extension of the rain gauges observations to more spatial coverage increases the degree of uncertainty, since it is influenced by numerous factors such as the degree of density and distribution of the rain gauges (Haberlandt, 2007; Tao, Chocat, Liu, & Xin, 2009; Tozer et al., 2012). Therefore, the addressing of the uncertainty that exists on each pixel is an important step prior to merging.

3.3.3 Merging Two Datasets

To remove the remaining bias on both bias corrected SPEs and the gridded rain gauges, the $RMSE^{-1}$ approach has been developed based on distance and precipitation rate as shown in Equation 3.4, Equation 3.5 and Equation 3.6.

$$M_{(i)} = wg_{(i)} * GI_i + ws_{(i)} * S_i \qquad 3.4$$

$$wg_{(i)} = \frac{\left(RMSE_{g(i)}\right)^{-1}}{\left(RMSE_{g(i)}\right)^{-1} + \left(RMSE_{s(i)}\right)^{-1}} \qquad 3.5$$

$$ws_{(i)} = \frac{\left(RMSE_{s(i)}\right)^{-1}}{\left(RMSE_{g(i)}\right)^{-1} + \left(RMSE_{s(i)}\right)^{-1}} \qquad 3.6$$

In Equations 3.4 – 3.6, where $M_{(i)}$ is the merged daily precipitation measurement at pixel i, GI_i is daily gridded rain gauge observations at pixel i, and S_i is adjusted bias SPE. $wg_{(i)}$ is weight assigned to the gridded rain gauges at pixel i, while $ws_{(i)}$ is weight that is assigned for adjusted bias SPE at pixel i. $RMSE_{g(i)}$ *and* $RMSE_{s(i)}$ are root mean square error for gridded rain gauges and adjusted bias SPE, respectively.

As mentioned above, the rain gauges measure the precipitation at the point of observation, and the degree of uncertainty increases when the observations are extended. (Ahrens, 2006; Wagner, Fiener, Wilken, Kumar, & Schneider, 2012) had approached the relationship between the uncertainty and the distance from the rain gauges. We assume that the bias that exists on the gridded rain gauges is related to the distance between the pixel and nearby rain gauges.

To address this relationship, leave-one out cross-validation is used to compute daily root mean square error for each gauge within climatic zones with the closest gauge used as the distance definition. This is done for each climatic zone. The calculation of daily root mean square error and distance is described by Equations 3.7 and 3.8:

$$RMSEGI_j = \sqrt{\frac{1}{m} * \sum_{k=1}^{m} \left(GI_{kj} - G_{kj}\right)^2} \qquad 3.7$$

$$\mathrm{RMSE}_{g(i)} = f(D_{min(i)}) \qquad 3.8$$

In Equation 3.7, RMSEGI_j is the daily root mean square error at rain gauge j, and GI_{kj} is gridded rain gauge observations over the rain gauge j. G_{kj} is the daily rain gauge observation, and m is the total number of precipitation rates from the gauge j.

According to Equation 3.8, the degree of the uncertainty for the gridded dataset is related to the distance. Therefore, the error function $f(D_{min(i)})$ can be calculated to estimate $\mathrm{RMSE}_{g(i)}$ the for the gridded pixel, i, based on the calculating the daily root mean square error, RMSEGI_j, at every rain gauge and the minimal distance from each gauge, j, and the other rain gauges within the same climatic zones.

The uncertainty associated with the adjusted bias SPE can be related to the precipitation rates, which refer to when the precipitation rate is heavy, the uncertainty of the estimates is relatively higher, and vice versa. To assign the weight to the pixel based on the precipitation rate, an equation that minimizes the daily RMSE has been developed and shown Equations 3.9 and 3.10.

$$\mathrm{RMSERT}_j = \sqrt{\frac{1}{m'} * \sum_{k=1}^{m'} \left(S_{kj} - G_{kj}\right)^2} \qquad 3.9$$

$$\mathrm{RMSE}_{s(i)} = f(R_{min(i)}) \qquad 3.10$$

In Equation 3.9, RMSERT_j is the daily root mean square error at rain gauge j, and S_{kj} is bias adjusted estimations over the rain gauge j. G_{kj} is the daily rain gauge observation, and m' is the total number of precipitation rates from the gauge j.

The degree of the uncertainty of the bias corrected estimations is associated with the precipitation rates, so Equation 3.10 interpolates this relationship where $f(R_{min(i)})$ can be fitted to calculate the daily root mean square error that is based on the precipitation rate, $RMSE_{s(i)}$, for each pixel based on estimations of the daily root mean square error at every rain gauge, $RMSERT_j$, and the precipitation rate that associated with it.

3.3.4 Evaluations

It is worth to mention that apart of this approach has been proposed and applied (Yang et al., 2017). Where the assumptions are that the merging between the rain gauges and the SPEs is done through the implementation of the IRMSE, but the degree of the uncertainty is mainly associated with the distant and the degree of the uncertainty of the precipitation rate is assumed to be constant. To justify the assumptions are this dissertation that are based on the degree of the uncertainties based on the distance and the precipitation rates are variables compare between both precipitation rate and precipitation constant. Therefore, Merged-PERSIANN-CCS with constant rate represents the assumption that is based on the degree of the uncertainty is constant with precipitation rate. Also, Merged-PERSIANN-CCS with precipitation rate not constant represents the assumption that is based on the degree of the uncertainty is changeable as the precipitation rate changes.

To exam in the results of merging, the results is presented in spatial distribution and temporal patters. Spatial distribution of the mean annually and monthly of the study area are examined by using correlation confession (CC), mean bias (MB), and root mean square error (RMSE). They are calculated based on Equations 3.11 – 3.13.

$$\mathrm{CC} = \frac{\sum_{g=1}^{n}(G_g - \bar{G}) \; * \; \sum_{g=1}^{n}(S_g - \bar{S})}{\sqrt{\sum_{g=1}^{n}(G_g - \bar{G})^2} \; * \; \sqrt{\sum_{g=1}^{n}(S_g - \bar{S})^2}} \qquad 3.11$$

$$\mathrm{MB} = \frac{\sum_{g=1}^{n}(S_g - G_g)}{n} \qquad 3.12$$

$$\mathrm{RMSE} = \sqrt{\frac{\sum_{g=1}^{n}(S_g - G_g)^2}{n}} \qquad 3.13$$

G is the rain gauge observations, $\bar{G}$ represents the mean rain gauge observations, S is the SPE estimations, and $\bar{S}$ is the mean of SEP. n represents the number of rain gauges.

The results of merging are evaluated via calculating CC, MB, and RMSE for mean areal cumulative daily, mean areal monthly, and mean areal daily in each zone. Probability of detection (POD), false alarm rate (FAR), and critical success index (CSI) are calculated for mean areal daily in each climate zone. They are calculated via Equations 3.14 – 3.16, and Table 3.1 interpolates the values.

$$\mathrm{POD} = \frac{A}{A + C} \qquad 3.14$$

$$\mathrm{FAR} = \frac{B}{A + B} \qquad 3.15$$

$$\mathrm{CSI} = \frac{A}{A + B + C} \qquad 3.16$$

Table 3.1 Contingency table for evaluation POD, FAR, and CSI

		Rain Gauge Observations	
		Yes	No
Merged SPE	Yes	A	B
	No	C	D

3.4 Results and Discussion

3.4.1 Bias adjustment

As illustrated in Figure. 3.2 , the bias corrected is needed prior to merge (Alharbi et al., 2018). The rain gauge observations are separated into calibration and validation periods to examine the results of the implementations of QM-CZ over the study area. The years between 2010 and 2015 are the calibration period, while the later year (2016) is the validation period. The spatial and temporal results of the calibration and validations show that the QM-CZ successfully removed the bias of Original PERSIANN-CCS, and the results of implementing the QM-CZ are presented as Adjusted PERSIANN-CCS. In fact, the results of the calibration and the validation periods are shown in detailed in Chapter 2.

3.4.2 Parameterization of Gridding the Rain Gauges

The study implemented the IWD as a tool to grid the daily rain gauge observations at 0.04º by 0.04º latitude-longitude between 2010 and 2016. IWD has two parameters: the number of rain gauges n, and power p. To calibrate the parameters, leave one out cross validation approach and daily RMSE as an objective function are used. As shown by Figure. 3.4, the daily RMSE is reduced rapidly until the number of nearest rain gauges is increased to ten, then the RMSE is flatly reduced. Therefore, the optimized number of rain gauges is ten. Figure. 3.4 shows the optimized power is one because it had the lowest RMSE with all combinations of the number of rain gauges.

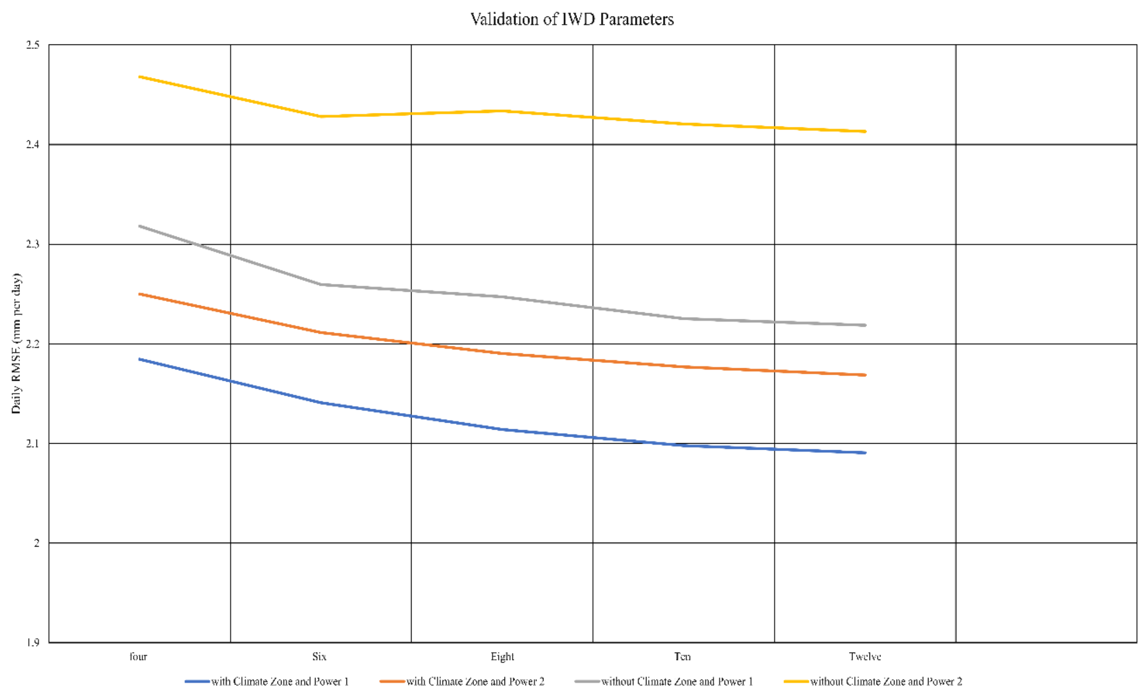

Figure 3.4 Optimized Number of Rain Gauges

3.4.3 Fitting Monthly Weighting Functions for Data Merging

Here, the fitting of monthly distance and precipitation rates functions are shown in Figures 3.5 and 3.6 where the months that are displayed are January, April, July, and November.

3.4.3.1 Fitting Monthly Weighting Functions for Gridding

A monthly error function for each climatic zone has been fitted for the daily RMSE and minimum distance (D_{min}). It is calculated based on Equation 3.5 and Equation 3.6 where the level

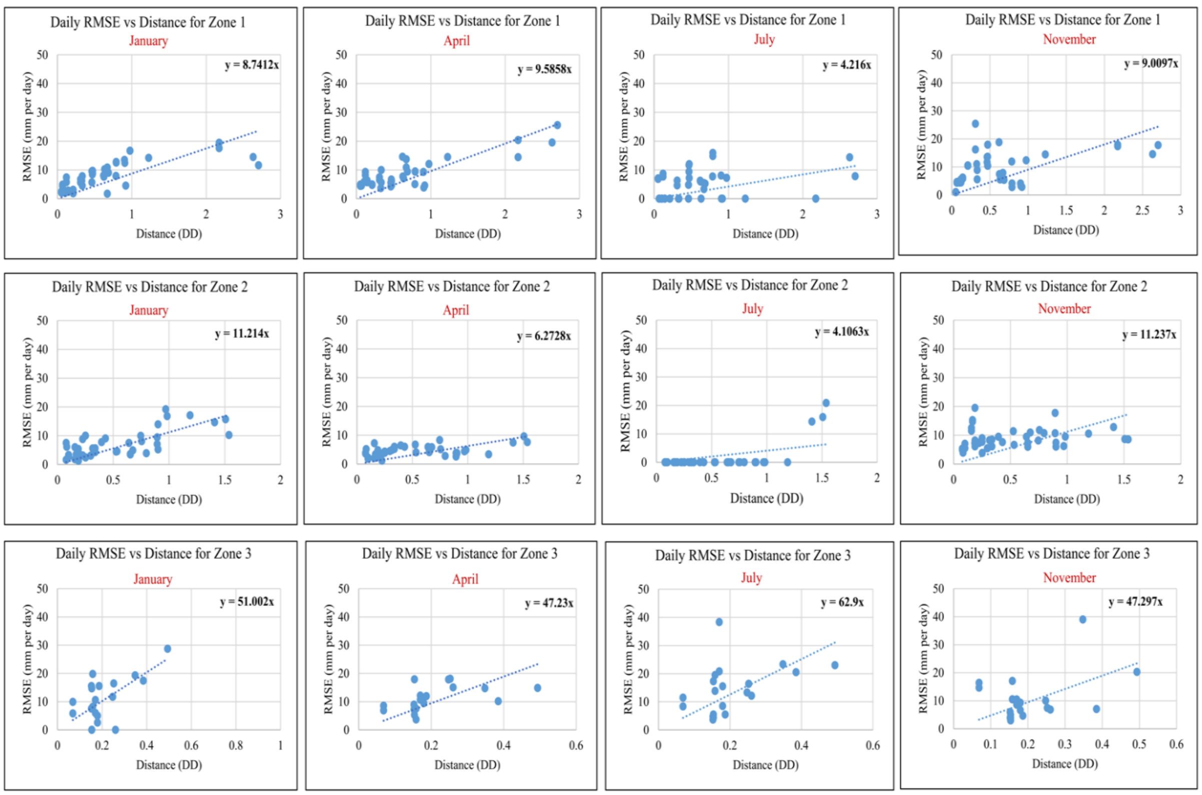

Figure 3.5 Monthly Daily RMSE and minimum distance relationships for Gridded Rain Gauge Observations. The blue lines are fitted to the samples for four months (January, April, July, and November) in each zone. The formulations are shown for each month and each zone

one out cross validation and daily RMSE are used. As shown in Figure. 3.5, x-axis is the daily RMSE that is calculated between interpolated gridded pixel, which shares the same location with a tested gauge that is not included in the interpolation with the gauge based in climatic zone. Y-axis is the nearest distance that is measured between the gridded pixel and the nearest rain gauge that is included in the interpolation, and the distance is measured by decimal degrees. The months that is shown in Figure. 3.5 are January, April, July, and November. As shown in Figure. 3.5, the daily RMSE linearly increases with the distance. Clearly, the degree of the sensitively of the daily RMSE to the distance is various based on the zones. For example, the most sensitivity is found to be Zone 3 where a small change in the distance results a high value of the daily RMSE. On other hand, Zone 1 and Zone 2 have the similar sensitively.

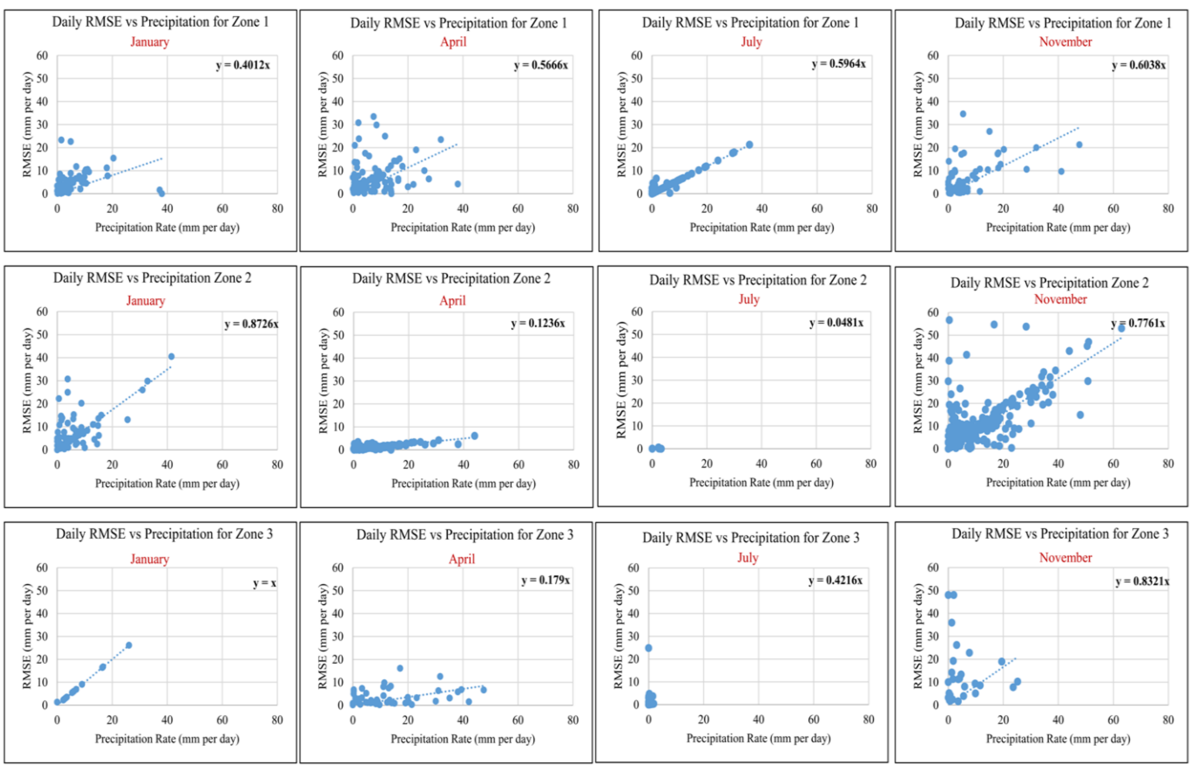

Figure 3.6 Monthly Daily RMSE and Daily Precipitation Rate for the bias corrected (Adj-PERSIANN-CCS).The blue lines are fitted to the samples for four months (January, April, July, and November) in each zone. The formulations are shown for each month and each zone

3.4.3.2 Fitting Monthly Weighting Function for Precipitation Rate

The Equation 3.6 and Equation 3.7 are implemented to fit the monthly error functions for each climatic zone that are used to calculate the daily RMSEs for precipitation rates. As shown in Figure. 3.6, after the bias correction approach, QM-CZ, is applied, the relationships between the daily RMSE and precipitation rate can be expressed as linear that are shown in Figure. 3.6. The degree of the goodness of the fitting is various based on the climatic zones. The fittings of Zone 1 and Zone 2 can be similar especially January, and November where the most of precipitation occurs in the zones. Noteworthy, the occurrence of the precipitation in Zone 2 rarely falls in July that what makes the fitting may not be strong, but the most occurrence of the precipitation falls in July for Zone 3 where the daily RMSE is highly correlated with precipitation rates. The same results are founded in April for Zone 3.

Based on the fitted functions that are shown in Figures. 3.5 and 3.6, the bias corrected Adjusted PERSIANN-CCS and Gridded rain gauges are blended together by implementing the rates and distances, respectively. As shown in Figure. 3.5, when a pixel is located far away from the nearest rain gauge, the influence of the gridded rain gauges is low. Therefore, the influence of bias corrected Adjusted PERSIANN-CCS on the merging becomes high, while the influence of the gridded rain gauges is high when the pixel is close. When the precipitation rates get heavy, the degree of uncertainty becomes relatively high, shown in Figure. 3.6. Therefore, the weight that is assigned to the bias corrected Adjusted PERSIANN-CCS is low when the precipitation rates are high.

3.4.4 Spatial distribution of precipitation in Saudi Arabia

The results of the spatial distribution of precipitation are shown in Figures. 3.7, 3.8,3. 9, and 3.10. Tables 3.2 and 3.3 represent the statistical evaluation. Figures. 9 and 10 compare the rain gauge observations, Original PERSIANN-CCS, Adjusted PERSIANN-CCS, Merged PERSIANN-CCS (Constant), and Merged PERSIANN-CC (Not Constant).

3.4.4.1 Annual distribution of precipitation in Saudi Arabia

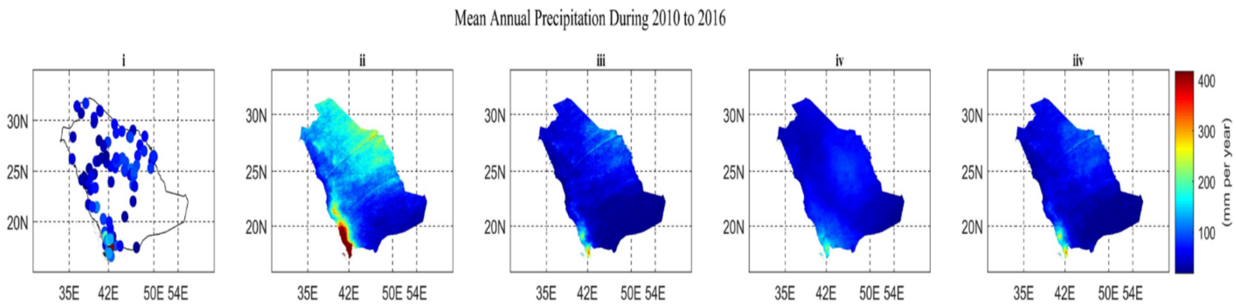

Figure 3.7 Annual mean precipitation of (i) rain gauge, (ii) Original PERSIANN-CCS, (iii) Adjusted PERSIANN-CCS, (iv) Merged PERSIANNCCS with constant Precipitation Rate, and (iiv) Merged PERSIANN-CCS with Precipitation Rate as a function during 2010 to 2016.

Table 3.2 Statistics evaluations for the mean annual precipitation

PERSIANN-CCS	CC	MB $\frac{\mathbf{mm}}{\mathbf{year}}$	RMSE $\frac{\mathbf{mm}}{\mathbf{year}}$
Original	0.632	143.014	212.804
Adjusted	0.636	-0.909	43.439
Merged (Constant)	0.679	11.378	42.429
Merged (Not Constant)	0.730	1.556	37.148

Figure. 3.7, and Figure. 3.8 and Table 3.2 represent the annual mean of precipitation over the study area between 2010 and 2016. Original PERSIANN-CCS overestimates the annual precipitation over the study area by more than 140 mm per year. Original PERSIANN-CCS mostly

overestimates in the southwest of the country and the center of the country that is clear as shown in Figure. 3.8. Original PERSIANN-CCS has a robust annual correlation with the rain gauge observations that is calculated to be 0.63. On the other hand, the implementation of the QM-CZ effectively removes the systematic bias by more than 95% of the mean bias, and more than 75% of annual RMSE. The QM-CZ does not improve the annual correlation coefficient since it keeps the same value, which is 0.63. As expected, when the rain gauges are blended with bias-corrected of PERSIANN-CCS, the results improve significantly.

In two merging methods, the annual correlation confession is improved, but the improvements have different magnitudes. First, not incorporation the climate zone to QM and implementing the error constant in the merging, which is represented by Merged-PERSIANN-CCS (Constant), helps to improve the annual correlation confession by 7%. On the other hand, implementing the climate zone to QM and using error function approach in the merging, which is presented by Merged-PERSIANN-CCS (Not Constant), successfully enhances the annual correlation confession by 15% (See Table 3.2). Not including the climate zone to QM and the constant error overestimates the mean annual precipitation, (Merged (Constant)), by 11.3 mm per year, which means the 92% of the bias in Original PERSIANN-CCS is removed by this merging method. On the other hand, the mean annual precipitation that is estimated by implementing the climate zone and the error function, (Merged (Not Constant)), slightly overestimates by 1.5 mm per year which means 99% of the bias is removed by applying this method. Merged PERSIANN-CCS (Not Constant) has the lowest annual RMSE, which is 37 mm per year when the annual RMSE of Merged-PERSIANN-CCS (Not Constant) is compared to annual RMSE of Original PERSIANN-CCS, it decreases by 83%. In comparison, Merged-PERSIANN-CCS (Constant) has the second lowest annual RMSE, which is calculated to be 42.4 mm per year, when Adjusted PERSIANN-CCS and the merged PERSIANN-CCS are compared, they have similar annual

RMSEs (See Table 3.2). Not including the climate zone and using constant error does not successfully reduce annual RMSE even after the merging.

When the comparison between the observed mean annual precipitation, (Rain Gauge), the estimated gauged mean annual precipitations pixels is calculated and plotted, Original PERSIANN-CCS, which is highlighted by orange points in Figure. 3.9, overestimates the mean precipitations. Conversely, the gauged pixels by Adjusted PERSIANN-CCS, Red Points, overestimates and underestimates mean annual precipitations.

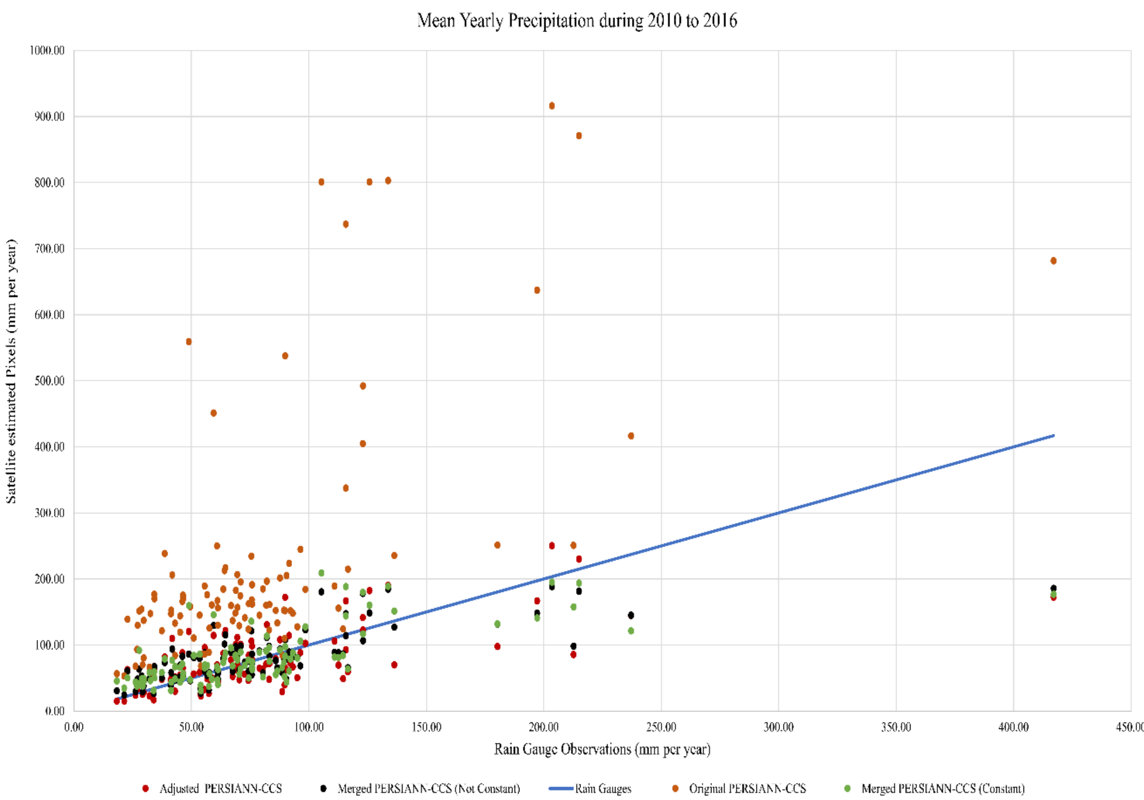

Figure 3.8 Annual Scatter Plot of mean annual precipitations during 2010 to 2016.

Clearly, the both merged gauged pixels, Black and Green points in Figure. 3.9, are closely near of the observed mean annual precipitations.

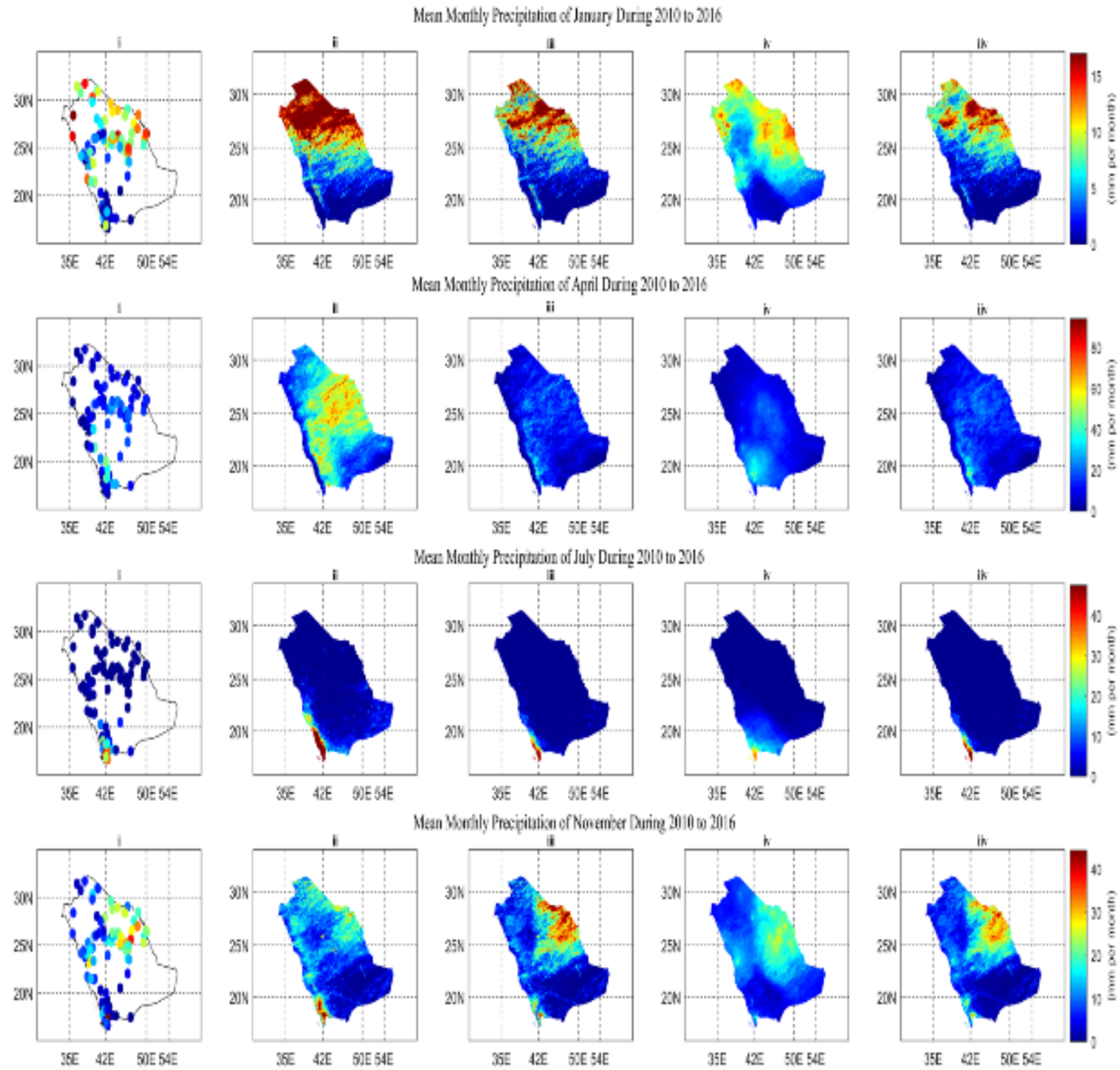

Figure 3.9 Monthly mean precipitation of (i) rain gauge, (ii) original PERSIANN-CCS, (iii) adjusted PERSIANN-CCS, (iv) Merged PERSIANNCCS with constant Precipitation Rate, and (iiv) Merged PERSIANN-CCS with Precipitation Rate as a function during 2010 to 2016.

3.4.4.2 Monthly distribution of precipitation in Saudi Arabia

The results of monthly precipitation spatial distribution are shown in Figure. 3.9, and Figure. 3.10 and Table 3.3. January, April, July, and November are the months that are presented. As expected, Original PERSIANN-CCS overestimates the mean monthly precipitation for displayed months by 2.6 mm per month, 20.6 mm per month, 14.3 mm per month, and 3.7 mm per month for January, April, July, and November, respectively (See Table 3.3). As shown in Figure. 3.9, Original PERSIANN-CCS strongly captures variations of the mean monthly over Saudi Arabia mainly in January and July. The estimated mean captures the precipitation variations where the north part of the country receives precipitations in January, while most of the precipitations fall in the southwest in July that is well captured by Original PERSIANN-CCS. When the observed mean monthly precipitation is compared with the gauged pixels of Original PERSIANN-CCS, the gauged pixels have strong correlations with the observed mean that are estimated to be 0.6 and 0.9 for January and July, respectively. When the comparison between the rain gauged, Blue Line, and gauged pixels, Orange Points, is plotted in Figure. 3.10 Original PRESIANN-CCS overestimated. On the other hand, Original PERSIANN-CCS does not well capture the mean monthly precipitation for April and November where the monthly CCs are calculated to be 0.3 and less than 0.1 (See Table 3.3). Also, the mean monthly precipitation overestimates by 20.6 mm per month and 3.7 mm per month for April and November.

When QM-CZ is applied, the systematic bias is removed as demonstrated by Figure. 3.9 and Table 3.3. The mean monthly precipitation that are estimated by Adjusted PERSIANN-CCS of January, July and November overestimates by 0.2 mm per month, 0.3 mm per month, and 1.1 mm per month, respectively, but QM-CZ successfully removes the bias that is existing in the mean monthly precipitations by 93%, 97% and 70% for January, July and November. However, the implementation of QM-CZ does not help to improve the wellness of capturing spatial variation of the mean monthly precipitations as seen in Figure. 3.9 and Figure. 3.10 and Table 3.3 where the monthly CC does not improve for the shown months expect November.

Table 3.3 Statistics evaluations mean monthly precipitations

	January			April			July			November		
	CC	MB	RMSE	CC	MB	RMSE	CC	MB	RMSE	CC	MB	RMSE
PERSIANN-CCS		$\frac{mm}{month}$	$\frac{mm}{month}$		$\frac{mm}{month}$	$\frac{mm}{month}$		$\frac{mm}{month}$	$\frac{mm}{month}$		$\frac{mm}{month}$	$\frac{mm}{month}$
Original	0.6	2.6	7.1	0.3	20.6	29.0	0.9	14.3	37.9	0.0	3.7	14.5
Adjusted	0.5	0.2	5.5	0.7	-1.3	10.2	0.8	0.3	7.0	0.5	1.1	9.1
Merged (Constant)	0.6	0.3	4.6	0.7	0.2	11.6	0.9	0.3	4.3	0.7	0.7	6.7
Merged (Not Constant)	0.7	0.1	3.9	0.8	0.3	10.0	0.9	0.2	4.6	0.8	0.1	6.3

As expected, when the observed rain gauges are blended with the estimated precipitations pixels, the results of the mean monthly precipitation enhance. Merged PERSIANN-CCS (Not Constant) shows the best performances where the monthly CCs are calculated to be more than 0.7 for the displayed months, which means that there are strong correlations between the mean observed and mean merged precipitations. The worth to mention that the correlation coefficient of

November is highly improved from less than 0.1 to be 0.8 (See Table 3.3). Merged PERSIANN-CCS (Not Constant) have the lowest overestimations where it overestimates by 0.1 mm per month (January), 0.3 mm per month (April), 0.2 mm per month (July), and 0.1 mm per month (November). Also, Merged PERSIANN-CCS (Constant) has slightly performance like Merged PERSIANN-CCS (Not Constant), but it overestimates the mean monthly precipitation more than Merged PERSIANN-CCS (Not Constant) that is shown in Table 3.3. When the mean monthly precipitations estimations form gauged pixels are compered to the rain gauged observations as displayed in Figure. 3.10, Merged PERSIANN-CCS (Not Constant) that is highlighted by black points follows the rain gauge observations for displayed months.

3.4.5 Time series of precipitations over Saudi Arabia

Monthly and daily time series over Saudi Arabia are presented in Figures. 3.11, 3.12, and 3.13. The statistical evaluations of the time series are shown in Tables 3.4, 3.5, and 3.6. The figures are divided into three climatic zones.

3.4.5.1 Monthly time series

In monthly time series, the areal monthly precipitation is plotted in Figure. 3.11 and Table 3.4 shows the statistical evaluations. Original PERSIANN-CC, Orange Line, overestimates the monthly estimations as shown in Figure. 3.11 where the highest overestimations is in Zone 3 where most of precipitations occurs between April, May, June, July, August and September. The average of overestimations in Zone 3 is calculated to be 26.54 mm per month. The lowest overestimations is in Zone 2 where precipitations usually falls in March, April, and May, and Original PRESIANN-CCS has middle correlation with the rain gauge observations that is calculated to be 0.57. Original PERSIANN-CCS overestimates the areal monthly precipitation for Zone 2 by 0.9 mm per month (See Table 3.4).

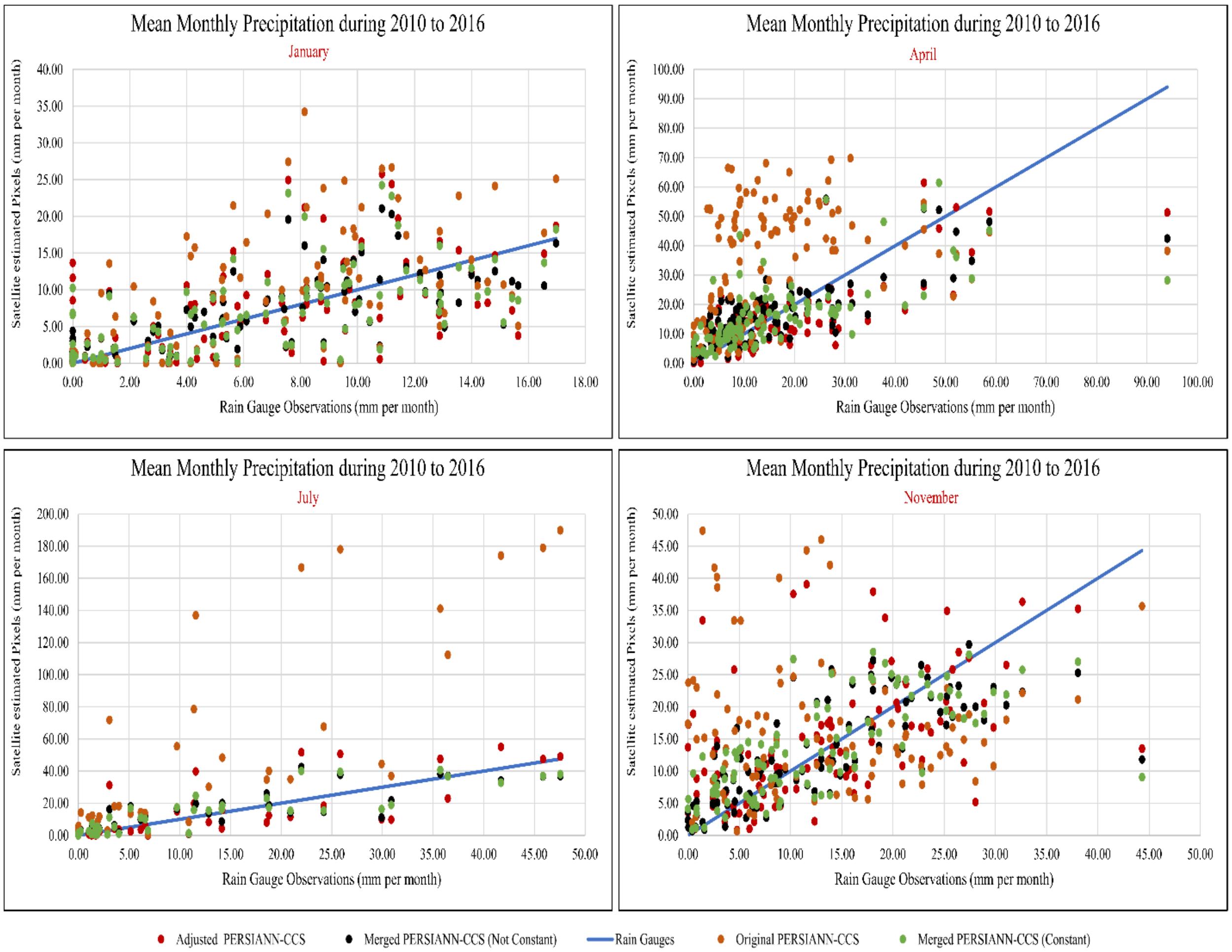

Figure 3.10 Monthly Scatter of mean monthly precipitations during 2010 and 2016

Table 3.4 Statistical evaluation of monthly time series

	Zone 1			Zone 2			Zone 3		
PERSIANN-CCS	CC	MB	RMSE	CC	MB	RMSE	CC	MB	RMSE
		$\frac{mm}{month}$	$\frac{mm}{month}$		$\frac{mm}{month}$	$\frac{mm}{month}$		$\frac{mm}{month}$	$\frac{mm}{month}$
Original	0.68	7	10.32	0.57	0.9	17.23	0.64	26.54	44.9
Adjusted	0.73	-1.1	4.06	0.74	6.26	7.41	0.76	-2.87	13.04
Merged (Constant)	0.82	0.56	3.31	0.84	0.58	5.8	0.91	1.78	8.37
Merged (Not Constant)	0.92	0.06	2.17	0.9	0.58	4.88	0.95	0.77	6.41

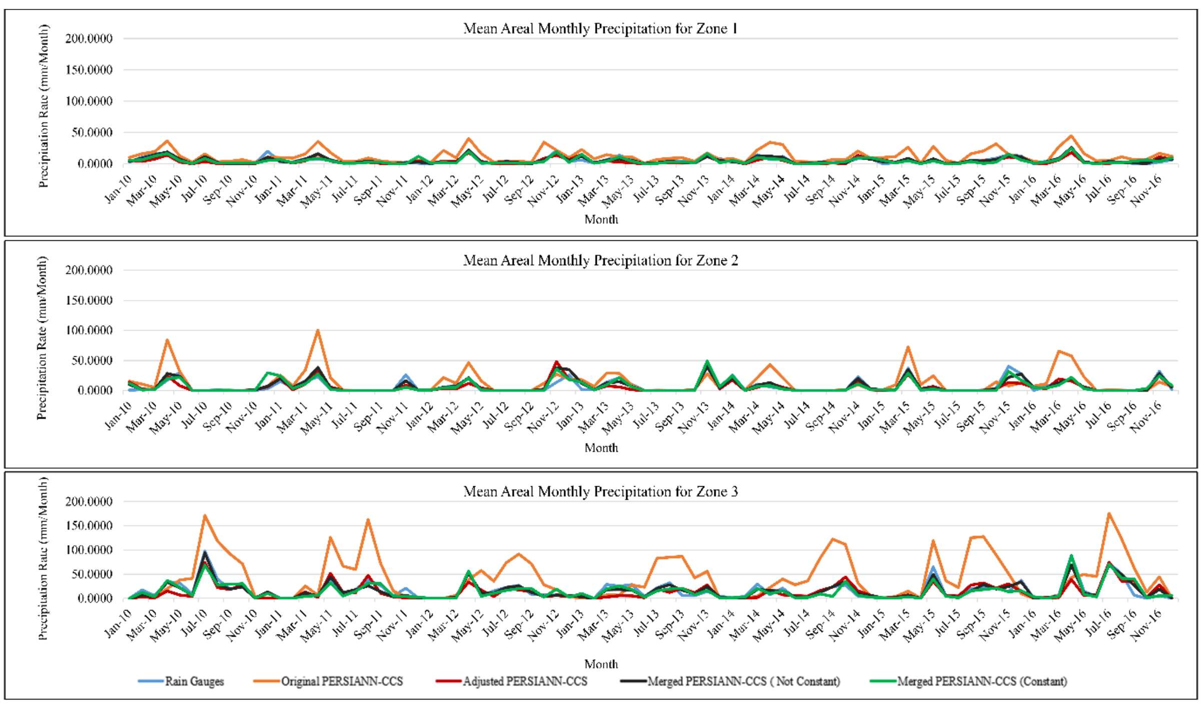

Figure 3.11 Mean areal monthly precipitation for three zones during 2010 and 2016

The areal monthly precipitations that are estimated by Adjusted PERSIANN-CCS (Red line). The CCs are more than 0.7 for all zones, which means that there are strong correlations between the estimated areal monthly precipitations and the observed monthly precipitations. Implementation of QM-CZ helps to reduce the bias; the estimated areal monthly matches well the observed monthly precipitation. However, the reductions of the bias underestimate the areal monthly precipitations in Zone 1 and Zone 3.

As expected of the merging between the rain gauges and the bias-corrected, Merged PERSIANN-CCS (Not Constant), Green Line, has best performances in all zones. The estimated areal monthly precipitations have robust correlations with the observed mean areal precipitations where the CCs are calculated to be more than 0.9 (See Table 3.4). Also, Merged PERSIANN-CCS (Not Constant) has the lowest mean bias in each zone when is compared to other estimations, Original- PERSIANN-CCS, Adjusted PERSIANN-CCS, and Merged PERSIANN-CCS (Constant). For example, the estimated areal monthly precipitation in Zone 3 overestimated by 0.77 mm per month that means 97% of the bias in Original PERSIANN-CCS is removed, and Zone 3 where is most of the precipitation falling in Saudi Arabia. In Additional, Merged PERSIANN-CCS shows the lowest monthly RMSE in each zone where the lowest monthly RMSE is 2.17 mm per month in Zone 1 that means it is reduced by 99%. When Merged PERSIANN-CCS (Constant) is evaluated against Merged PERSIANN-CCS (Not Constant), the latter one is dominating based on the results that are presented in Table 3.4.

3.4.5.2 Daily time series

The daily precipitation over Saudi Arabia is shown in Figures. 12 and 13, and Tables 3.5 and 3.6. Figure. 3.12 represents the mean areal daily cumulative precipitation for each climatic zone for each year between 2010 and 2016. Figure. 3.13 shows the mean areal daily precipitation for each climatic zone. Table 3.5 mentions the statistical evaluation of the cumulative daily precipitation for each climatic zone. Table 3.6 illustrates the statistical evaluation of the mean daily precipitation for each climatic zone.

3.4.5.2.1 The mean areal daily cumulative precipitation

In the comparison of the cumulative daily precipitation that is shown in Figure. 3.12 where the rain gauge observations (Blue Line), original PERSIANN-CCS (Orange Line), Adjusted PERSIANN-CCS (Red Line), Merged PERSIANN-CCS Constant (Black Line) and Merged PERSIANN-CCS Not Constant (Green Line) are emphasized, Original PERSIANN-CCS well captures the daily distributions of the precipitations in the study area as illustrating in Figure. 3.12. For example, the observed cumulative daily precipitation in Zone 2 for each year shows that the precipitation mainly falls during the first 120 days of a year that is well. The similar performance is found for Zone 3 where the precipitation generally falls after the early 100 days of a year as shown in Figure. Original PERSIANN-CCS captures 3.12. However, Original PERSIANN-CCS overestimates the cumulative daily precipitations in each zone, and the overestimations are 54 mm per day, 66 mm per day, and 142 mm per day for Zone 1, Zone 2, and Zone 3, respectively (See Table 3.5).

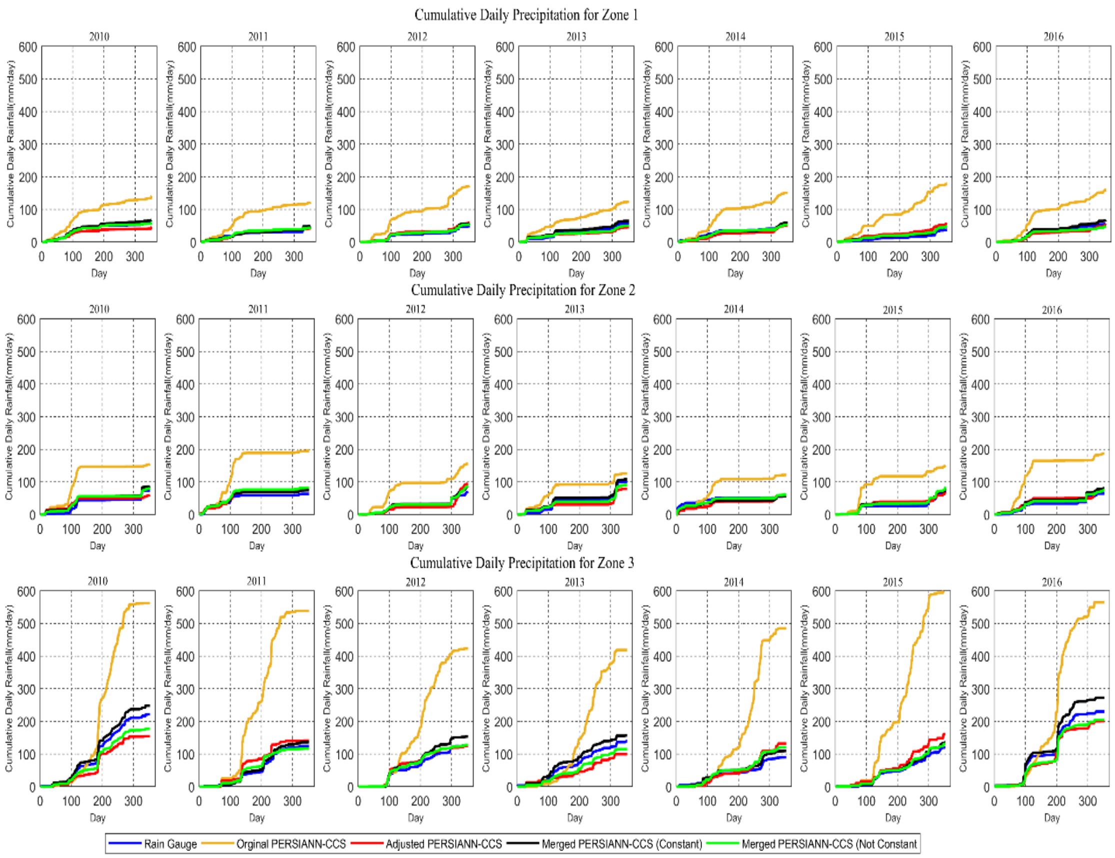

Figure 3.12 Mean daily cumulative precipitation for all zones during 2010 and 2016.

On the other hand, when QM-CZ is applied, the significant reductions in the bias are made. The average reductions in the bias in the zones are calculated to be 98%, and 90%, and 94% in Zone 1, Zone 2, and Zone 3, respectively. However, Adjusted PERSIANN-CCS still overestimates the cumulative daily precipitations in each zones as shown in Table 3.5.

Table 3.5 Statistical Evaluation of the cumulative daily

PERSIANN-CCS	Zone 1			Zone 2			Zone 3		
	CC	MB	RMSE	CC	MB	RMSE	CC	MB	RMSE
		$\frac{mm}{day}$	$\frac{mm}{day}$		$\frac{mm}{day}$	$\frac{mm}{day}$		$\frac{mm}{day}$	$\frac{mm}{day}$
Original	0.98	54.56	62.92	0.92	65.79	74.57	0.97	141.69	205.97
Adjusted	0.98	1.24	8.07	0.94	6.92	11.29	0.98	7.15	23.45
Merged (Constant)	1	3	4.47	0.98	4.78	7.83	0.94	11.15	14.17
Merged (Not Constant)	0.99	0.25	4.33	0.99	4.05	7.7	0.99	3.42	4.68

As benefits of the merging, Merged PERSIANN-CCS (Not Constant) shows the lowest average of the bias in all zones, and the reductions in the bias are calculated to be more than 99%. Also, Merged PERSIANN-CCS (Not Constant) has the strongest correlations with the observed cumulative daily precipitations in the zones where CCs are calculated to be around one as shown in Table 3.5. In the comparison between Merged PERSIANN-CCS (Constant) and (Not Constant), the latter one shows the best performances in all zones, while Merged PERSIANN-CCS (Not Constant) does not perform well where it overestimates the precipitation in more than Adjusted PERSIANN-CCS in Zone 3 and Zone 1.

3.4.5.2.2 The mean areal daily precipitation in Saudi Arabia

In order to evaluate the effectiveness of the merging method that is proposed in this study, the results of Probability of detection (POD), false alarm rate (FAR), and critical success index (CSI) are show in Table 3.6 where the comparison of day by day is done.

Table 3.6 Statistical Evaluation of daily time series

	Zone 1					
PERSIANN-CCS	CC	MB $\frac{mm}{day}$	RMSE $\frac{mm}{day}$	POD	FAR	CSI
Original	0.24	0.28	0.98	0.67	0.55	0.37
Adjusted	0.22	0	0.62	0.4	0.5	0.28
Merged (Constant)	0.93	0.02	0.3	0.99	0.36	0.64
Merged (Not Constant)	0.97	0	0.38	0.97	0.33	0.65
	Zone 2					
PERSIANN-CCS	CC	MB $\frac{mm}{day}$	RMSE $\frac{mm}{day}$	POD	FAR	CSI
Original	0.25	0.24	1.42	0.67	0.48	0.41
Adjusted	0.17	0	1.12	0.51	0.4	0.38
Merged (Constant)	0.83	0.03	0.35	0.94	0.27	0.7
Merged (Not Constant)	0.89	0.02	0.22	0.9	0.28	0.67

PERSIANN-CCS	Zone 3					
	CC	MB	RMSE	POD	FAR	CSI
		$\frac{mm}{day}$	$\frac{mm}{day}$			
Original	0.32	1.03	3.7	0.67	0.48	0.41
Adjusted	0.37	-0.02	1.67	0.38	0.46	0.29
Merged (Constant)	0.66	0.06	0.9	0.93	0.26	0.7
Merged (Not Constant)	0.74	0.02	0.96	0.91	0.26	0.69

Original PERSIANN-CCS has the chance (POD) 67% of detecting the occurrences of the daily precipitations in the zones as shown in Table 3.6, while it falsely identifies the events of the daily precipitations 48% in Zone 2 and Zone 3, and 55% in Zone 1. Original PERSIANN-CCS overestimates the daily precipitations by 0.28 mm per day, 0.24 mm per day, and 1.03 mm per day in Zone 1, Zone 2 and Zone 3, respectively. As expected of the implementation of QM-CZ, the existence of the bias is reduced the daily overestimation of the original PERSIANN-CCS by less than 0.1 mm per day. The falsely detects the occurrences of the daily precipitations is reduced to be 50%, 40%, and 46% in Zone 1, Zone 2, and Zone 3, respectively. However, PODs of Adjusted PERSIANN-CCS are reduced to be 40%, 51%, and 38% in Zone 1, Zone 2, and Zone 3, respectively. This is expected because the correction is based on implementing QM, which is calculated based on historical observations. Therefore, some amount of the precipitation events are assigned to be no precipitation events, which influences the calculation of POD and CSI as shown in Table 3.6.

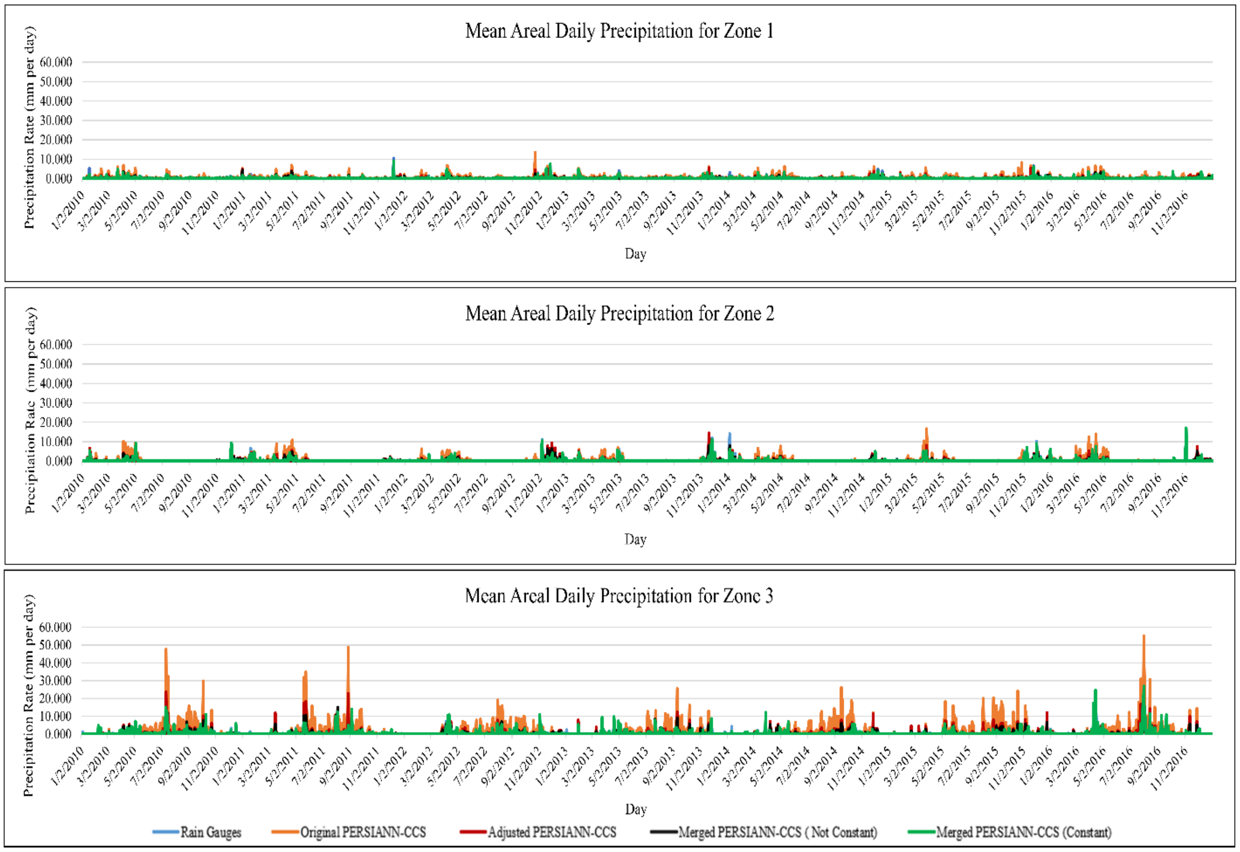

Figure 3.13 Mean areal daily precipitation for all zones during 2010 and 2016

When the merging is done for the two merging products, which are Merged PERSIANN-CCS (Constant), and Merged PERSIANN-CCS (Not Constant), CCs, MBs, RMSEs, PODs, FARs, and CSIs are improved. Based on the results shown in Table 3.6, Merged PERSIANN-CCS (Not Constant) has robust correlations with CCs are calculated to be 0.97, 0.89, and 0.74 for Zone 1, Zone 2, and Zone 3. The calculated CCs are improved by more than twice the correlations of Original PERSIANN-CCS as shown in Table 3.6. Merged PERSIANN-CCS (Not Constant) has the lowest overestimates in all the zones where it exceeds the daily precipitations by less than 0.02 mm per day that means the 99% of the bias that exists in Original PERSIANN-CCS is removed.

One of the benefits of the merging is to enhance the correctly detecting of the occurrences of the daily precipitations that what is shown in Table 3.6. Where Merged PERSIANN-CCS (Not Constant) accurately identifies the events of the daily precipitations by 97%, 90%, and 91% in Zone 1, Zone 2, and Zone 3, respectively. Also, Merged PERSIANN-CCS (Not Constant) incorrectly detects the occurrences of the daily precipitations by 33%, 28% and 26% in Zone 1, Zone 2, and Zone 3, respectively. PODs of Merged PERSIANN-CCS are improved by 44% in Zone 1, 34% in Zone 2, and 35% in Zone 3. Finally, When Merged PERSIANN-CCS (Constant) is compared to Merged PERSIANN-CCS (Not Constant), the latter one has best performances regarding CCs, MBs, and RMSEs, while it does not have best performances in PODs, FARs, and CSIs.

3.5 Conclusion and Recommendations

Based on the presented yearly, monthly, and daily results, this merging approach that is found in the distance and error functions can be used to improve dataset quality when the SPEs estimations and the rain gauge observations are merged. The proposed method blends the estimated daily estimations of PERSIANN-CCS with the rain gauges observations and removes the bias via two significant steps. First, the implementations of QM-CZ (Quantile Mapping and Climatic Zone) where the method is based on assuming that the rain gauges in the same climate zone share the same probability distribution function removes the majority of the existing bias in yearly and monthly the uncorrected PERSIANN-CCS estimations. Six years (2010 – 2015) are used to calibrate QM-CZ and one year (2016) is used to validate it. However, the major limitation of QM is that QM may not capture the occurrences of the daily precipitation (Jakob Themeßl et al., 2011) that is confirmed from day-by-day comparison. Second, to overcome this limitation and achieve a significant reduction in the bias, the blending the daily rain gauge observations with bias-corrected PERSIANN-CCS is done based on the uncertainty of each estimate, being presented as RMSE. The blending method is based on the degree of uncertainty is the function to the distance and daily precipitation rates where the degree of uncertainty linearly increases for a pixel with distance and estimated daily precipitation rate. This merging approach is effectively removing the bias of PERSIANN-CCS and highly improves the occurrences of the precipitations during the time the study is conducted. The high correlation and significant reductions in the bias during the annual, monthly, and daily scales confirm that this proposal merging is a useful tool to provide the high quality of bias-corrected PRESIANN-CCS.

Hence, this study can be used as a suitable tool to provide a high quality of precipitation datasets when the rain gauges are limited. Two recommendations can be drawn from this experiment. First, care should be taken when calculating the parameters, especially for the relationship between the precipitation rate and daily RMSE, and the relationship between the distance and daily RMSE. This is important because the estimations of the two equations influence the calculation of the weights. Second, the implementation of the QM-CZ is affected by the historical data timeline. When the timelines are short, there is a high degree of uncertainty.

Since the primary goal of this method is to provide the high quality of dataset that is based on the rain gauge observations, and SPE estimations that can be used in hydrological and climate studies, the in-depth examination of the proposed method will be investigated in future.

CHAPTER 4: Assessing the Efficacy of Bias Corrected Satellite-based Precipitation Estimation and Merging over Three Watersheds in Saudi Arabia

4.1 Introduction

Precipitation is the engine of the hydrological cycle, so the needs of accuracy precipitation observation are critical for hydrological and climatic studies (Cole & Moore, 2008; Fekete et al., 2004; Moradkhani & Sorooshian, 2008). Precipitation is primarily observed by rain gauges. Rain gauges provide precipitation observations at the point of the observation and obtaining a regional precipitation estimation from a rain gauge observation is done by using of one of the interpolation methods (such as Thiessen polygons, Kriging method, Shepard's Method etc.). However, (Andreassian et al., 2001; Faurès et al., 1995; Huff, 1970; King et al., 2013; Tozer et al., 2012; Villarini et al., 2008) have found that there is a degree of uncertainty associated with the extension of the rain gauges observations to estimate an areal precipitation that is associated with density and location of rain gauges. (J. D. Michaud & Sorooshian, 1994) examined the effect of rainfall sampling errors on hydrological modeling and found that the sampling rainfall from insufficient rain gauges especially on sparse rain gauges networks underestimated simulated runoff by more than 50% of the peak observed runoff. (Anctil, Lauzon, Andréassian, Oudin, & Perrin, 2006) examined the model performance when the mean areal precipitation was completed by using a number of the rain gauges, and the study found that the model performance was highly impacted by the number of the rain gauges that were used to obtain the mean areal precipitation. (Xu, Xu, Chen, Zhang, & Li, 2013) evaluated the influence of the rain gauge density on the hydrological modeling of Xiangjiang River basin, and one of the study findings was that the result of the hydrological modeling was improved when the number the rain gauge that was used to complete mean areal precipitation were increased. Also, economic and geographical situations repeatedly limit rain gauge availability. On the other hand, satellite-based precipitation estimations (SPEs) provide global measurements at fine resolutions, and SPEs becomes an alternative source of the precipitation measurement when rain gauges are limited (Al et al., 2004; Ashouri et al., 2015; Hong et al., 2004; Hou et al., 2014; K. Hsu et al., 1997; George J. Huffman et al., 1997, 2010, 2007; Kubota et al., 2006; Sorooshian et al., 2000).

SPEs have been widely used in hydrological modeling because of their ability to provide continuous and accurate estimations. (Z. Li et al., 2015) inspected use of Remotely Sensed Information Using Artificial Neural Networks-Climate Data Record (PERSIANN-CDR), the Global Land Data Assimilation System (GLDAS), and rain gauges on modeling the stream flow over upper the Yellow and Yangtze River basins. As a result, the simulated streamflow using PERSIANN-CDR and GLDAS showed good performance compared to observed streamflow. (Nguyen, Thorstensen, Sorooshian, Hsu, & AghaKouchak, 2015) examined the ability of Precipitation Estimation from Remotely Sensed Information Using Artificial Neural Networks–Cloud Classification System (PERSIANN-CCS) and NEXRAD Stage 2 precipitation data to simulate the 2008 Iowa flood in the United States. The simulated hydrograph by using PERSIANN-CCS matched the observed hydrograph better than stage 2. (Pakoksung & Takagi, 2016) modeled the streamflow on the Nan River basin using the products of six, and the results showed that the simulated streamflow of the six SPEs had a high correlation with observed streamflow. However, the existence of bias in SPEs limits the application of SPEs which has been confirmed by (Adler et al., 2000; Aghakouchak et al., 2011; J. Chen et al., 2013; Melo et al., 2015; Pereira Filho et al., 2010; Shah & Mishra, 2016; Teutschbein & Seibert, 2012a). Therefore, the removal of bias is curial to prior implement the SPEs on hydrological modeling (Hagemann et al., 2011; Piani et al., 2010; D. Sharma, Gupta, & Babel, 2007; Andrew W. Wood et al., 2002).

Numerous bias correction approaches are developed to remove the bias and improve the outcomes of SPEs. Among the bias correction approaches, the Quantile Mapping (QM) approach is widely used which it effectively removes the bias of SPEs (Ajaaj et al., 2016; Cannon, Sobie, & Murdock, 2015; Ines & Hansen, 2006; Teutschbein & Seibert, 2012a). QM is a distribution based approach that removes the bias by matching between two probability distribution functions (PDF) (Piani et al., 2010; Teutschbein & Seibert, 2012a). Therefore, QM is sensitive to the number of the samples, so the effectiveness of QM on removing bias is highly influenced by the sample size (Alharbi et al., 2018). Moreover, the performance of QM at daily scale has been investigated, and results showed that the QM was unable to adjust on the daily scale (Ajaaj et al., 2016; J. Chen et al., 2013; Teutschbein & Seibert, 2012a).

(Alharbi et al., 2018) proposed a bias correction approach based on QM and climatic zone, and the results of the study showed that the systematic bias of PERSIANN-CCS was removed by more than 87% over Saudi Arabia between 2010 and 2016. In order to improve the performance of QM and climatic zone, (Alharbi et al. 2019) tried to improve the performance of QM at the daily scale by merging between the rain gauge observations and bias corrected PERSIANN-CCS estimations. The study results confirmed that the merging assisted the performance of QM to remove the systematic and random bias.

The aim of this study is to examine the effectiveness of the bias corrected approach that is proposed by (Alharbi et al., 2018) and (Alharbi et al. 2019) in hydrological applications. Therefore, monthly and yearly observations of Bisha, Byash, and Hail watersheds and the Soil Conservation Service model are chosen for this purpose. The study time is six years between 2011 and 2016.

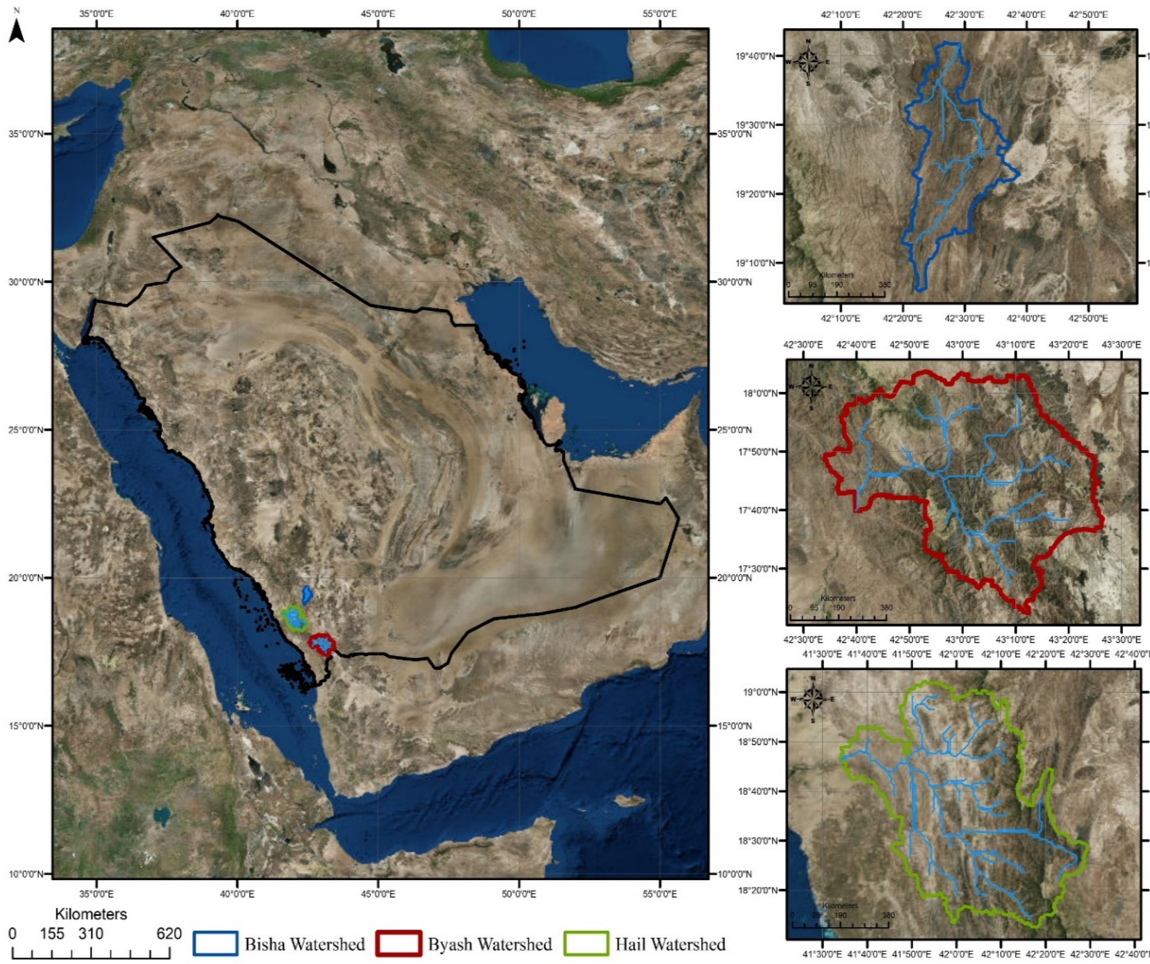

Figure 4.1 Map of three watersheds

4.2 Methodology and data acquisition

4.2.1 Study Area

For the purpose of this study, three watersheds are selected in Saudi Arabia, shown in Figure. 4.1. The three selected watersheds are Bisha, Byash, and Hail watersheds, and they are located in the southwest of Saudi Arabia. They are selected as the study area due to the diversity in their topography and climate. First, Bisha watershed is located in the Asir region, and the area of the watershed is 1002 Km^2 (see Table 4.1). Bisha watershed has the largest dam in Saudi Arabia, which is King Fahad Dam. Second, Byash watershed is located within the Asir region, and the area of the watershed is 4716 Km^2 (see Table 4.1). Hail watershed is one of the major five wadis of Tihamah coastal plain wadis, and the watershed has the second largest dam in Saudi Arabia. Third, Byash watershed is one of Tihamah coastal plain wadis, and it is located within the Jizan region, and the area of the watershed is estimated to be 3943 Km^2 (see Table 4.1). Byash watershed has third largest dams in Saudi Arabia, which is Byash Dam.

Table 4.1 Area of watersheds

Name of Watershed	Area Km^2
Bisha Watershed	1002
Hali Watershed	4716
Byash Watershed	3943

4.2.2 Precipitation

Four datasets are used on this study, and the description of data sources can be found in detail in Chapter 2 and Chapter 3. These datasets are rain gauges, the original PERSIANN-CCS, bias corrected PERSIANNN-CCS (Adjusted), and merged PERSIANN-CCS (Merged) at 0.04º by 0.04º latitude-longitude. The daily rain gauge observations between 2011 and 2016 are provided by the Ministry of Environment, Water, and Agriculture (MEWA) and the General Authority of Meteorology and Environmental Protection (GAMEP). The daily estimation of PERSIANN-CCS is provided by the Center for Hydrometeorology and Remote Sensing (CHRS).

4.2.3 Runoff Measurements

Unfortunately, existing stream measurements over Saudi Arabia are not available. However, Ministry of Environment Water & Agriculture tracks daily water volumes of dams, therefore, the water volume is used to estimate the runoff measurements. Three dams, which are Baysh Dam, King Fahad Dam, and Hali Dam, are used.

4.3 Rainfall–runoff modeling

In order to model the runoff, Soil Conservation Service curve number (SCS-CN) model is used (SCS, 1972). The model is found to be good or even better than complex runoff-rainfall models in gauged and ungauged watersheds (Al-Khalaf, 1997; J. Michaud & Sorooshian, 1994; Wagener, Wheater, & Gupta, 2004). The model is extensively used over Saudi Arabia. Studies use geographical information system (GIS) and remote sensing to compute SCS-CN and model the runoff over some parts of the study area (Al-Hasan & Mattar, 2014; Dawod, Mirza, & Al-Ghamdi, 2013; Mahmoud, Mohammad, & Alazba, 2014; Mohammad & Adamowski, 2015; Sharif, Al-Zahrani, & El Hassan, 2017).

The model estimates potential runoff based on curve number which is calculated based on soil type, land uses, and slope. SCS-CN estimates surface runoff by Equations 4.1, 4.2, and 4.3.

$$\mathrm{Q} = \frac{(\mathrm{P} - 0.2 * \mathrm{S})^2}{\mathrm{P} + 0.8 * \mathrm{S}} \tag{4.1}$$

$$\mathrm{S} = \left(\frac{25400}{\mathrm{CN}}\right) - 254 \tag{4.2}$$

$$\mathrm{V} = \mathrm{Q} * \mathrm{Area} \tag{4.3}$$

Q is potential runoff depth (mm), and P is the precipitation depth (mm). S is the soil retention (mm), and $CN$is the curve number. SCS-CN calculates the runoff based on the estimation of the effective precipitation depth, which is influenced by Curve Number “CN”. V is the runoff volume, and Area is the area of the watershed.

(Mohammad & Adamowski, 2015) calculated the curve number of Asir region. The study used Landsat-5 and Landsat-7 images that were provided by King Abdulaziz City for Science and Technology (KACST) with 15-meter ground resolution and were classified under the supervision and validated with ground true points. A soil texture map was generated by importing GPS points for soil texture that were collected during the field survey. The slope of the Asir region was calculated based on the DEM map that was provided by KACST with 15-meter resolutions. Validation the classification of land use and soil type using ground true points for the Asir region. As Bisha and Hail watersheds are located in the Asir region, the curve number developed by (Mohammad & Adamowski, 2015) are applied in this study.

4.3.1.1 Land cover

To classify Byash watershed, a free cloud image of Landsat 8 was obtained from the USGS Earth Explorer site. The image was collected on 9 June 2016 with path 167 and row 48. The image was projected to UTM zone 38.

4.3.1.2 Digital elevation model

In order to obtain the slope map for Byash watershed, DEM was downloaded from USGS Earth Explorer with the resolution a 30 meter. The DEM was collected on 19 November 2015. DEM was projected to UTM zone 38, and the fill sink function on ArcMap was used to fill the sink on the DEM grid.

4.3.1.3 Soil Texture

Generating the curve number requires knowing the soil texture of the Byash watershed. Therefore, information about the soil texture was obtained from the Saudi Geological Survey, and FAO-UN Digital Soil Map of the World sit (FAO, 2009).

4.4 Evaluation

The simulated runoff volumes that are estimated from rain gauges observations, the Original PERSIANN-CCS, the Adjusted PERSIANN-CCS, Merged PERSIANN-CCS, are tested against the monthly and yearly dam observations. The correlation coefficient (CC), mean bias (MB), and root mean square error (RMSE) are used to evaluate the simulated runoff volumes and are calculated by Equations 4.4,4.5, and 4.6.

$$\mathrm{CC} = \frac{\sum_{t=1}^{n}(O_t - \bar{O}) \;*\; \sum_{t=1}^{n}(S_t - \bar{S})}{\sqrt{\sum_{t=1}^{n}(O_t - \bar{O})^2} \;*\; \sqrt{\sum_{t=1}^{n}(S_t - \bar{S})^2}} \tag{4.4}$$

$$\mathrm{MB} = \frac{\sum_{t=1}^{n}(S_t - O_t)}{n} \tag{4.5}$$

$$\mathrm{RMSE} = \sqrt{\frac{\sum_{t=1}^{n}(S_t - O_t)^2}{n}} \tag{4.6}$$

In Equations 4.4, 4.5, and 4.6, O represents of observed water volume at the dam locations in specified month or year, and $\bar{O}$ is mean observed water volume at the dam. S represents the simulated monthly or yearly runoff volumes, and $\bar{S}$ is the mean monthly or yearly simulated runoff volume.

4.5 Results and Discussion

4.5.1 Calculating Curve Number

As mentioned above the land uses classification, soil texture, and elevation maps for Bisha and Hail watersheds are adopted from (Mohammad & Adamowski, 2015). The calculation for curve number, land uses, soil texture and elevation maps are shown in Figure. 4.2 and Figure. 4.3.

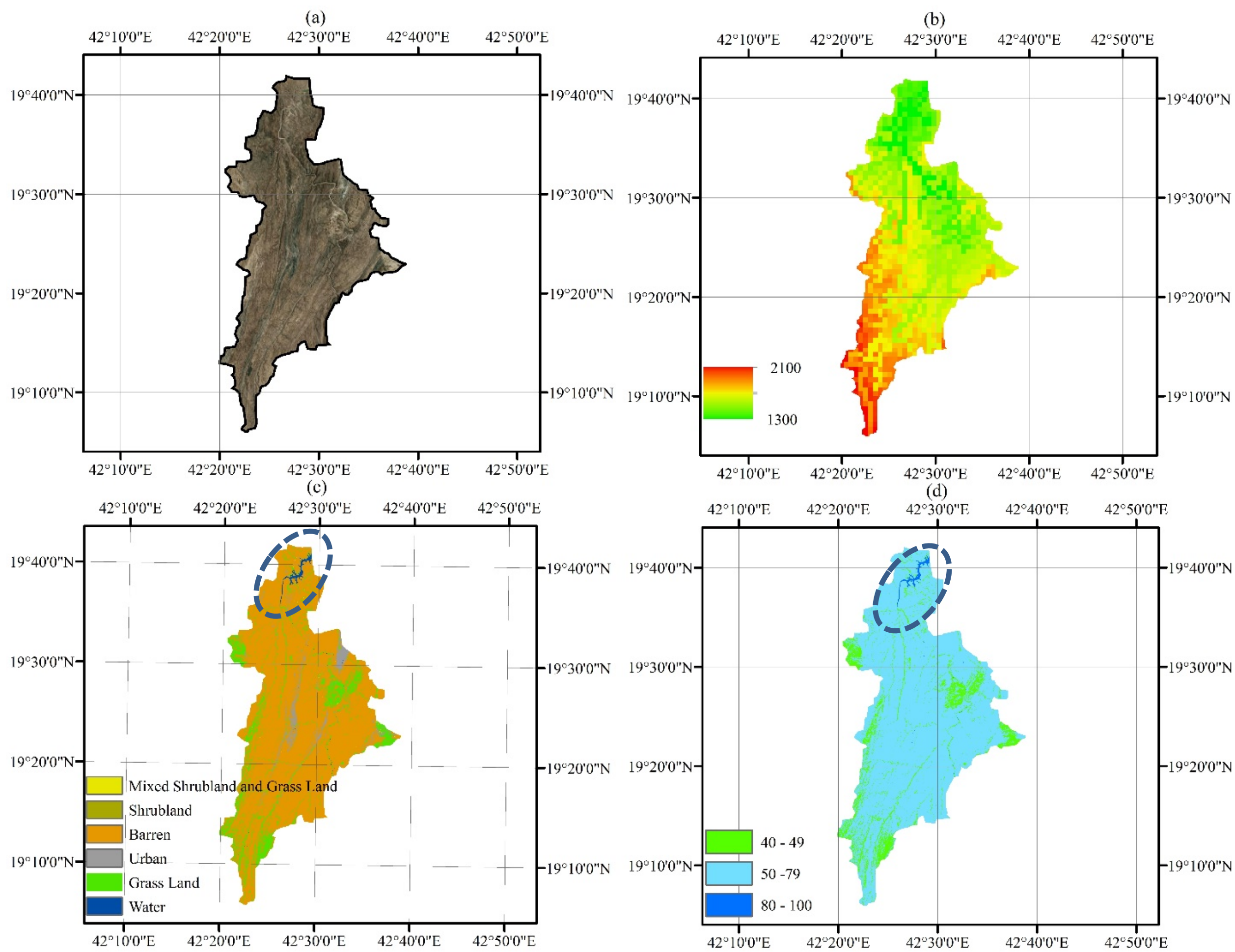

Figure 4.2 Bisha Watershed Map where (a) the map of the watershed, (b) the map of the elevation, (c) the map of land uses, and (d) the map of curve number.

Table 4.2 Distribution of land cover Bisha Watershed

Class	Area (Km^2)	Percentage
Mixed Shrubland and Grass Land	0.74	0.07%
Shrubland	0.61	0.06%
Barren	816.0	81.36%
Urban	51.0	5.06%
Grass Land	129.0	12.78%
Water	6.5	0.66%

Figure. 4.2 shows that the map of the watershed, and the map of the watershed's elevation, which ranges from 1 km to more than 2 km. As seen in Figure. 4.2, King Fahad Dam is located at the watershed mouth, and it is highlighted in blue line in the watershed land uses map. Table 4.2 shows the area and the percentage of land uses of the watershed. The largest land uses class is barren soil, accounting for more than 80%. The second largest class is grassland, covers more than 10% of the watershed. Finally, the distribution of the curve number is shown in Figure. 4.2.C, and it is clear that more than 50% of the potential rainfall may become potential surface runoff according to (Mohammad & Adamowski, 2015).

The land uses classification and the classification distribution of Hail watershed are presented in Figure. 4.3 and Table 4.3. In Figure. 4.3, the watershed's elevation ranges from less than 100 meters to 3 km, and the total area of the watershed, as mentioned in Table 4.3, is 4717 Km^2. Hail Dam is located at the watershed mouth that is shown in blue. The largest land uses is barren soil, which accounts for more than 50% of the watershed land use, and the second largest land use class is the urban area (see Table 4.3). As a result, the distribution of curve numbers is presented in Figure. 4.3, and the curve numbers range between 40 and 100, which means the potential of the precipitation that may convert to runoff ranges between those numbers. As mentioned above the distribution of the curve number and the land uses are adopted form (Mohammad & Adamowski, 2015).

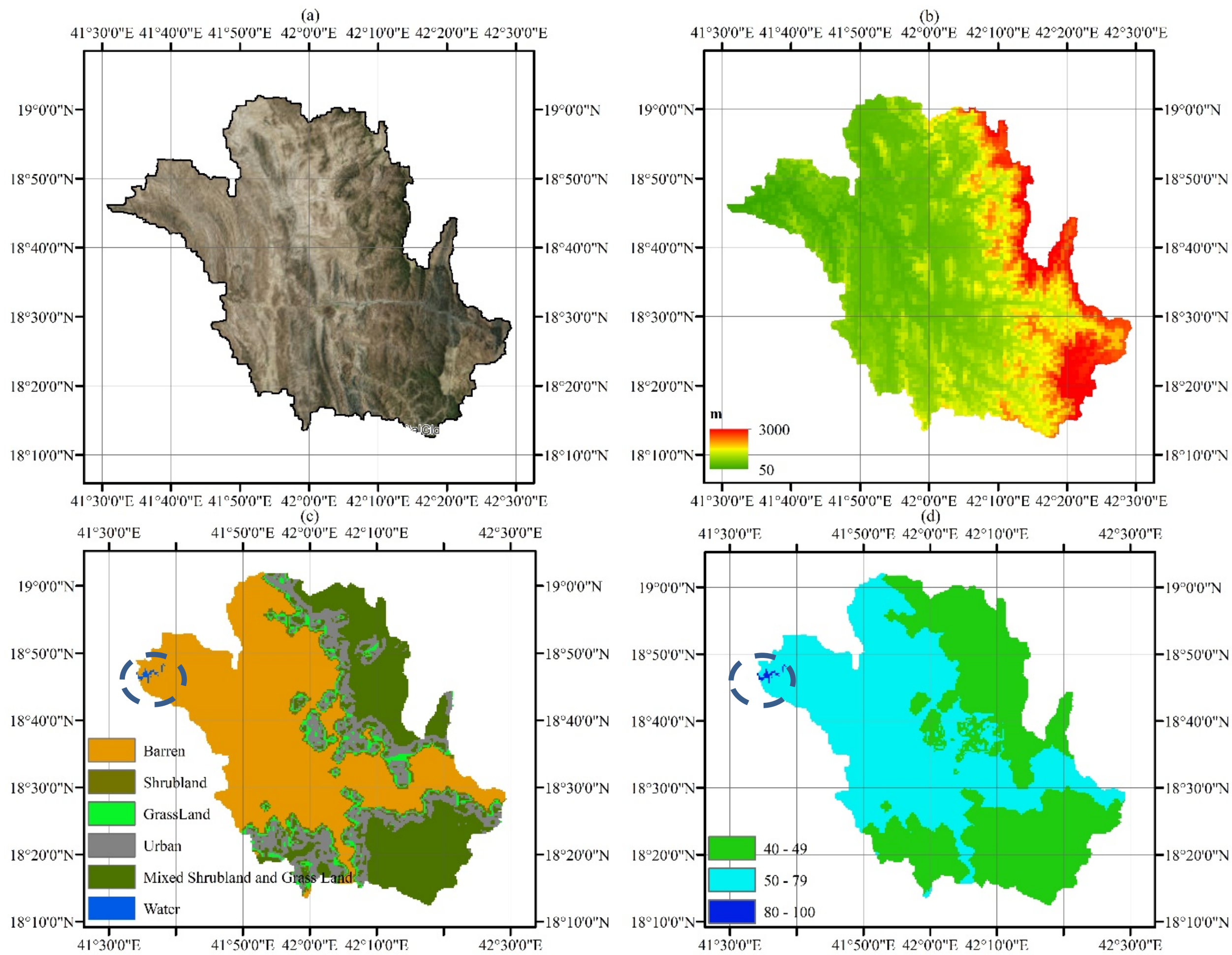

Figure 4.3 Hail Watershed Map where (a) the map of the watershed, (b) the map of the elevation, (c) the map of land uses, and (d) the map of curve number.

Table 4.3 Distribution of land cover Hail Watershed

Class	Area (Km^2)	Percentage
Barren	2472.0	52.42%
Shrubland	175.0	3.71%
Grass Land	23.0	0.49%
Urban	698.0	14.80%
Mixed Shrubland and Grass Land	1340.0	28.41%
Water	8	0.17%

The ArcMap was implemented to classify the land uses for the Byash watershed and the max likelihood was applied. The results of the classification are shown in Figure. 4.4 and Table 4.

Table 4.4 Distribution of land cover Byash Watershed

Class	Area (Km^2)	Percentage
Barren or Sparsely Vegetated	1259.9	31.96%
Urban	8.3	0.21%
Water	6.4	0.16%
Shrubland	1676.4	42.52%
Mixed Shrubland and Grass Land	835.1	21.18%
Grass Land	156.4	3.97%

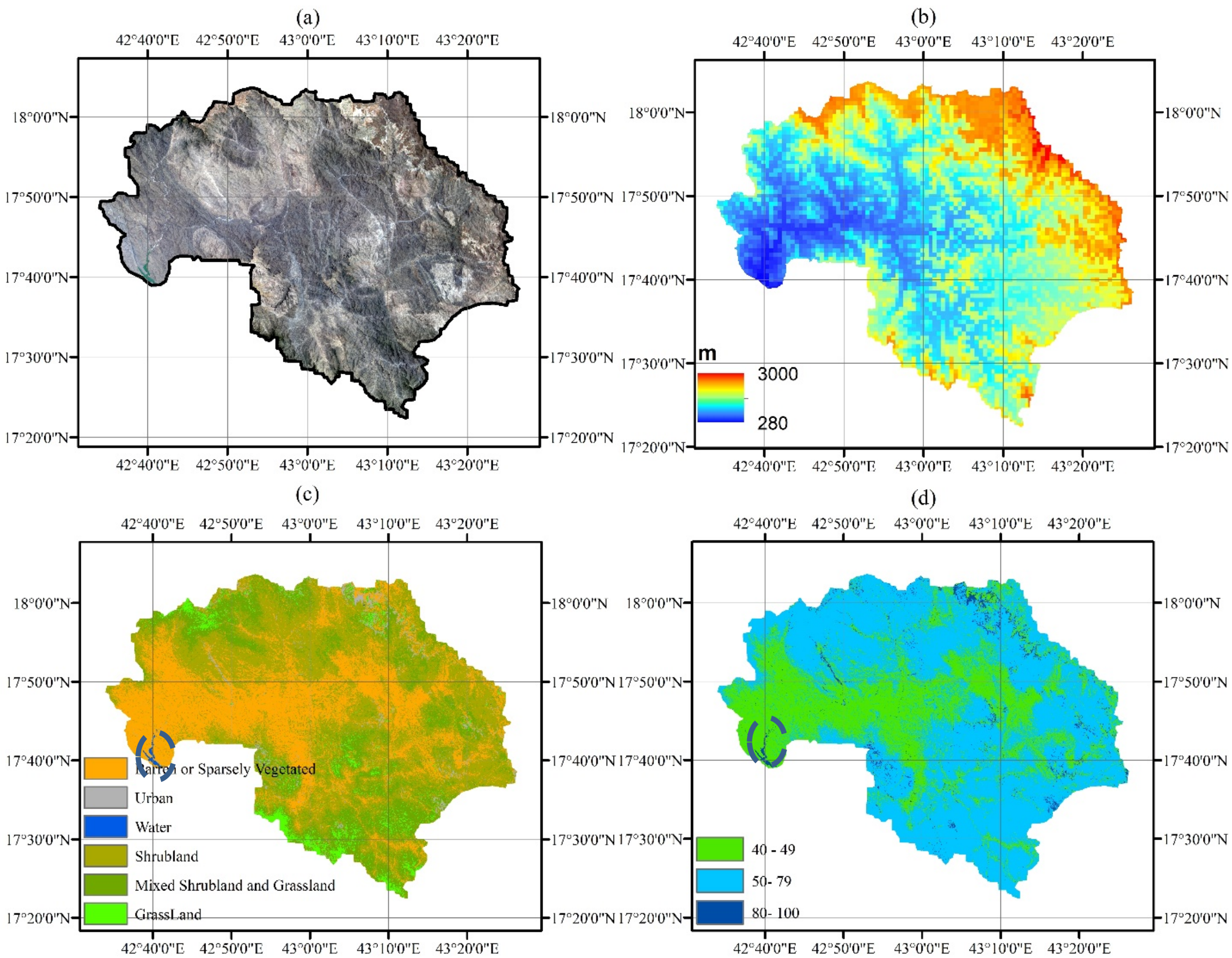

Figure 4.4 Byash Watershed Map where (a) the map of the watershed, (b) the map of the elevation, (c) the map of land uses, and (d) the map of curve number.

Figure. 4.4 shows that the Byash watershed has an elevation between less than 300 meters to 3 Km. Byash Dam is located at the watershed mouth, and it is clearly shown in Figure. 4.4. The largest land uses class is shrubland as presented by Table 4.4, and it covers around 43% of the watershed. The second largest land uses class is barren soil or sparsely vegetation that covers 32% of the watershed. The distribution of the curve numbers of the watershed is shown in Figure. 4.4 The distribution ranges between 40 and 100, and the potential of precipitations could become runoff is located on the watershed mouth where the water, and the upper of the watershed. The majority of the watershed has runoff number that ranges between 50 and 79.

The SCS model was implemented to estimate the monthly and yearly water volumes for each watershed and was compared to the observed water volumes. The results of the simulated runoff are presented for each watershed in the following sections.

4.5.2 Simulated Runoff Volume

4.5.2.1 Bisha Watershed

The monthly and yearly precipitations are shown in Figure. 4.5, where the monthly and yearly rain gauges, the Original PERSIANN-CCS, the Adjusted PERSIANN-CCS, and the Merged PERSIANN-CCS are presented in blue, red, green, and yellow respectively. The monthly

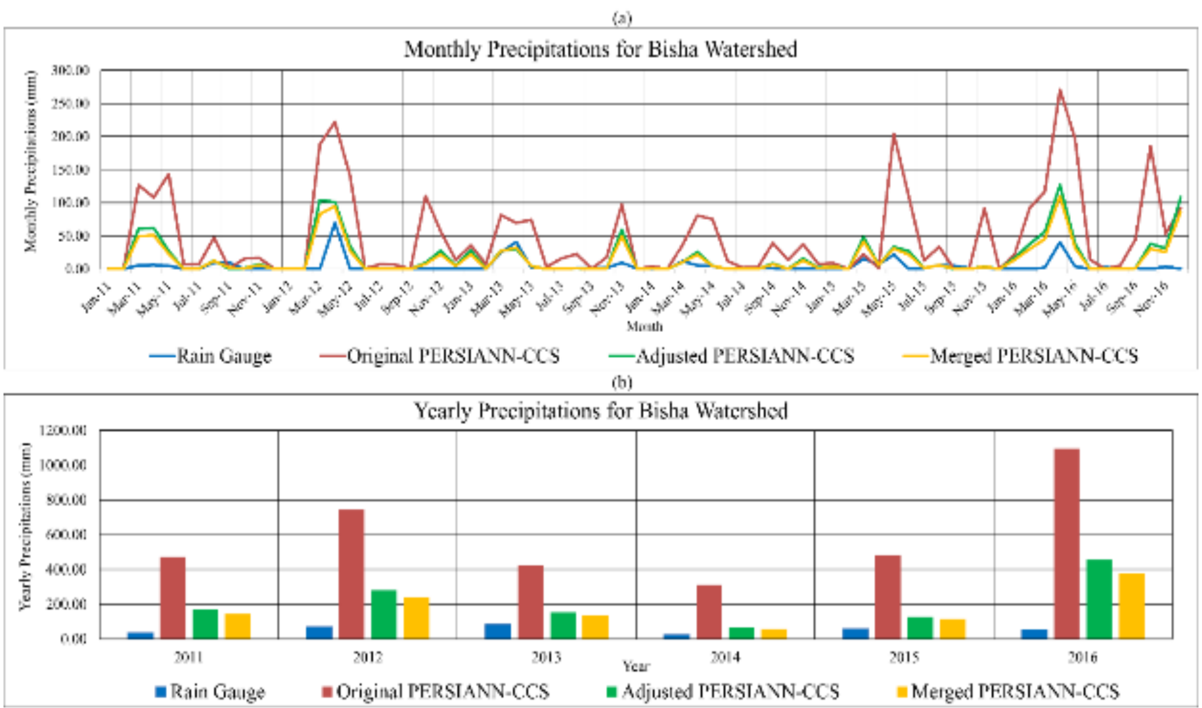

Figure 4.5 Mean areal precipitations over Bisha Watershed where (a) mean areal monthly, and (b) mean areal yearly.

and yearly runoff water volumes are shown in Figure. 4.6, and Figure. 4.7 where the simulated runoff volumes are shown, and the monthly and yearly dam observations are also presented. Finally, Table 4.5 and Table 4.6 present the results of the runoff volumes.

Figure. 4.5 shows the mean areal monthly and yearly precipitations over the watershed. Clearly, the rain gauges captured different in variation temporal precipitation compared to other datasets. Meaning, the highest precipitation depth of 85 mm recorded by the rain gauges was during 2013. On the other hand, the highest precipitation depths recorded by the Original, Adjusted, and Merged PERSIANN-CCSs were in 2016, with the depths were of than 1000 mm, 455.74 mm, and 375.7 mm respectively. Also, the second highest precipitation depths were estimated in 2012 where the rain gauges estimation was 72 mm, and the Original, the Adjusted,

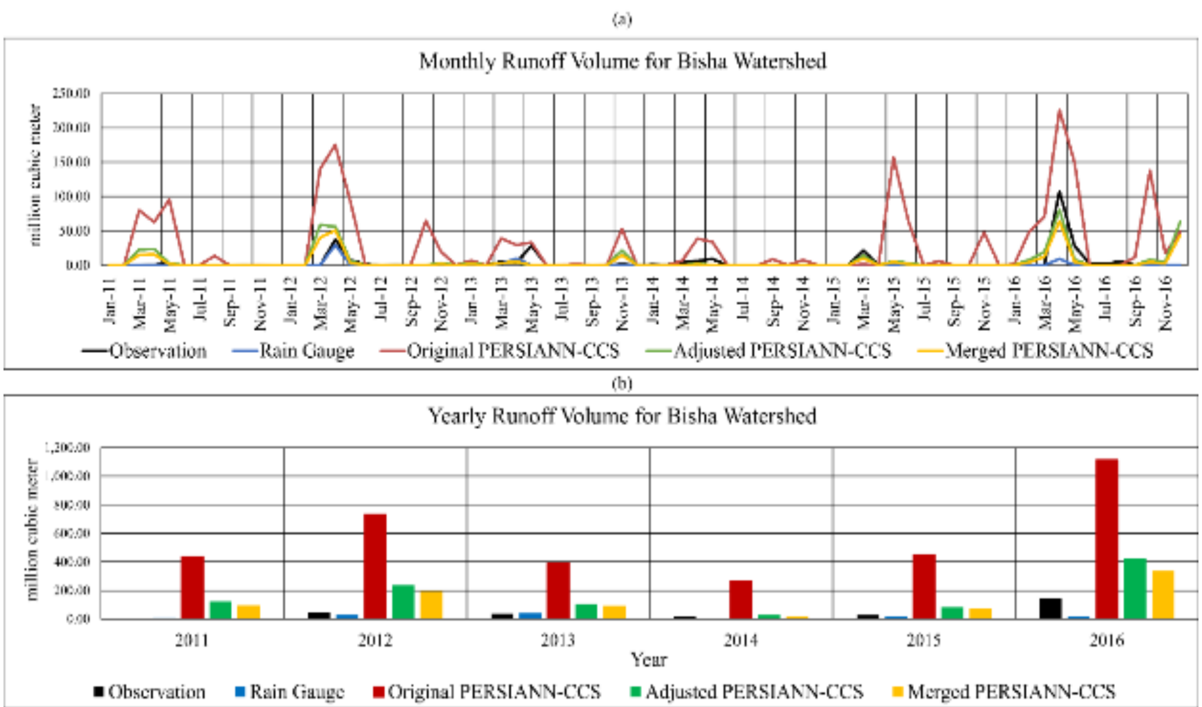

Figure 4.6 Mean Runoff Volume where (a) mean monthly runoff volumes, and (b) mean yearly runoff volumes

and the Merged PERSIANN-CCSs were 750 mm, 283 mm, and 240 mm, respectively. On the other hand, the lowest precipitation depths were estimated in 2014, where the depths were 25 mm, 310 mm, 68 mm, and 59 mm for the rain gauges, the Original, the Adjusted, and the Merged PERSIANN-CCSs, respectively.

In the monthly scales, the highest precipitation depth of 69 mm recorded by the rain gauges was in April- 2012, while the highest precipitation depth of 270 mm recorded by the Original PERSIANN-CCS was estimated in April-2016. Also, the highest precipitation depths were estimated by the Adjusted PERSIANN-CCS and the Merged PERSIANN-CCS 130 mm, and 109 mm respectively. The second highest precipitation depth of 41 mm recorded by rain gauges was in April-2013, while the Original PERSIANN-CCS estimated to be 222 mm. Also, the Adjusted PERSIANN-CCS has the second highest precipitation of 101 mm depth in Dec-2016. The Merged PERSIANN-CCS's second highest precipitation depth of 98 mm in April-2012.

Figure. 4.6 shows mean monthly and yearly runoff volumes. The observations are shown in the black, and the highest yearly runoff volume is estimated to be 145 million cubic meters during 2016, while the lowest yearly runoff volume is 3.2 million cubic meters during 2011. The highest monthly runoff volume is observed is 107 million cubic meters in April-2016. Based on the mean areal monthly and yearly rain gauge observations, the highest monthly simulated runoff volume is calculated to be 29.5 million cubic meters in April-2012, and the highest amount of the yearly simulated runoff volume is 30.9 million cubic meters in 2013. For the Original PERSIANN-CCS, the highest amount of yearly simulated runoff is calculated to be 1.110 billion cubic meters during 2016, and the highest monthly is 225.95 million cubic meters in April-2016. For the Adjusted, and the Merged PERSIANN-CCSs, the highest yearly runoff volumes are 422 million cubic meters (Adjusted PERSIANN-CCS), and 377 million cubic meters (Merged PERSIANN-

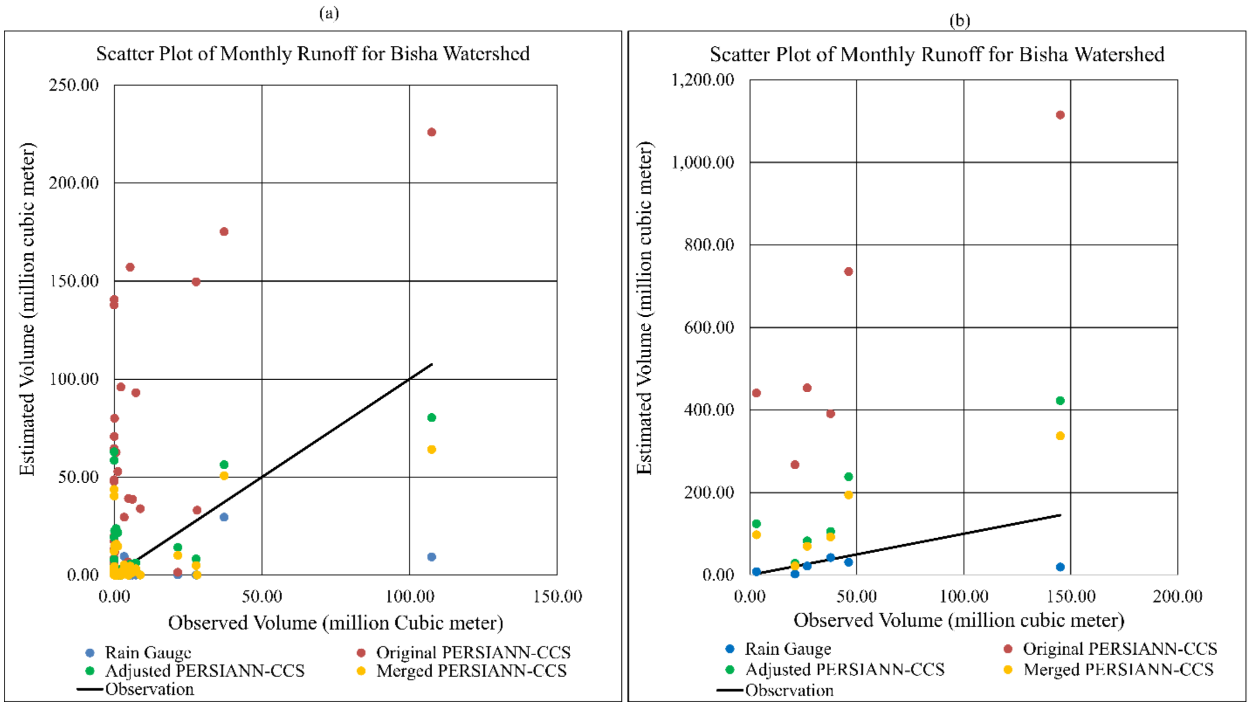

Figure 4.7 Scatter plots of the simulated runoff volumes where (a) Mean monthly, and (b) Mean yearly

CCS), respectively. On a monthly scale, the max amount of simulated runoff volumes are 80 million cubic meters, and 64.03 million cubic meters respectively.

Table 4.5 Monthly statistical evaluation for Bisha watershed

	Rain Gauges	Original PERSIANN-CCS	Adjusted PERSIANN-CCS	Merged PERSIANN-CCS
CC	0.51	0.63	0.63	0.677
MB (Million cubic meters per month)	-3.18	23.7	1.95	0.321
RMSE (Million cubic per month)	13	47.7	12.8	10.6

(a)

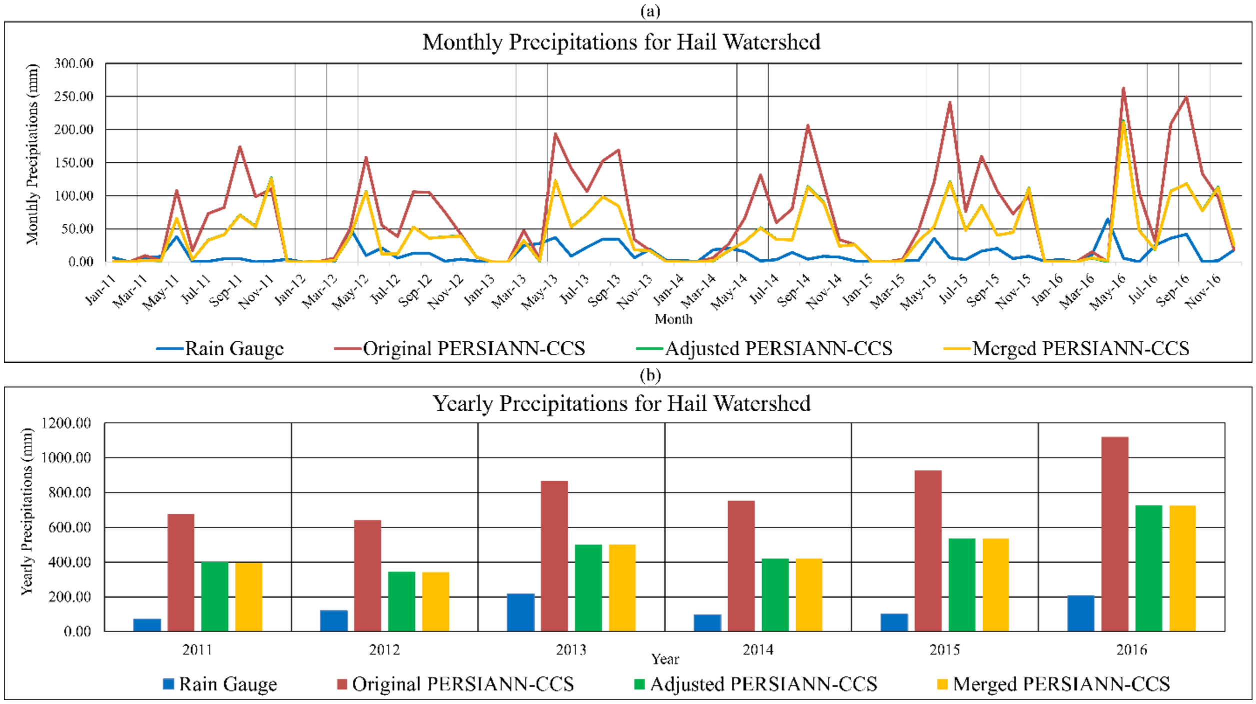

Figure 4.8 Mean areal precipitation over Hail Watershed (a) monthly, and (b) yearly

When comparing between the simulated monthly and yearly runoff volumes that are generated from the rain gauges, the simulated runoff volumes underestimate by 3.18 million cubic meters per month and 26.2 million cubic meters per year. Also, the rain gauges have poor correlation with the observations, where the monthly and yearly correlations are calculated to be 0.51 and 0.178 (See Table 4.5 and Table 4.6). On the other hand, the Original, the Adjusted, and the Merged PERSIANN-CCSs have strong yearly correlations of 0.908, 0.908, and 0.909 respectively. Also, simulated monthly and yearly runoff volumes by the PERSIANN-CCS overestimate, but the Merged PERSIANN-CCS shows the lowest values of the overestimations on monthly and yearly scales (See Table 4.5 and Table 4.6).

Figure. 4.7 where the simulated monthly and yearly runoff volumes are plotted. Clearly, the rain gauges do not follow the observations, which is plotted in black, on both scales, but the PERSIANN-CCSs may follow the observations. As shown in Figure. 4.7, the Adjusted PERSIANN-CCS, and the Merged PERSIANN-CCS show the lowest overestimations comparing to the Original PERSIANN-CCS.

Table 4.6 Yearly statistical evaluation for Bisha watershed

	Rain Gauges	**Original PERSIANN-CCS**	**Adjusted PERSIANN-CCS**	**Merged PERSIANN-CCS**
CC	0.178	0.908	0.908	0.909
MB (Million cubic meters per year)	-26.2	520	120	88.5

RMSE (Million cubic meters per year)	52.5	574	151	110

4.5.2.2 Hail Watershed

The mean areal monthly and yearly precipitations are shown in Figure. 4.8, and the observed and simulated runoff water volumes are shown in Figure. 4.9, and the scatter plots of the runoff are presents in Figure. 4.10. The statistical evaluations of the datasets are shown in Table 4.7 and Table 4.8.

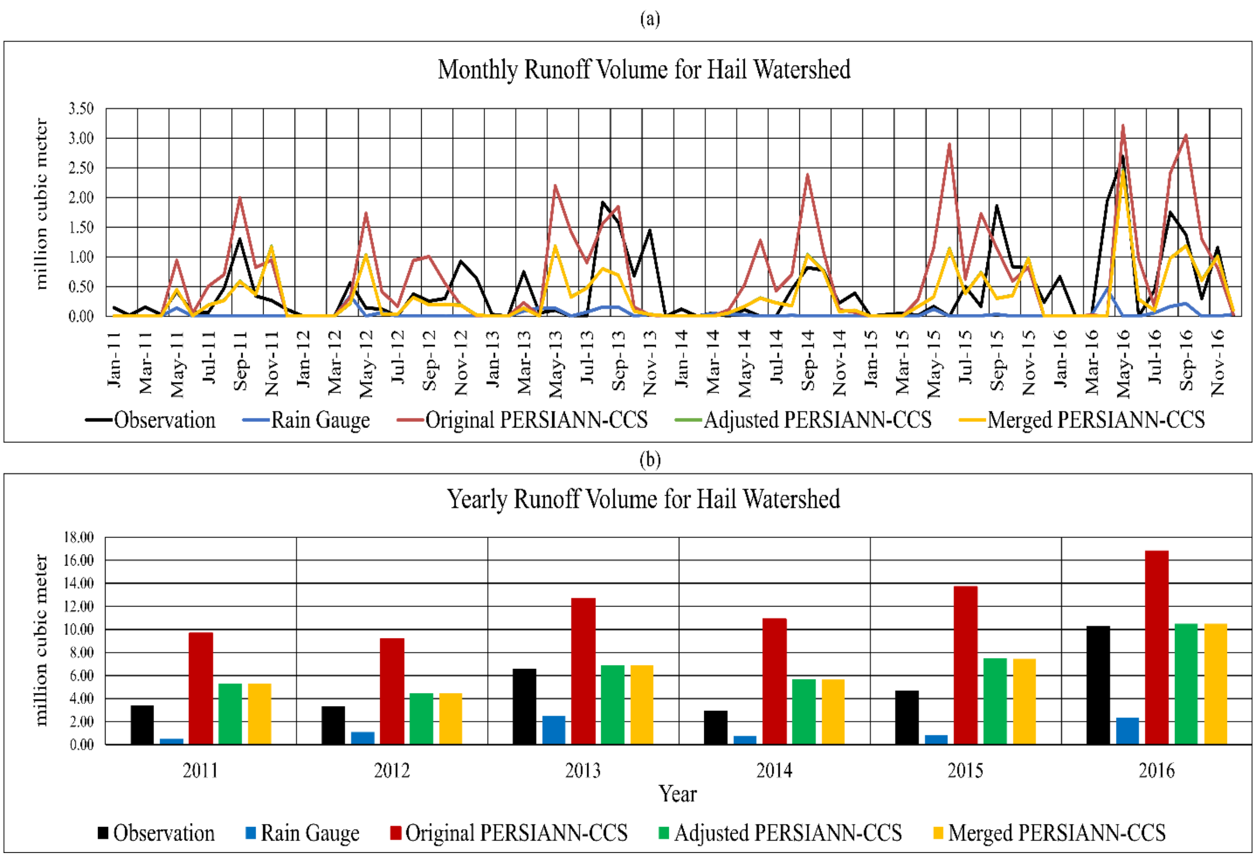

Figure 4.9 Mean Runoff Volume where (a) mean monthly runoff volumes, and (b) mean yearly runoff volumes

Figure. 4.8 presents the mean areal monthly and yearly precipitation depths by the four datasets. The max precipitation depth that was recorded by the rain gauges was more than 210 mm during 2013, and the second highest depth of 206 mm was observed during 2016. The highest precipitation depths that were estimated by the Original, the Adjusted, the Merged PERSIANN-CCSs were 1100 mm, 727.25 mm, and 725 mm respectively that was during 2016. They recorded the second highest precipitation depths during 2015 with 928 mm for the Original PERSIANN-CCS, 538 mm for the Adjusted PERSIANN-CCS, and 534 mm for the Merged PERSIANN-CCS.

On the monthly scale, the max monthly precipitation rates are shown in Figure. 4.8 is. First, the rain gauges observed 65 mm per month in April-2016, while the Original PERSIANN-CCS estimated 263 mm per month in May-2016, and the Adjusted PERSIANN-CCS estimated 213 mm per month, and the Merged PERSIANN-CCS estimated 211 mm per month. The second highest precipitations are shown in Figure. 4.8 are 51 mm per month for rain gauges during April-2012, 250 mm per month, during Sep-2016 for the Original PERSIANN-CCS, 127 and 125mm per month during November- 2011 for the Adjusted PERSIANN-CCS and the Merged PERSIANN-CCS.

In Figure. 4.9 where the monthly and yearly runoff volumes are shown, the max yearly observed runoff volume was recorded in 2016 to be 10.03 million cubic meters, and the max monthly runoff was 2.69 million cubic meters in May-2016. For the rain gauges, the highest similitude yearly and monthly runoff volumes were 2.5 million cubic meters in 2013 and 0.46 million cubic meters in April-2016. On the other hand, the max yearly and monthly runoffs that were generated by the Original PERSIANN-CCS were 16.7 million cubic meters and 3.2 million cubic meters during 2016 and May-2016 respectively. For the Adjusted and Merged PERSIANN-CCS, the highest yearly runoff volumes were 10.5 and 10.47 million cubic meters in 2016 respectively. In the monthly scale, the max runoff volumes were calculated to be 2.45 and 2.42 million cubic meters in May-2016 respectively.

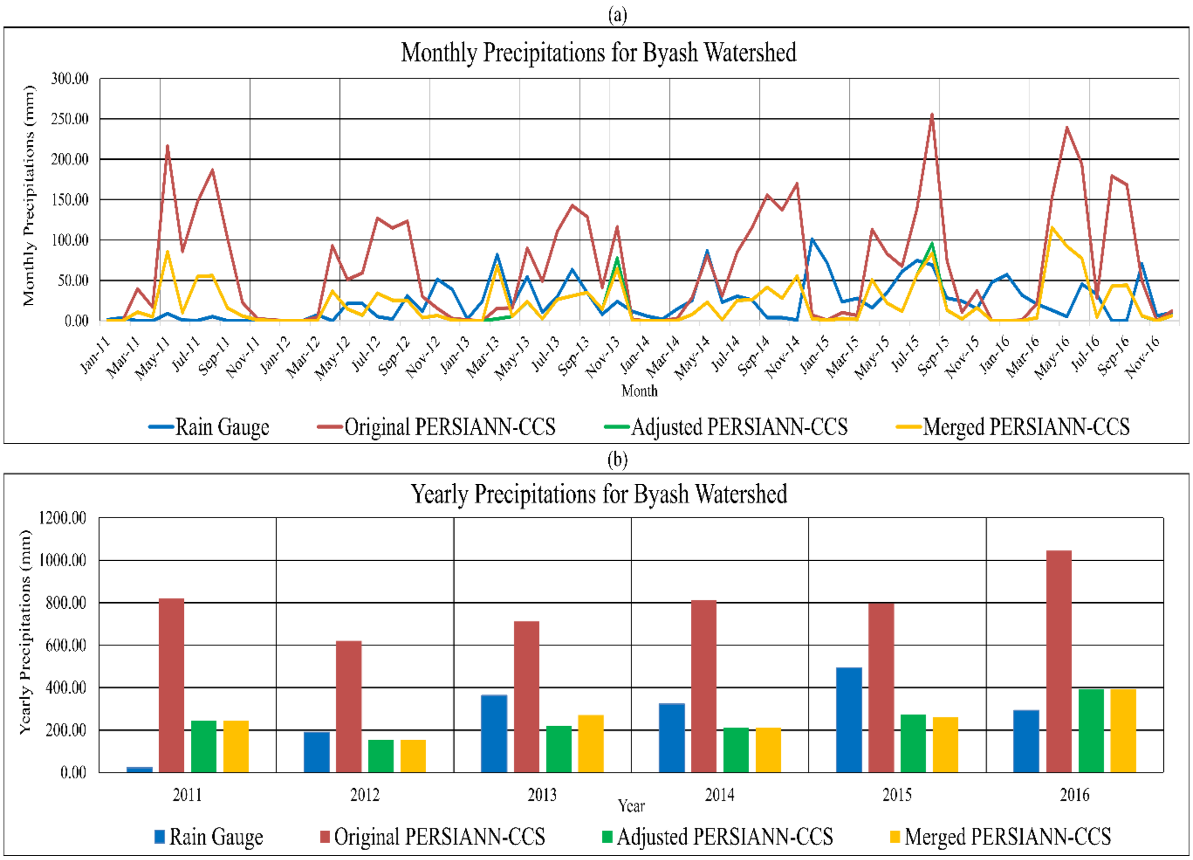

Figure 4.10 Mean areal precipitation over Byash Watershed (a) monthly, and (b) yearly

As shown in Figure. 4.10, and Table 4.7 and Table 4.8, the simulated monthly and yearly runoff volumes that were generated from the rain gauges underestimated compared to the observed volumes. In the monthly scale, the rain gauges underestimated by 0.39 million cubic meters per month and had monthly correlation around 0.42. The rain gauges have the second highest RMSE, which is 0.68 million cubic meters per month after the Original PERSIANN-CCS. As it is clarified in Figure. 4.10, the rain gauges on the monthly and yearly scales underestimate the runoff volumes.

On the other hand, the performance of the Adjusted and Merged PERSIANN-CCSs are the best, when compared to other simulated monthly and yearly runoff volumes. On a yearly scale, CCs are 0.54 and 0.54 respectively, and they have the lowest RMSEs, which are 0.523 million cubic meters per month and 0.522 million cubic meters per month. For the yearly scale, the Adjusted and Merged PERSIANN-CCSs are strongly correlated with the yearly observations by more than 0.92 and have lowest RMSEs by around 1.83 million cubic meters per year, but they overestimate the yearly runoff by around 1.5 million cubic meters per year.

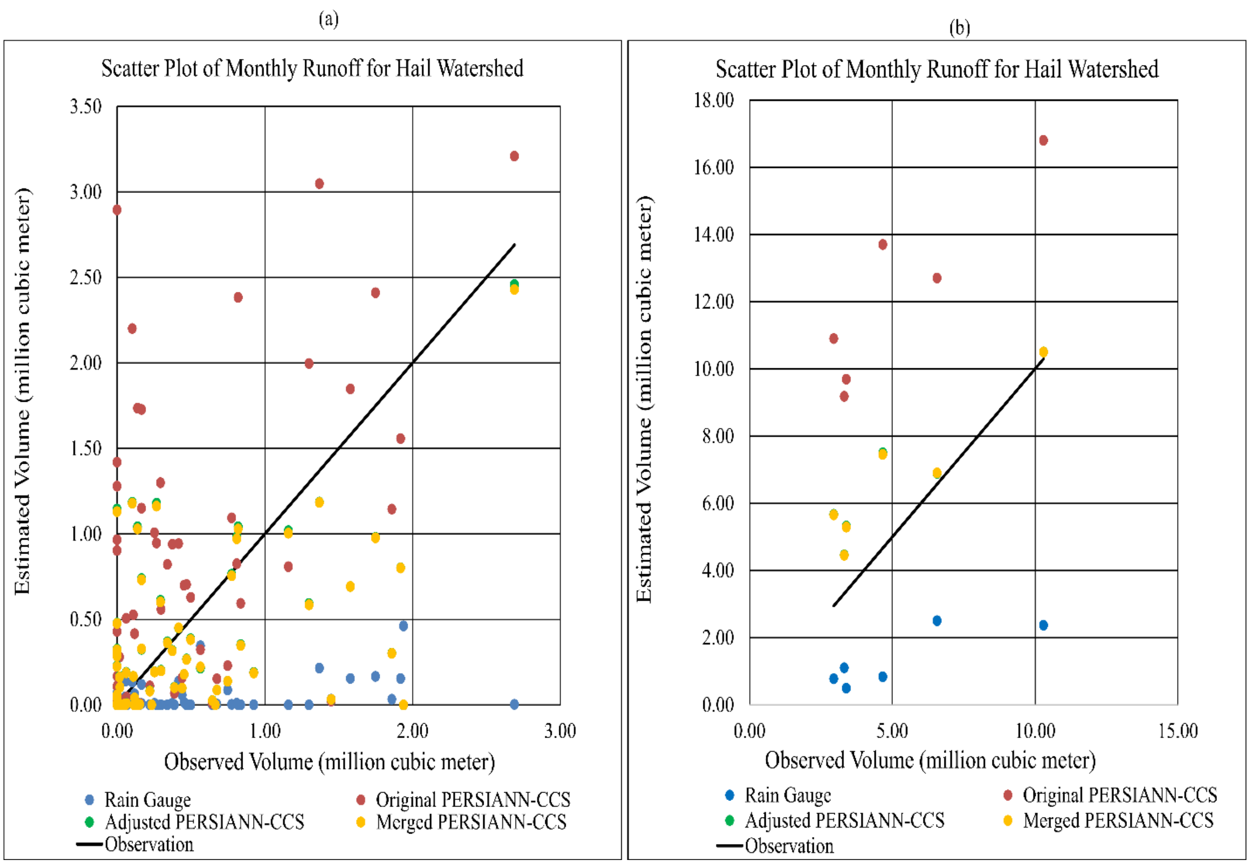

Figure 4.11 Scatter plots of the simulated runoff volumes where (a) Mean monthly, and (b) Mean yearly

Table 4.7 Monthly statistical evaluation for Hail watershed

	Rain Gauges	Original PERSIANN-CCS	Adjusted PERSIANN-CCS	Merged PERSIANN-CCS
CC	0.42	0.48	0.54	0.54
MB (Million cubic meters per month)	-0.398	0.227	-0.112	-0.115
RMSE (Million cubic meters per month)	0.686	0.777	0.523	0.522

4.5.2.3 Byash Watershed

As mentioned, Figure. 4.11, Figure. 4.12, and Figure. 4.13 present the mean areal monthly and yearly precipitations depths, the monthly and yearly runoff volumes with dam observations, and the scatter plots for the monthly and the yearly runoffs. Tables 4.9 and 4.10 show the statistical evaluations respectively.

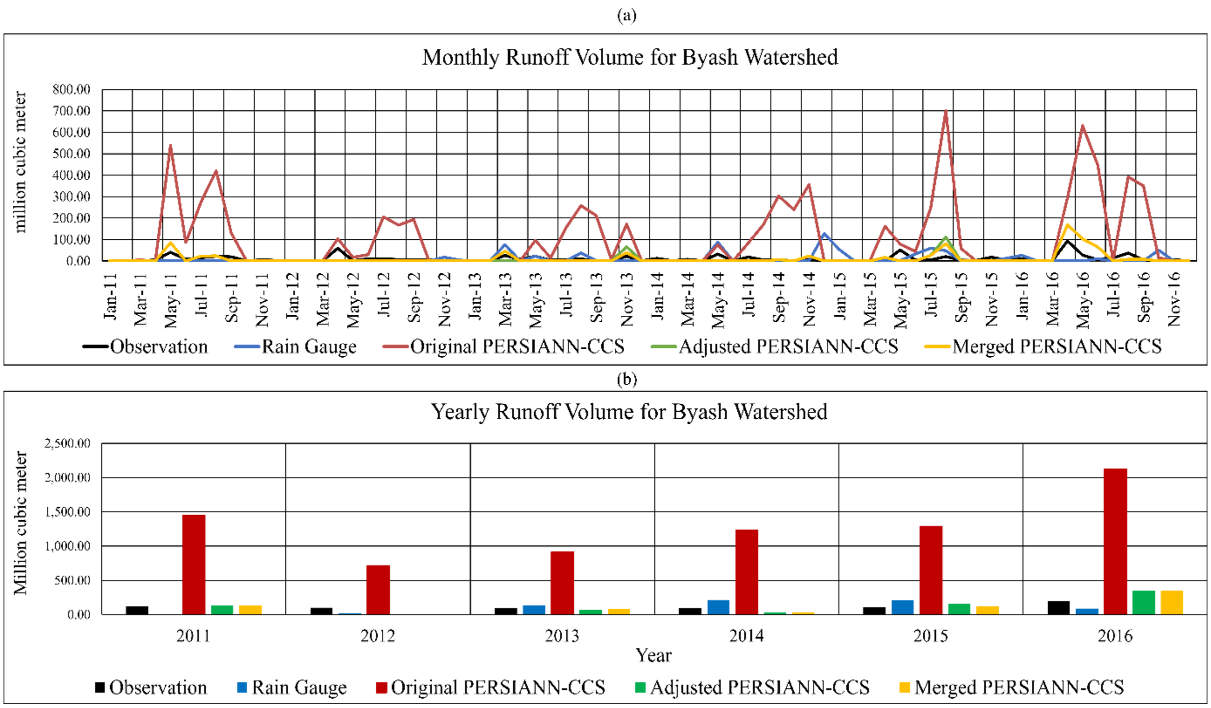

Figure 4.12 Mean Runoff Volume where (a) mean monthly runoff volumes, and (b) mean yearly runoff volumes

As expected, the max yearly precipitation depth was estimated by the Original PERSIANN-CCS in 2016 was depth 1044 mm. Also, the Adjusted PERSIANN-CCS and the Merged PERSIANN-CSS showed the same max variation as the Original PERSIANN-CCS in 2016 where the depths were more than 390 mm. On the other hand, the highest yearly precipitation depth recorded by the rain gauges was 493 mm in 2015. In addition, the second highest precipitation rate was 369 mm in 2013, and the same temporal variation was captured by the Merged PERSIANN-CCS where the depth was 271 mm. On the other hand, the second highest precipitation depth for the Original and the Merged PERSIANN-CCSs were 813 mm in 2014, and 273 mm in 2015 respectively. In the monthly scale, the max precipitation depth captured by the rain gauge was 102 mm in December-2014, while the Original PERSIANN-CCS captured 256 mm in August-2015. Also, the highest precipitation depths that were captured by the Adjusted PERSIANN-CCS and the Merged PERSIANN-CCS were 152 mm, and 116 mm in April-2016 respectively

Table 4.8 Yearly statistical evaluation for Hail watershed

	Rain Gauges	**Original PERSIANN-CCS**	**Adjusted PERSIANN-CCS**	**Merged PERSIANN-CCS**
CC	0.843	0.901	0.929	0.932
MB (Million cubic meters per year)	-3.857	6.968	1.521	1.497
RMSE (Million cubic meters per year)	4.332	7.063	1.853	1.827

The max yearly and monthly observed runoff volumes were 198.1 million cubic meters in 2016, and 93.2 million cubic meters that happened during April-2016 (See Figure. 4.12). For the rain gauges, the max monthly and yearly runoff volumes are 208 million cubic meters during 2015, and 126.5 cubic meters in December-2016. For the Original PERSIANN-CCS, the highest yearly and monthly runoff volumes are 2128 million cubic meters during 2016, and 700 million cubic meters. In addition, the max highest amount of simulated volumes by the Adjusted and Merged PERSIANN-CCSs are 352.9 and 353.07 million cubic meters. On the monthly scale, the highest monthly runoff volumes are 168.8 and 168.8 million cubic meters for the Adjusted PERSIANN-CCS and the Merged PERSIANN-CCS.

As shown by Tables 4.9 and 4.10, when the comparison between the performance of the Adjusted PERSIANN-CCS and the Merged PERSIANN-CCS with the other dataset, they show the best performance on monthly and yearly scales. Meaning, they have strong yearly correlation and good monthly correlation as shown in Tables 4.9 and 4.10. Also, they overestimated the yearly runoff by 0.32 and 0.14 million cubic meters. As shown in Figure. 4.13, the Adjusted PERSIANN-CCS and the Merged PERSIANN-CCS followed the observations. On the other hand, the rain gauges have poor yearly and monthly correlations, and they underestimated the runoff volumes by 7.85 million cubics for yearly and 0.65 million cubic meters for the monthly runoff. The Original PERSIANN-CCS overestimated the runoff monthly and yearly by 97.39 million cubic meters per month and 1168.67 million cubic meters per year.

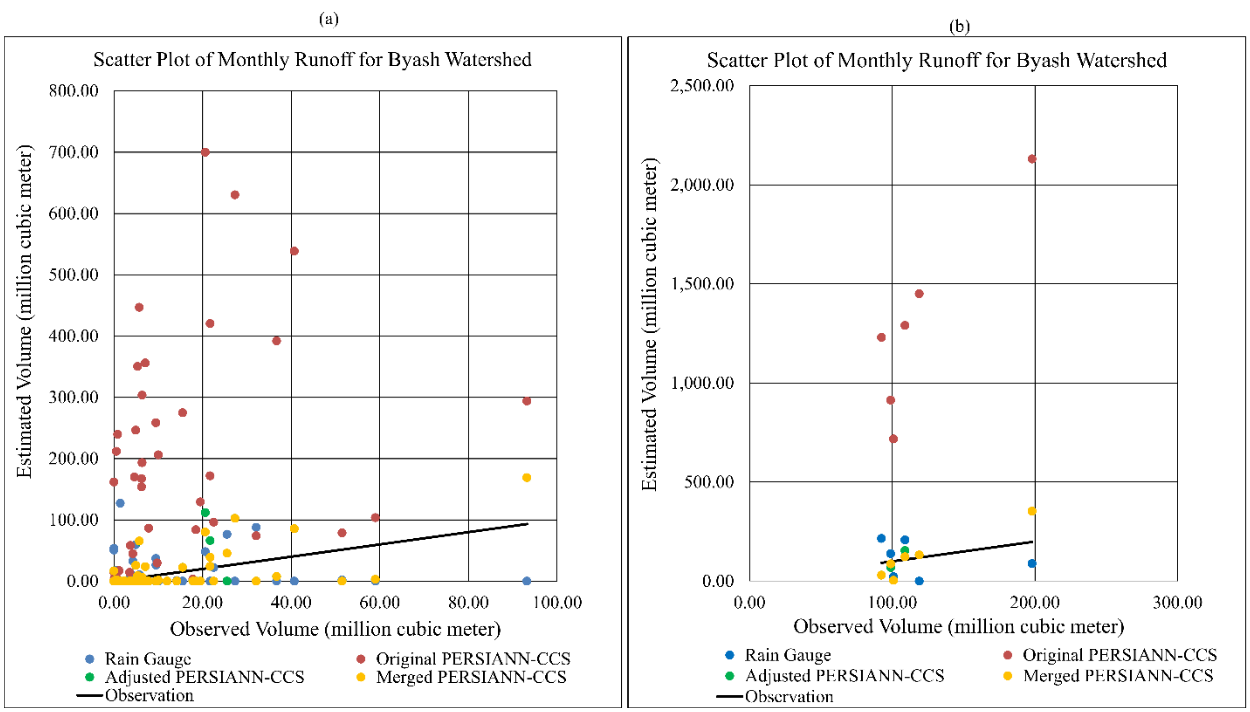

Figure 4.13 Scatter plots of the simulated runoff volumes where (a) Mean monthly, and (b) Mean yearly

Table 4.9 Monthly statistical evaluation for Byash watershed

	Rain Gauges	Original PERSIANN-CCS	Adjusted PERSIANN-CCS	Merged PERSIANN-CCS
CC	0.04	0.41	0.62	0.65
MB (Million cubic per month)	-0.65	97.39	0.32	0.14
RMSE (Million cubic per month)	27.48	184.37	23.37	21.29

Table 4.10 Yearly statistical evaluation for Byash watershed

	Rain Gauges	Original PERSIANN-CCS	Adjusted PERSIANN-CCS	Merged PERSIANN-CCS
CC	-0.24	0.89	0.95	0.96
MB (Million cubic per year)	-7.85	1168.67	3.88	1.70
RMSE (Million cubic per year)	98.75	1240.60	81.92	79.27

4.6 Conclusion

The main goal of this study is to evaluate of the effectiveness of the bias correction method that was developed by (Alharbi et al., 2018) against the non-bias corrected PERSIANN-CCS and rain gauge observations in hydrological modeling. Therefore, three watersheds have been selected, and the study was carried out between 2011 to 2016 where the monthly and the yearly dam observations are available. In the examination of the performance of the bias correction method, the bias corrected products, which are the Adjusted PERSIANN-CCS and the Merged PERSIANN-CCS, three conclusions can be drawn. First, when the performance of the bias corrected methods is compared to other products, this bias corrected method showed the best performance for all watersheds on monthly and yearly scales that confirmed the ability of the method to implement in the hydrological and calamitic modeling. Second, the bias corrected method works by removing the systematic and random biases from the Original PERSIANN-CCS that helps to reduce the overestimations in hydrological modeling. Third, when the performances of the non-bias corrected PERSIANN-CCS are evaluated against the rain gauges, it has better results that confirm the non-bias corrected can be applied in the modeling with reasonable estimations. Overall, the results approve that implementing the climatic zones to quantile mapping are effective, and the bias corrected method can be applied to correct the SPEs for prior implementation in the hydrological and climatic modeling when rain gauges are limited.

CHAPTER 5: Summery and Future Works

5.1 Summery

Satellite precipitation-based estimations become widely used in the hydrological and climatic studies, but the estimates usually are biased. The primary goal of this dissertation is to enhance and improve the applications of SPEs over a region where the ground observations are limited. To enhance the utilization of SPEs, the QM is chosen as an effective method to remove the bias of SPEs estimations. However, the QM has some drawbacks that limit the effectiveness of the QM in removing the bias. The disadvantages are discussed as following:

1) The QM is a distribution-based approach that matches between two PDFs, and the sample size is critical for the calculating of PDF. With sufficient samples, the PDF can be reliably estimated, and vice versa.
2) The purpose of the QM is to remove the bias by adjusting the PDF of a SPE to the reference data (gauge), and the QM works well in removing the bias in of the estimations accumulated to the monthly, seasonal, and the yearly scales. However, high variability in performance was found for the QM on the daily scale because of high variability of PDFs across climate zones.

To overcome the above limitation, this study examined the effectiveness of incorporating the climatic zone into the QM. Saudi Arabia is chosen to be the study area where the country has three climatic zones with limited rain gauge network. Findings and recommendations are summarized and listed below:

1) The performance of the localized QM has been tested over Saudi Arabia where the rain gauges are sparse where the number of samples that were used to calculate the PDFs were

small. The sensitivity of the sampling size was significant for localized QM where the assumption was that the rain gauges with the same climatic zones did not share the same the PDFs. Therefore, based on this assumption the existence of the bias was not effective removed. According to Table 2.2 and Table 2.3, the bias-corrected product with localized QM which is written as Adjusted PERSIANN-CCS without CZ, still overestimated or underestimated even after the QM was implemented. On the other hand, the including the climatic zones may overcome the sampling size limitations. Assuming the rain gauges that share the same climatic zones are sharing the same PDFs helps to remove the most the bias as presented in Table 2.2 and Table 2.3 where the bias-corrected using the climatic zone product, which is written as Adjusted PERSIANN-CCS with CZ has the lowest mean monthly and yearly biases and root mean square errors.

2) One of the most challenges are that how to interpolate the results of the implementation of the QM to remove the bias over a region where the rain gauges are limited. A notable and applicable approach is proposed to interpolate the results of the QM over Saudi Arabia. The approach is based in dividing the study area to many 1° by 1°, latitude and longitude, grids then the results of the QM is distributed found in the climatic zones. To interpolate the results of the QM to fine resolutions, the inversed weighted distance (IWD) is applied where four grids of 1° by 1°, latitude, and longitude, are included. To justify the including the climatic zones helps in removing the existence bias, the interpolation approach has been tested by comparing between incorporating and not incorporating the climatic zones. Not including the climatic zones leads to misallocate the spatial precipitation distribution over the study area where the results of the QM will be incorrectly interpolated as shown in Figure 2.24 where the Adjusted PERSIANN-CCS without Climatic Zone wrongly interpolated the results of the QM to regions where the precipitation rare occurs. Based on

the allocation of the Adjusted PERSIANN-CCS without Climatic Zone, the Empty Quarter, which is the largest sand desert in the world, receives a monthly precipitation rate during July around 30 mm per month. However, the only part of the country gets precipitation during July is the Hijaz and Asir Mountains, and the occurs of the precipitation rate is hardly ever in the country. On the other hand, the implementation of the interpolation approach with incorporating the climatic zones keeps the correct spatial distribution of precipitation sine using of the climatic zone prevents the misallocating of the results of the QM. As shown in Figure 2.24, the Adjusted PERSIANN-CCS with Climatic Zones matches the rain gauges observations in the monthly and yearly scales. During July where most of the country does not receive the precipitation, the Adjusted PERSIANN-CCS with Climatic Zones keeps the spatial distribution of precipitation that matches the rain gauge observations. No doubt, using the interpolation approach with incorporating the climatic zones keeps the spatial distribution of the precipitation, and it can be a useful tool to remove and interpolate the bias of SPEs over a region where the rain gauges are limited or unavailable.

3) One of the QM limitations is that the lack of the correction and the removing of the bias in the daily scale. The QM matches well in PDFs but cannot match well the corresponding day-by-day precipitation time series. To further improving the data quality, effective integration of rain gauges and SPEs is an option.

4) Therefore, the merging between the daily rain gauge observations and the daily satiates estimates helps to enhance the outcomes of the QM as the results show in Chapter 3. The merging approach is done by three steps: (1) the implementation of the QM by incorporating the climatic zones; (2) the gridding the daily rain gauge observations to match spatial resolutions of satellite estimates by implementing Inverse weighted distance

(IWD); (3) the two data sets which are the bias-corrected product and the gridded rain gauge observations are merged where the degree of the uncertainty of each data sets is addressed by the implementation of inversed root mean square error (IRMSR).

5) IRMSR is a useful tool to be implemented for merging between the rain gauges and satellite precipitation estimates especially when the rain gauges are limited or unavailable because IRMSE helps to assign the weights for each pixel based on the distance and the precipitation rates.
6) Assuming the degree of the uncertainty is a function of the precipitation rates, and the degree of the uncertainty changes as the precipitation rates changes is an applicable approach to comping between the rain gauge observations and satellite precipitation estimates when the rain gauges are limited. As the results of the implementation of this approach, which is named as "the Merged PERSIANN-CCS Not Constant" is improved especially at the daily scales where tremendous reductions are shown in mean daily bias, root mean square, and flash alarm. Also, the utilization of this approach hugely improves the daily correlation coefficient and the probability of detection.
7) Assuming the degree of the uncertainty is function of the precipitation rates and it does not change as the precipitation rate changes, which is named as is "the Merged PERSIANN-CCS Constant" not a valid tool when the rain gauges are limited since it the estimations of the gridded rain gauges overtaken satellite precipitation estimates. That eliminates the benefits of the satellite precipitation estimates.

The implementation of the QM with incorporating climatic zones can be very useful for hydrological and climatic studies for regions where ground observations are limited. Experiments are extended to the hydrological modeling is performed using rain gauge observations, the uncorrected PERSIANN-CCAS (the Original PERSIANN-CCS), the bias-corrected (the Adjusted PERSIANN-CCS), and the Merged PERSIANN-CCS.

The three selected watersheds are Bisha, Byash, and Hail watersheds, and they are in the southwest of Saudi Arabia. They are chosen as the study area due to the diversity in their topography and climate. All those watersheds have dams which are the biggest dams in Saudi Arabia. The Soil Conservation Service curve number (SCS-CN) is selected. The primary model input is the curve numbers which were provided by Mohammad & Adamowski (2015) for two watersheds (Bisha and Hail), and calculated from the land sat image, soil type, and DEM maps for Byash watershed. Precipitation data, including the daily rainfall from (1) rain gauge, (2) the Original PERSIANN-CCS, (3) the Adjusted PERSIANN-CCS, and (4) the Merged PERSIANN-CCS Not Constant for each watershed, are used to generate the monthly and yearly runoff volumes at the test basins.

When the monthly and yearly runoff volumes generated from the rain gauge observations are compared against the dam observations, the SCS-CN generated runoff volumes did not match well with the observations in test watersheds. It can be that, the sparse rain gauge network can result in unreliable observations of basin area rainfall for runoff volumes generation.

The benefits of the implementation of the SPEs in the hydrological modeling is clearly shown in all watersheds where the satellites estimations have the strong correlations with the observations. The monthly and yearly volumes that are generated by the biased and uncorrected, the Original PERSIANN-CCS, matches the monthly and annual observed water volumes in all the watersheds, but the created water volumes overestimate. The behind reason is that the existing bias in the Original PERSIANN-CCS makes the generated runoff volumes overestimations regarding monthly and yearly mean bias and RMSE.

The implementations of the QM with incorporating of the climatic zones helps to remove the existence bias in the Original PERSIANN-CCS, and the yearly and monthly generated runoff volumes using the precipitations that are estimated by the Original PERSIANN-CCS strongly correlate with the dam observations. The created runoff volumes using the Adjusted PERSIANN-CCS follows the dam observations with much reductions in the mean bias and RMSE of the runoff volumes.

The combining between the rain gauge observations and SEPs based on the distance and the precipitation rates as functions for the degree of the uncertainty helps to achieve more reductions in the bias and improving the performance of the QM. That is confirmed where the generated monthly, and yearly runoff volumes have the lowest mean bias and RMSE in all watersheds. The bias that exists in the Original PERSIANN-CCS and makes the created runoff volumes of the Original PERSIANN-CCS overestimation is successfully removed by the implementation of the QM and the merging approach.

The results of the implementation of the QM with incorporating the climatic zone helps to remove the bias over Saudi Arabia where the rain gauges are limited. The results confirmed that including of the climatic zones is a suitable solution to remove the bias. Furthermore, without any doubt, the merging approach that is based involving the IWD as the interpolation tools, and weighing the pixel based on the distance from the rain gauge and the precipitation rates is a reliable tool to use to achieve more reduction in the bias and improving the results of the QM with climatic zones.

5.2 Recommendations

Based on the results, the QM with incorporating climatic zones and the merging approach are the applicable tool that can consistently adjust a large amount of the bias when the ground observations are limited since the QM uses the advantages of the historical ground observations and SPEs. Also, the merging approach uses the benefits of the rain gauge observations. Here, some recommendations will help to implement this method over other regions of the world when the rain gauges are limited or unavailable.

1) The adjustment of the bias is made by matching between CDFs, so the model calibration needs the high-quality historical ground observations. When the high-quality historical is unavailable, the using for seasonal CDFs may overcome the limitation and improve the model calibration.
2) Dividing the study area to 1° by 1° box and implementing IWD is not needed when the study area has one CZ.
3) Care should be taken when calculating the parameters, especially for the relationship between the precipitation rate and daily RMSE, and the relationship between the distance and daily RMSE. This is important because the estimations of the two equations influence the calculation of the weights.

5.3 Future Directions

The primary goal of this dissertation is to enhance and improve the applications of SPEs over a region where the ground observations are limited. Needless to say, that future extensions can be made, and the following are some of the areas for the future extensions:

Using Near Real-Time Remote Sensing Precipitation Data for Flood Forecasting over Study Area

The shortage of the reliable precipitation measurements may lead to catastrophic results. For example, my country which is Saudi Arabia, has suffered from floods, and the shortages of the precipitation measurements effects the managements against floods. The utilizing of Satellite-based precipitation estimations (SPEs) may help my country to mitigate flood damages since the SPEs provide globally and hourly precipitations estimations that could use to forecast flood events. This is one of the dissertation motivations.

The Implementation of the Bias-Correction Approach in Hydrological Cycle.

As I mentioned in the motivation section, the needs for sustainable water management in my country are critical needs. To successfully achieve this goal, there is a need for reliable precipitation data. Therefore, examining the effectiveness of the bias correction over one of the watersheds in Saudi Arabia where the data is available and accurate is one of my future goals where one of the advance hydrological models will be implemented to test the effectiveness of the bias corrections in the hydrological cycle.

Evaluation of effectiveness of the Bias-Corrections Approach in Near Real Time observations.

The performance of the proposal bias-correction approach has been tested and successfully removes the bias in the yearly, seasonal, monthly and daily scales, but the approach has not tested in the near real time. Evaluation of the bias corrections in near real times may enhance the application of the proposal method in flood forecasting.

Comparison Between the Outcomes of the Bias-Correction Approach and Major Satellite-Based Precipitation Estimations

The performance of the proposed bias-correction approach is evaluated against the observations of the rain gauge in the study area, but the performance of the bias-correction has not been tested against other major satellite-based precipitation estimations. The evaluations of the outcomes of the bias-corrections against the other SPEs may support the using of the bias-correction when the rain gauges are limited.

REFERENCES

(MAW), M. of A. and W. (1984). Water Atlas of Saudi Arabia. Saudi Arabia, Ministry of Agriculture and Water Riyadh.

Abderrahman, W. A. (2005). Groundwater management for sustainable development of urban and rural areas in extremely arid regions: A case study. *International Journal of Water Resources Development*, *21*(3), 403–412.

Abdullah, M. A., & Al-Mazroui, M. A. (1998). Climatological study of the southwestern region of Saudi Arabia. I. Rainfall analysis. *Climate Research*. https://doi.org/10.3354/cr009213

Adler, R. F., Huffman, G. J., Bolvin, D. T., Curtis, S., & Nelkin, E. J. (2000). Tropical Rainfall Distributions Determined Using TRMM Combined with Other Satellite and Rain Gauge Information. *Journal of Applied Meteorology*. https://doi.org/10.1175/1520-0450(2001)040<2007:TRDDUT>2.0.CO;2

Adler, R. F., Huffman, G. J., Chang, A., Ferraro, R., Xie, P.-P., Janowiak, J., … Nelkin, E. (2003). The Version-2 Global Precipitation Climatology Project (GPCP) Monthly Precipitation Analysis (1979–Present). *Journal of Hydrometeorology*. https://doi.org/10.1175/1525-7541(2003)004<1147:TVGPCP>2.0.CO;2

Aghakouchak, A., Behrangi, A., Sorooshian, S., Hsu, K., & Amitai, E. (2011). Evaluation of satellite-retrieved extreme precipitation rates across the central United States. *Journal of*

Geophysical Research Atmospheres. https://doi.org/10.1029/2010JD014741

Ahmed, B. Y. M. (1997). Climatic classification of Saudi Arabia: An application of factor--Cluster analysis. *GeoJournal*, *41*(1), 69–84.

Ahrens, B. (2006). Distance in spatial interpolation of daily rain gauge data. *Hydrology and Earth System Sciences*. https://doi.org/10.5194/hess-10-197-2006

Ajaaj, A. A., Mishra, A. K., & Khan, A. A. (2016). Comparison of BIAS correction techniques for GPCC rainfall data in semi-arid climate. *Stochastic Environmental Research and Risk Assessment*. https://doi.org/10.1007/s00477-015-1155-9

Al-Hasan, A. A. S., & Mattar, Y. E. S. (2014). Mean runoff coefficient estimation for ungauged streams in the Kingdom of Saudi Arabia. *Arabian Journal of Geosciences*, *7*(5), 2019–2029. https://doi.org/10.1007/s12517-013-0892-7

Al-Khalaf, H. A. (1997). Predicting short-duration, high-intensity rainfall in Saudi Arabia. MS Thesis, Faculty of the College of Graduate Studies, King Fahad University of Petroleum and Minerals, Dhahran, KSA.

Al-Qurashi, M. (1981). Synoptic climatology of the rainfall in the southwestern region of Saudi Arabia. *Unpublished MSc Thesis, Western Michigan University, Michigan, USA*.

Al-Rashed, M. F., & Sherif, M. M. (2000). Water resources in the GCC countries: An overview.

Water Resources Management. https://doi.org/10.1023/A:1008127027743

Al-Zahrani, K. H., & Baig, M. B. (2011). Water in the kingdom of Saudi Arabia: Sustainable management options. *Journal of Animal and Plant Sciences*.

Al-Jerash, M. A. (1985). Climatic subdivisions in Saudi Arabia: an application of principal component analysis. *International Journal of Climatology*, *5*(3), 307–323.

Al, J. E. T., Joyce, R. J., Janowiak, J. E., Arkin, P. A., & Xie, P. (2004). CMORPH: A Method that Produces Global Precipitation Estimates from Passive Microwave and Infrared Data at High Spatial and Temporal Resolution. *Journal of Hydrometeorology*. https://doi.org/10.1175/1525-7541(2004)005<0487:CAMTPG>2.0.CO;2

Alharbi, R., Hsu, K., & Sorooshian, S. (2018). Bias adjustment of satellite-based precipitation estimation using artificial neural networks-cloud classification system over Saudi Arabia. *Arabian Journal of Geosciences*, *11*(17), 508. https://doi.org/10.1007/s12517-018-3860-4

Almazroui, M. (2011). Calibration of TRMM rainfall climatology over Saudi Arabia during 1998-2009. *Atmospheric Research*. https://doi.org/10.1016/j.atmosres.2010.11.006

Almazroui, M., Dambul, R., Islam, M. N., & Jones, P. D. (2015a). Principal components-based regionalization of the Saudi Arabian climate. *International Journal of Climatology*. https://doi.org/10.1002/joc.4139

Almazroui, M., Dambul, R., Islam, M. N., & Jones, P. D. (2015b). Principal components-based regionalization of the Saudi Arabian climate. *International Journal of Climatology*, *35*(9), 2555–2573.

Alpert, P., Krichak, S. O., Shafir, H., Haim, D., & Osetinsky, I. (2008). Climatic trends to extremes employing regional modeling and statistical interpretation over the E. Mediterranean. *Global and Planetary Change*. https://doi.org/10.1016/j.gloplacha.2008.03.003

Alyamani, M. S. (2001). Isotopic composition of rainfall and ground-water recharge in the western province of Saudi Arabia. *Journal of Arid Environments*. https://doi.org/10.1006/jare.2001.0815

Anctil, F., Lauzon, N., Andréassian, V., Oudin, L., & Perrin, C. (2006). Improvement of rainfall-runoff forecasts through mean areal rainfall optimization. *Journal of Hydrology*. https://doi.org/10.1016/j.jhydrol.2006.01.016

Andreassian, V., Perrin, C., Michel, C., Sanchez, I. U., & Lavabre, J. (2001). Impact of imperfect rainfall knowledge on the ef®ciency and the parameters of watershed models. *Journal of Hydrology*.

Arnell, N. W. (1999). Climate change and global water resources. In *Global Environmental Change*. https://doi.org/10.1016/S0959-3780(99)00017-5

Arnell, N. W. (2003). Climate change scenarios from a regional climate model: Estimating change in runoff in southern Africa. *Journal of Geophysical Research*. https://doi.org/10.1029/2002JD002782

Ashouri, H., Hsu, K. L., Sorooshian, S., Braithwaite, D. K., Knapp, K. R., Cecil, L. D., … Prat, O. P. (2015). PERSIANN-CDR: Daily precipitation climate data record from multisatellite observations for hydrological and climate studies. *Bulletin of the American Meteorological Society*. https://doi.org/10.1175/BAMS-D-13-00068.1

Basistha, A., Arya, D. S., & Goel, N. K. (2008). Spatial distribution of rainfall in Indian Himalayas - A case study of Uttarakhand Region. *Water Resources Management*. https://doi.org/10.1007/s11269-007-9228-2

Beck, H. E., Van Dijk, A. I. J. M., Levizzani, V., Schellekens, J., Miralles, D. G., Martens, B., & De Roo, A. (2017). MSWEP: 3-hourly 0.25° global gridded precipitation (1979-2015) by merging gauge, satellite, and reanalysis data. *Hydrology and Earth System Sciences*. https://doi.org/10.5194/hess-21-589-2017

Bennett, J. C., Grose, M. R., Post, D. A., Corney, S. P., & Bindoff, N. L. (2011). Performance of quantile-quantile bias-correction for use in hydroclimatological projections. In *19th International Congress on Modelling and Simulation*.

Bitew, M. M., & Gebremichael, M. (2011). Evaluation of satellite rainfall products through hydrologic simulation in a fully distributed hydrologic model. *Water Resources Research*. https://doi.org/10.1029/2010WR009917

Block, P. J., Souza Filho, F. A., Sun, L., & Kwon, H. H. (2009). A streamflow forecasting framework using multiple climate and hydrological models. *Journal of the American Water Resources Association*. https://doi.org/10.1111/j.1752-1688.2009.00327.x

Bong, T., Son, Y.-H., Yoo, S.-H., & Hwang, S.-W. (2017). Nonparametric quantile mapping using the response surface method – bias correction of daily precipitation. *Journal of Water and Climate Change*, *9*(3), 525–539. Retrieved from http://dx.doi.org/10.2166/wcc.2017.127

Boserup, E. (2013). *The conditions of agricultural growth: The economics of agrarian change under population pressure*. *The Conditions of Agricultural Growth: The Economics of Agrarian Change Under Population Pressure*. https://doi.org/10.4324/9781315016320

Boushaki, F. I., Hsu, K.-L., Sorooshian, S., Park, G.-H., Mahani, S., & Shi, W. (2009). Bias Adjustment of Satellite Precipitation Estimation Using Ground-Based Measurement: A Case Study Evaluation over the Southwestern United States. *Journal of Hydrometeorology*. https://doi.org/10.1175/2009JHM1099.1

Cannon, A. J., Sobie, S. R., & Murdock, T. Q. (2015). Bias correction of GCM precipitation by quantile mapping: How well do methods preserve changes in quantiles and extremes? *Journal of Climate*. https://doi.org/10.1175/JCLI-D-14-00754.1

Chaplot, V., Saleh, A., & Jaynes, D. B. (2005). Effect of the accuracy of spatial rainfall information on the modeling of water, sediment, and NO3-N loads at the watershed level. *Journal of Hydrology*. https://doi.org/10.1016/j.jhydrol.2005.02.019

Cheema, M. J. M., & Bastiaanssen, W. G. M. (2012). Local calibration of remotely sensed rainfall from the TRMM satellite for different periods and spatial scales in the Indus Basin. *International Journal of Remote Sensing*. https://doi.org/10.1080/01431161.2011.617397

Chen, J., Brissette, F. P., Chaumont, D., & Braun, M. (2013). Finding appropriate bias correction methods in downscaling precipitation for hydrologic impact studies over North America. *Water Resources Research*. https://doi.org/10.1002/wrcr.20331

Chen, J., Li, C., Brissette, F. P., Chen, H., Wang, M., & Essou, G. R. C. (2018). Impacts of correcting the inter-variable correlation of climate model outputs on hydrological modeling. *Journal of Hydrology*. https://doi.org/10.1016/j.jhydrol.2018.03.040

Chen, J., St-Denis, B. G., Brissette, F. P., & Lucas-Picher, P. (2016). Using Natural Variability as a Baseline to Evaluate the Performance of Bias Correction Methods in Hydrological Climate Change Impact Studies. *Journal of Hydrometeorology*. https://doi.org/10.1175/JHM-D-15-0099.1

Chen, M., Xie, P., Janowiak, J. E., & Arkin, P. a. (2002). Global Land Precipitation: A 50-yr Monthly Analysis Based on Gauge Observations. *Journal of Hydrometeorology*. https://doi.org/10.1175/1525-7541(2002)003<0249:GLPAYM>2.0.CO;2

Cheng, K. S., Lin, Y. C., & Liou, J. J. (2008). Rain-gauge network evaluation and augmentation using geostatistics. *Hydrological Processes*. https://doi.org/10.1002/hyp.6851

Christensen, J. H., Boberg, F., Christensen, O. B., & Lucas-Picher, P. (2008). On the need for bias correction of regional climate change projections of temperature and precipitation. *Geophysical Research Letters*. https://doi.org/10.1029/2008GL035694

Cole, S. J., & Moore, R. J. (2008). Hydrological modelling using raingauge- and radar-based estimators of areal rainfall. *Journal of Hydrology*. https://doi.org/10.1016/j.jhydrol.2008.05.025

Condom, T., Rau, P., & Espinoza, J. C. (2011). Correction of TRMM 3B43 monthly precipitation data over the mountainous areas of Peru during the period 1998-2007. *Hydrological Processes*. https://doi.org/10.1002/hyp.7949

Cook, C., & Bakker, K. (2012). Water security: Debating an emerging paradigm. *Global Environmental Change*. https://doi.org/10.1016/j.gloenvcha.2011.10.011

CRED, & UNISDR. (2015). The human cost of weather-related disasters 1995-2015. *UNISDR Publications*. https://doi.org/10.1017/CBO9781107415324.004

Creel, L., & Souza, R. De. Finding the Balance : Population and Water Scarcity in the Middle East and North Africa, MENA Policy Brief (2002).

Cressie, N. A. C. (1994). Statistics for Spatial Data, Revised Edition. *Biometrics*. https://doi.org/10.2307/2533238

Davis, R. E. (1976). Predictability of sea surface temperature and sea level pressure anomalies over the North Pacific Ocean. *Journal of Physical Oceanography*, *6*(3), 249–266.

Dawod, G. M., Mirza, M. N., & Al-Ghamdi, K. A. (2013). Assessment of several flood estimation methodologies in Makkah metropolitan area, Saudi Arabia. *Arabian Journal of Geosciences*, *6*(4), 985–993. https://doi.org/10.1007/s12517-011-0405-5

De Vera, A., & Terra, R. (2012). Combining CMORPH and Rain Gauges Observations over the Rio Negro Basin. *Journal of Hydrometeorology*. https://doi.org/10.1175/JHM-D-12-010.1

de Vries, A. J., Feldstein, S. B., Riemer, M., Tyrlis, E., Sprenger, M., Baumgart, M., … Lelieveld, J. (2016). Dynamics of tropical-extratropical interactions and extreme precipitation events in Saudi Arabia in autumn, winter and spring. *Quarterly Journal of the Royal Meteorological Society*. https://doi.org/10.1002/qj.2781

DeNicola, E., Aburizaiza, O. S., Siddique, A., Khwaja, H., & Carpenter, D. O. (2015). Climate change and water scarcity: The case of Saudi Arabia. *Annals of Global Health*. https://doi.org/10.1016/j.aogh.2015.08.005

Diaz-Nieto, J., & Wilby, R. L. (2005). A comparison of statistical downscaling and climate change factor methods: Impacts on low flows in the River Thames, United Kingdom. *Climatic Change*. https://doi.org/10.1007/s10584-005-1157-6

Dinku, T., Hailemariam, K., Maidment, R., Tarnavsky, E., & Connor, S. (2014). Combined use of satellite estimates and rain gauge observations to generate high-quality historical rainfall time series over Ethiopia. *International Journal of Climatology*. https://doi.org/10.1002/joc.3855

Dirks, K. N., Hay, J. E., Stow, C. D., & Harris, D. (1998). High-resolution studies of rainfall on Norfolk Island Part II: Interpolation of rainfall data. *Journal of Hydrology*. https://doi.org/10.1016/S0022-1694(98)00155-3

Duan, Z., & Bastiaanssen, W. G. M. (2013). First results from Version 7 TRMM 3B43 precipitation product in combination with a new downscaling-calibration procedure. *Remote Sensing of Environment*. https://doi.org/10.1016/j.rse.2012.12.002

Duncan, M. R., Austin, B., Fabry, F., & Austin, G. L. (1993). The effect of gauge sampling density on the accuracy of streamflow prediction for rural catchments. *Journal of Hydrology*. https://doi.org/10.1016/0022-1694(93)90023-3

Durman, C. F., Gregory, J. M., Hassell, D. C., Jones, R. G., & Murphy, J. M. (2001). A comparison of extreme European daily precipitation simulated by a global and a regional model for present and future climates. *Quarterly Journal of the Royal Meteorological Society*. https://doi.org/10.1256/smsqj.57315

Ehret, U., Zehe, E., Wulfmeyer, V., Warrach-Sagi, K., & Liebert, J. (2012). HESS Opinions "should we apply bias correction to global and regional climate model data?" *Hydrology and Earth System Sciences*. https://doi.org/10.5194/hess-16-3391-2012

Fang, G. H., Yang, J., Chen, Y. N., & Zammit, C. (2015). Comparing bias correction methods in downscaling meteorological variables for a hydrologic impact study in an arid area in China. *Hydrology and Earth System Sciences*. https://doi.org/10.5194/hess-19-2547-2015

fao. (2008). Irrigation in the Middle East region in figures – AQUASTAT Survey 2008. *Report*. https://doi.org/978-92-5-106316-3

FAO. (2009). *Harmonized World Soil Database*. *Food and Agriculture Organization*. https://doi.org/3123

FAO. (2014). Water withdrawal by sector, around 2007. *AQUASTAT Database*.

Faurès, J. M., Goodrich, D. C., Woolhiser, D. A., & Sorooshian, S. (1995). Impact of small-scale spatial rainfall variability on runoff modeling. *Journal of Hydrology*. https://doi.org/10.1016/0022-1694(95)02704-S

Fekete, B. M., Vörösmarty, C. J., Roads, J. O., & Willmott, C. J. (2004). Uncertainties in precipitation and their impacts on runoff estimates. *Journal of Climate*. https://doi.org/10.1175/1520-0442(2004)017<0294:UIPATI>2.0.CO;2

Food and Agriculture Organization. (2002). *World agriculture : towards 2015 / 2030 World agriculture : towards 2015 / 2030*. *FAO, Rome*. https://doi.org/10.1016/S0264-8377(03)00047-4

Food and Agriculture Organization. (2009). *How to Feed the World in 2050. Insights from an expert meeting at FAO*. https://doi.org/10.1111/j.1728-4457.2009.00312.x

Gao, X., & Giorgi, F. (2008). Increased aridity in the Mediterranean region under greenhouse gas forcing estimated from high resolution simulations with a regional climate model. *Global and Planetary Change*. https://doi.org/10.1016/j.gloplacha.2008.02.002

Gebregiorgis, A. S., Tian, Y., Peters-Lidard, C. D., & Hossain, F. (2012). Tracing hydrologic model simulation error as a function of satellite rainfall estimation bias components and land use and land cover conditions. *Water Resources Research*. https://doi.org/10.1029/2011WR011643

Gellert, W., Hellwich, M., Kästner, H., & Küstner, H. (2012). *The VNR concise encyclopedia of mathematics*. Springer Science & Business Media.

Grillakis, M. G., Koutroulis, A. G., & Tsanis, I. K. (2013). Multisegment statistical bias correction of daily GCM precipitation output. *Journal of Geophysical Research Atmospheres*. https://doi.org/10.1002/jgrd.50323

Gudmundsson, L., Bremnes, J. B., Haugen, J. E., & Engen-Skaugen, T. (2012). Technical Note: Downscaling RCM precipitation to the station scale using statistical transformations – A comparison of methods. *Hydrology and Earth System Sciences*. https://doi.org/10.5194/hess-16-3383-2012

Haberlandt, U. (2007). Geostatistical interpolation of hourly precipitation from rain gauges and radar for a large-scale extreme rainfall event. *Journal of Hydrology*. https://doi.org/10.1016/j.jhydrol.2006.06.028

Habib, E., Krajewski, W. F., & Kruger, A. (2001). Sampling Errors of Tipping-Bucket Rain Gauge Measurements. *Journal of Hydrologic Engineering*. https://doi.org/10.1061/(ASCE)1084-0699(2001)6:2(159)

Haddeland, I., Heinke, J., Biemans, H., Eisner, S., Flörke, M., Hanasaki, N., … Wisser, D. (2014). Global water resources affected by human interventions and climate change. *Proceedings of the National Academy of Sciences*. https://doi.org/10.1073/pnas.1222475110

Hagemann, S., Chen, C., Haerter, J. O., Heinke, J., Gerten, D., & Piani, C. (2011). Impact of a Statistical Bias Correction on the Projected Hydrological Changes Obtained from Three GCMs and Two Hydrology Models. *Journal of Hydrometeorology*. https://doi.org/10.1175/2011JHM1336.1

Hay, L. E., Wilby, R. L., & Leavesley, G. H. (2000). A comparison of delta change and downscaled GCM scenarios for three mountainous basins in the United States. *Journal of the American Water Resources Association*. https://doi.org/10.1111/j.1752-1688.2000.tb04276.x

Hepbasli, A., & Alsuhaibani, Z. (2011). A key review on present status and future directions of solar energy studies and applications in Saudi Arabia. *Renewable and Sustainable Energy Reviews*. https://doi.org/10.1016/j.rser.2011.07.052

Hong, Y., Hsu, K.-L., Sorooshian, S., & Gao, X. (2004). Precipitation Estimation from Remotely Sensed Imagery Using an Artificial Neural Network Cloud Classification System. *Journal of Applied Meteorology*. https://doi.org/10.1175/JAM2173.1

Hou, A. Y., Kakar, R. K., Neeck, S., Azarbarzin, A. A., Kummerow, C. D., Kojima, M., … Iguchi, T. (2014). The global precipitation measurement mission. *Bulletin of the American Meteorological Society*. https://doi.org/10.1175/BAMS-D-13-00164.1

Hsu, K., Gao, X., Sorooshian, S., & Gupta, H. V. (1997). Precipitation Estimation from Remotely Sensed Information Using Artificial Neural Networks. *Journal of Applied Meteorology*. https://doi.org/10.1175/1520-0450(1997)036<1176:PEFRSI>2.0.CO;2

Hsu, K. L., Gupta, H. V., Gao, X., & Sorooshian, S. (1999). Estimation of physical variables from multichannel remotely sensed imagery using a neural network: Application to rainfall estimation. *Water Resources Research*. https://doi.org/10.1029/1999WR900032

Huff, F. A. (1970). Sampling Errors in Measurement of Mean Precipitation. *Journal of Applied Meteorology*. https://doi.org/10.1175/1520-0450(1970)009<0035:SEIMOM>2.0.CO;2

Huffman, G. J., Adler, R. F., Arkin, P., Chang, A., Ferraro, R., Gruber, A., … Schneider, U. (1997). The Global Precipitation Climatology Project (GPCP) Combined Precipitation Dataset. *Bulletin of the American Meteorological Society*. https://doi.org/10.1175/1520-0477(1997)078<0005:TGPCPG>2.0.CO;2

Huffman, G. J., Adler, R. F., Bolvin, D. T., & Nelkin, E. J. (2010). The TRMM Multi-satellite Precipitation Analysis (TMPA). In *Satellite Rainfall Applications for Surface Hydrology*. https://doi.org/10.1007/978-90-481-2915-7_1

Huffman, G. J., Bolvin, D. T., Braithwaite, D., Hsu, K., Joyce, R., Kidd, C., … Xie, P. (2018). Algorithm Theoretical Basis Document (ATBD) Version 5.2 NASA - NASA Global Precipitation Measurement (GPM) Integrated Multi-satellitE Retrievals for GPM (IMERG) - Algorithm Theoretical Basis Document (ATBD) Version 5.2. *IMERG Algorithm Theoretical Basis Document (ATBD)*. https://doi.org/https://pmm.nasa.gov/resources/documents/gpm-integrated-multi-satellite-retrievals-gpm-imerg-algorithm-theoretical-basis-

Huffman, G. J., Bolvin, D. T., Nelkin, E. J., Wolff, D. B., Adler, R. F., Gu, G., … Stocker, E. F. (2007). The TRMM Multisatellite Precipitation Analysis (TMPA): Quasi-Global, Multiyear, Combined-Sensor Precipitation Estimates at Fine Scales. *Journal of Hydrometeorology*. https://doi.org/10.1175/JHM560.1

Hussain, G., Alquwaizany, A., & Al-Zarah, A. (2010). Guidelines for irrigation water quality and water management in the Kingdom of Saudi Arabia: An overview. *Journal of Applied Sciences*. https://doi.org/10.3923/jas.2010.79.96

Ines, A. V. M., & Hansen, J. W. (2006). Bias correction of daily GCM rainfall for crop simulation studies. *Agricultural and Forest Meteorology*. https://doi.org/10.1016/j.agrformet.2006.03.009

Intergovernmental Panel on Climate Change (IPCC). (2014). Summary for Policymakers. In *Climate Change 2014: Impacts, Adaptation, and Vulnerability. Part A: Global and Sectoral Aspects*. https://doi.org/10.1017/CBO9781107415324

International Water Management Institute. (2007). *Comprehensive Assessment of Water Management in Agriculture*. *Water for food, water for life: A Comprehensive Assessment of Water Management in Agriculture*.

IWMI. (2007). *Comprehensive Assessment of Water Management in Agriculture*. *Water for Food, Water for Life: A Comprehensive Assessment of Water Management in Agriculture*. https://doi.org/10.1007/s10795-008-9044-8

Jakob Themeßl, M., Gobiet, A., & Leuprecht, A. (2011). Empirical-statistical downscaling and error correction of daily precipitation from regional climate models. *International Journal of Climatology*. https://doi.org/10.1002/joc.2168

Jongjin, B., Jongmin, P., Dongryeol, R., & Minha, C. (2016). Geospatial blending to improve spatial mapping of precipitation with high spatial resolution by merging satellite-based and ground-based data. *Hydrological Processes*. https://doi.org/10.1002/hyp.10786

Kharin, V. V., & Zwiers, F. W. (2002). Climate predictions with multimodel ensembles. *Journal of Climate*. https://doi.org/10.1175/1520-0442(2002)015<0793:CPWME>2.0.CO;2

Kheimi, M. M., & Gutub, S. (2015). Assessment of Remotely-Sensed Precipitation Products

Across the Saudi Arabia Region. *International Journal of Water Resources and Arid Environments*.

King, A. D., Alexander, L. V., & Donat, M. G. (2013). The efficacy of using gridded data to examine extreme rainfall characteristics: A case study for Australia. *International Journal of Climatology*. https://doi.org/10.1002/joc.3588

Kottek, M., Grieser, J., Beck, C., Rudolf, B., & Rubel, F. (2006). World Map of Köppen-Geiger climate class. updated.pdf. *Meteorologische Zeitschrift*. https://doi.org/10.1127/0941-2948/2006/0130.

Kreft, S., & Eckstein, D. (2014). Global Climate Risk Index 2014. *Germanwatch*. https://doi.org/10.1093/schbul/sbn133

Kubota, T., Hashizume, H., Shige, S., Okamoto, K., Aonashi, K., Takahashi, N., … Kachi, M. (2006). Global precipitation map using satelliteborne microwave radiometers by the GSMaP project: Production and validation. In *International Geoscience and Remote Sensing Symposium (IGARSS)*. https://doi.org/10.1109/IGARSS.2006.668

Lafon, T., Dadson, S., Buys, G., & Prudhomme, C. (2013). Bias correction of daily precipitation simulated by a regional climate model: A comparison of methods. *International Journal of Climatology*. https://doi.org/10.1002/joc.3518

Leander, R., & Buishand, T. A. (2007). Resampling of regional climate model output for the simulation of extreme river flows. *Journal of Hydrology*. https://doi.org/10.1016/j.jhydrol.2006.08.006

Leander, R., Buishand, T. A., van den Hurk, B. J. J. M., & de Wit, M. J. M. (2008). Estimated changes in flood quantiles of the river Meuse from resampling of regional climate model output. *Journal of Hydrology*. https://doi.org/10.1016/j.jhydrol.2007.12.020

Lelieveld, J., Proestos, Y., Hadjinicolaou, P., Tanarhte, M., Tyrlis, E., & Zittis, G. (2016). Strongly increasing heat extremes in the Middle East and North Africa (MENA) in the 21st century. *Climatic Change*. https://doi.org/10.1007/s10584-016-1665-6

Lenderink, G., Buishand, A., & Van Deursen, W. (2007). Estimates of future discharges of the river Rhine using two scenario methodologies: Direct versus delta approach. *Hydrology and Earth System Sciences*. https://doi.org/10.5194/hess-11-1145-2007

Li, M., & Shao, Q. (2010). An improved statistical approach to merge satellite rainfall estimates and raingauge data. *Journal of Hydrology*. https://doi.org/10.1016/j.jhydrol.2010.01.023

Li, Z., Yang, D., Gao, B., Jiao, Y., Hong, Y., & Xu, T. (2015). Multiscale Hydrologic Applications of the Latest Satellite Precipitation Products in the Yangtze River Basin using a Distributed Hydrologic Model. *Journal of Hydrometeorology*. https://doi.org/10.1175/JHM-D-14-0105.1

Liu, X., Yang, T., Hsu, K., Liu, C., & Sorooshian, S. (2017). Evaluating the streamflow simulation capability of PERSIANN-CDR daily rainfall products in two river basins on the Tibetan

Plateau. *Hydrology and Earth System Sciences*. https://doi.org/10.5194/hess-21-169-2017

Luo, M., Liu, T., Meng, F., Duan, Y., Frankl, A., Bao, A., & De Maeyer, P. (2018). Comparing bias correction methods used in downscaling precipitation and temperature from regional climate models: A case study from the Kaidu River Basin in Western China. *Water (Switzerland)*. https://doi.org/10.3390/w10081046

Ly, S., Charles, C., & Degré, A. (2013). Different methods for spatial interpolation of rainfall data for operational hydrology and hydrological modeling at watershed scale: a review. *Base*.

Mahmoud, S. H., Mohammad, F. S., & Alazba, A. A. (2014). Determination of potential runoff coefficient for Al-Baha Region, Saudi Arabia using GIS. *Arabian Journal of Geosciences*, *7*(5), 2041–2057. https://doi.org/10.1007/s12517-014-1303-4

Maliva, R., & Missimer, T. (2012). *Arid lands water evaluation and management*. Springer Science & Business Media.

Mancosu, N., Snyder, R. L., Kyriakakis, G., & Spano, D. (2015). Water scarcity and future challenges for food production. *Water (Switzerland)*. https://doi.org/10.3390/w7030975

Melo, D. de C. D., Xavier, A. C., Bianchi, T., Oliveira, P. T. S., Scanlon, B. R., Lucas, M. C., & Wendland, E. (2015). Performance evaluation of rainfall estimates by TRMM multi-satellite precipitation analysis 3B42V6 and V7 over Brazil. *Journal of Geophysical Research*. https://doi.org/10.1002/2015JD023797

Miao, C., Su, L., Sun, Q., & Duan, Q. (2016). A nonstationary bias-correction technique to remove bias in GCM simulations. *Journal of Geophysical Research*. https://doi.org/10.1002/2015JD024159

Michaud, J. D., & Sorooshian, S. (1994). Effect of rainfall-sampling errors on simulations of desert flash floods. *Water Resources Research*. https://doi.org/10.1029/94WR01273

Michaud, J., & Sorooshian, S. (1994). Comparison of simple versus complex distributed runoff models on a midsized semiarid watershed. *Water Resources Research*, *30*(3), 593–605. https://doi.org/10.1029/93WR03218

Milly, P. C. D., Dunne, K. A., & Vecchia, A. V. (2005). Global pattern of trends in streamflow and water availability in a changing climate. *Nature*. https://doi.org/10.1038/nature04312

Mishra, A. K. (2013). Effect of rain gauge density over the accuracy of rainfall: A case study over Bangalore, India. *SpringerPlus*. https://doi.org/10.1186/2193-1801-2-311

Moazami, S., Golian, S., Kavianpour, M. R., & Hong, Y. (2013). Comparison of PERSIANN and V7 TRMM multi-satellite precipitation analysis (TMPA) products with rain gauge data over Iran. *International Journal of Remote Sensing*. https://doi.org/10.1080/01431161.2013.833360

Mohammad, F. S., & Adamowski, J. (2015). Interfacing the geographic information system, remote sensing, and the soil conservation service–curve number method to estimate curve number and runoff volume in the Asir region of Saudi Arabia. *Arabian Journal of Geosciences*, *8*(12), 11093–11105. https://doi.org/10.1007/s12517-015-1994-1

Molden, D. (2013). *Water for food water for life: A Comprehensive assessment of water management in agriculture*. *Water for Food Water for Life: A Comprehensive Assessment of Water Management in Agriculture*. https://doi.org/10.4324/9781849773799

Moradkhani, H., & Sorooshian, S. (2008). General review of rainfall-runoff modeling: Model calibration, data assimilation, and uncertainty analysis. In *Hydrological Modelling and the Water Cycle*.

Morrissey, M. L., Maliekal, J. A., Greene, J. S., & Wang, J. (1995). The Uncertainty of Simple Spatial Averages Using Rain Gauge Networks. *Water Resources Research*. https://doi.org/10.1029/95WR01232

Moulin, L., Gaume, E., & Obled, C. (2009). Uncertainties on mean areal precipitation: Assessment and impact on streamflow simulations. *Hydrology and Earth System Sciences*. https://doi.org/10.5194/hess-13-99-2009

N'Tcha M'Po, Y. (2016). Comparison of Daily Precipitation Bias Correction Methods Based on Four Regional Climate Model Outputs in Ouémé Basin, Benin. *Hydrology*. https://doi.org/10.11648/j.hyd.20160406.11

Nerini, D., Zulkafli, Z., Wang, L.-P., Onof, C., Buytaert, W., Lavado-Casimiro, W., & Guyot, J.-

L. (2015). A Comparative Analysis of TRMM–Rain Gauge Data Merging Techniques at the Daily Time Scale for Distributed Rainfall–Runoff Modeling Applications. *Journal of Hydrometeorology*. https://doi.org/10.1175/JHM-D-14-0197.1

Ngai, S. T., Tangang, F., & Juneng, L. (2017). Bias correction of global and regional simulated daily precipitation and surface mean temperature over Southeast Asia using quantile mapping method. *Global and Planetary Change*. https://doi.org/10.1016/j.gloplacha.2016.12.009

Nguyen, P., Thorstensen, A., Sorooshian, S., Hsu, K., & AghaKouchak, A. (2015). Flood Forecasting and Inundation Mapping Using HiResFlood-UCI and Near-Real-Time Satellite Precipitation Data: The 2008 Iowa Flood. *Journal of Hydrometeorology*. https://doi.org/10.1175/JHM-D-14-0212.1

Oki, T., & Shinjiro, K. (2006). Global Hydrological Cycles and. *Science*. https://doi.org/10.1126/science.1128845

Ouda, O. K. M. (2014). Water demand versus supply in Saudi Arabia: current and future challenges. *International Journal of Water Resources Development*. https://doi.org/10.1080/07900627.2013.837363

Overeem, A., Leijnse, H., & Uijlenhoet, R. (2013). Country-wide rainfall maps from cellular communication networks. *Proceedings of the National Academy of Sciences*. https://doi.org/10.1073/pnas.1217961110

Pakoksung, K., & Takagi, M. (2016). Effect of satellite based rainfall products on river basin responses of runoff simulation on flood event. *Modeling Earth Systems and Environment*. https://doi.org/10.1007/s40808-016-0200-0

Panofsky, H. A., Brier, G. W., & Best, W. H. (1958). Some application of statistics to meteorology.

Pereira Filho, A. J., Carbone, R. E., Janowiak, J. E., Arkin, P., Joyce, R., Hallak, R., & Ramos, C. G. M. (2010). Satellite rainfall estimates over South America - Possible applicability to the water management of large watersheds. *Journal of the American Water Resources Association*. https://doi.org/10.1111/j.1752-1688.2009.00406.x

Piani, C., Haerter, J. O., & Coppola, E. (2010). Statistical bias correction for daily precipitation in regional climate models over Europe. *Theoretical and Applied Climatology*. https://doi.org/10.1007/s00704-009-0134-9

Pierce, D. W., Cayan, D. R., Maurer, E. P., Abatzoglou, J. T., & Hegewisch, K. C. (2015). Improved Bias Correction Techniques for Hydrological Simulations of Climate Change*. *Journal of Hydrometeorology*. https://doi.org/10.1175/JHM-D-14-0236.1

Pierce, D. W., Das, T., Cayan, D. R., Maurer, E. P., Miller, N. L., Bao, Y., … Tyree, M. (2013). Probabilistic estimates of future changes in California temperature and precipitation using statistical and dynamical downscaling. *Climate Dynamics*. https://doi.org/10.1007/s00382-012-1337-9

Program, U. S. G. C. R. (2018). *Impacts of climate change on human health in the United States: a scientific assessment*. Skyhorse Publishing.

Qin, Y., Chen, Z., Shen, Y., Zhang, S., & Shi, R. (2014). Evaluation of satellite rainfall estimates over the Chinese Mainland. *Remote Sensing*. https://doi.org/10.3390/rs61111649

Ramanathan, V., Crutzen, P. J., Kiehl, J. T., & Rosenfeld, D. (2001). Atmosphere: Aerosols, climate, and the hydrological cycle. *Science*. https://doi.org/10.1126/science.1064034

Reddy, P. J. R. (2005). *A text book of Hydrology*. Firewall Media.

Reiter, P., Gutjahr, O., Schefczyk, L., Heinemann, G., & Casper, M. (2017). Does applying quantile mapping to subsamples improve the bias correction of daily precipitation? *International Journal of Climatology*. https://doi.org/10.1002/joc.5283

Rosenzweig, C., Tubiello, F. N., Goldberg, R., Mills, E., & Bloomfield, J. (2002). Increased crop damage in the US from excess precipitation under climate change. *Global Environmental Change*. https://doi.org/10.1016/S0959-3780(02)00008-0

Sagga, A. M. (1998). Physical Geography of Saudi Arabia. Sagga, Dar Kunoz Press, Jeddah, Saudi Arabia.

Schmidhuber, J., & Tubiello, F. N. (2007). Global food security under climate change. *Proceedings of the National Academy of Sciences*. https://doi.org/10.1073/pnas.0701976104

Schmidli, J., Frei, C., & Vidale, P. L. (2006). Downscaling from GCM precipitation: A benchmark for dynamical and statistical downscaling methods. *International Journal of Climatology*. https://doi.org/10.1002/joc.1287

SCS. (1972). *National Engineering Handbook*. Hydrology US Department of Agriculture.

Searcy, J. K., & Hardison, C. H. (1960). *Double-Mass Curves, Manual of Hydrology: part1. General Surface Water Techniques, U.S. Geological Survey, Water-Supply Paper 1541-B. WaterSupply Paper 1541B*. https://doi.org/http://udspace.udel.edu/handle/19716/1592

Sennikovs, J., & Bethers, U. (2009). Statistical downscaling method of regional climate model results for hydrological modelling. *18th World IMACS Congress and MODSIM09 International Congress on Modelling and Simulation. Modelling and Simulation Society of Australia and New Zealand and International Association for Mathematics and Computers in Simulation*.

Shabalova, M. V., van Deursen, W. P. A., & Buishand, T. A. (2003). Assessing future discharge of the river Rhine using regional climate model integrations and a hydrological model. *Climate Research*. https://doi.org/10.3354/cr023233

Shah, H. L., & Mishra, V. (2016). Uncertainty and Bias in Satellite-Based Precipitation Estimates over Indian Subcontinental Basins: Implications for Real-Time Streamflow Simulation and Flood Prediction*. *Journal of Hydrometeorology*. https://doi.org/10.1175/JHM-D-15-0115.1

Sharif, H. O., Al-Zahrani, M., & El Hassan, A. (2017). Physically, fully-distributed hydrologic simulations driven by GPM satellite rainfall over an urbanizing arid catchment in Saudi Arabia. *Water (Switzerland)*, *9*(3). https://doi.org/10.3390/w9030163

Sharma, A., & Mehrotra, R. (2010). Rainfall generation. *Rainfall: State of the Science*, 215–246.

Sharma, D., Gupta, A. Das, & Babel, M. S. (2007). Spatial disaggregation of bias-corrected GCM precipitation for improved hydrologic simulation: Ping River Basin, Thailand. *Hydrology and Earth System Sciences*. https://doi.org/10.5194/hess-11-1373-2007

Shen, Y., Zhao, P., Pan, Y., & Yu, J. (2014). A high spatiotemporal gauge-satellite merged precipitation analysis over China. *Journal of Geophysical Research*. https://doi.org/10.1002/2013JD020686

Shiklomanov, I. a. (1998). *World Water Rssources- A new Appraisal and Assessment for the 21st century*. *Scientific and Cultural Organization*. https://doi.org/10.4314/wsa.v30i4.5101

Simpson, M. J. (2011). Global Climate Change Impacts in the United States. *Journal of Environment Quality*. https://doi.org/10.2134/jeq2010.0010br

Singh, R. B. (2012). Climate Change and Food Security. In *Improving Crop Productivity in Sustainable Agriculture*. https://doi.org/10.1002/9783527665334.ch1

Sorooshian, S., Hsu, K. L., Gao, X., Gupta, H. V., Imam, B., & Braithwaite, D. (2000). Evaluation of PERSIANN system satellite-based estimates of tropical rainfall. *Bulletin of the American Meteorological Society*. https://doi.org/10.1175/1520-0477(2000)081<2035:EOPSSE>2.3.CO;2

Sowers, J., Vengosh, A., & Weinthal, E. (2011). Climate change, water resources, and the politics of adaptation in the Middle East and North Africa. *Climatic Change*. https://doi.org/10.1007/s10584-010-9835-4

Subyani, A., Al-Modayan, A., & Al-Ahmadi, F. (2010). Topographic, Seasonal and Aridity influences on rainfall variability in western Saudi Arabia. *Journal of Environmental Hydrology*. https://doi.org/10.1109/UIC-ATC.2012.115

Subyani, A. M. (2004). Geostatistical study of annual and seasonal mean rainfall patterns in southwest Saudi Arabia. *Hydrological Sciences–Journal–Des Sciences Hydrologiques*. https://doi.org/10.1623/hysj.49.5.803.55137

Sun, Q., Miao, C., Duan, Q., Ashouri, H., Sorooshian, S., & Hsu, K.-L. (2017). A review of global precipitation datasets: data sources, estimation, and intercomparisons. *Reviews of Geophysics*. https://doi.org/10.1002/2017RG000574

Takahashi, K., & Arakawa, H. (1981). *Climates of southern and western Asia*. Elsevier Scientific Pub. Co.

TAO, T., CHOCAT, B., LIU, S., & XIN, K. (2009). Uncertainty Analysis of Interpolation Methods in Rainfall Spatial Distribution–A Case of Small Catchment in Lyon. *Journal of Water Resource and Protection*. https://doi.org/10.4236/jwarp.2009.12018

Teng, H., Ma, Z., Chappell, A., Shi, Z., Liang, Z., & Yu, W. (2017). Improving rainfall erosivity estimates using merged TRMM and gauge data. *Remote Sensing*. https://doi.org/10.3390/rs9111134

Terink, W., Hurkmans, R. T. W. L., Torfs, P. J. J. F., & Uijlenhoet, R. (2009). Bias correction of temperature and precipitation data for regional climate model application to the Rhine basin. *Hydrology and Earth System Sciences Discussions*. https://doi.org/10.5194/hessd-6-5377-2009

Terink, W., Hurkmans, R. T. W. L., Torfs, P. J. J. F., & Uijlenhoet, R. (2010). Evaluation of a bias correction method applied to downscaled precipitation and temperature reanalysis data for the Rhine basin. *Hydrology and Earth System Sciences*. https://doi.org/10.5194/hess-14-687-2010

Tesfagiorgis, K., Mahani, S. E., Krakauer, N. Y., & Khanbilvardi, R. (2011). Bias correction of satellite rainfall estimates using a radar-gauge product – a case study in Oklahoma (USA). *Hydrology and Earth System Sciences*. https://doi.org/10.5194/hess-15-2631-2011

Teutschbein, C., & Seibert, J. (2010). Regional climate models for hydrological impact studies at the catchment scale: A review of recent modeling strategies. *Geography Compass*. https://doi.org/10.1111/j.1749-8198.2010.00357.x

Teutschbein, C., & Seibert, J. (2012a). Bias correction of regional climate model simulations for hydrological climate-change impact studies: Review and evaluation of different methods. *Journal of Hydrology*. https://doi.org/10.1016/j.jhydrol.2012.05.052

Teutschbein, C., & Seibert, J. (2012b). Bias correction of regional climate model simulations for hydrological climate-change impact studies: Review and evaluation of different methods. *Journal of Hydrology*. https://doi.org/10.1016/j.jhydrol.2012.05.052

Themeßl, M. J., Gobiet, A., & Heinrich, G. (2012). Empirical-statistical downscaling and error correction of regional climate models and its impact on the climate change signal. *Climatic Change*. https://doi.org/10.1007/s10584-011-0224-4

Thiemig, V., Rojas, R., Zambrano-Bigiarini, M., & De Roo, A. (2013). Hydrological evaluation of satellite-based rainfall estimates over the Volta and Baro-Akobo Basin. *Journal of Hydrology*. https://doi.org/10.1016/j.jhydrol.2013.07.012

Tozer, C. R., Kiem, A. S., & Verdon-Kidd, D. C. (2012). On the uncertainties associated with using gridded rainfall data as a proxy for observed. *Hydrology and Earth System Sciences*. https://doi.org/10.5194/hess-16-1481-2012

UN Water. (2007). *Coping With Water Scarcity - Challenge of the twenty-first century*. *Water Management*. https://doi.org/10.3362/0262-8104.2005.038

Vila, D. A., de Goncalves, L. G. G., Toll, D. L., & Rozante, J. R. (2009). Statistical Evaluation of

Combined Daily Gauge Observations and Rainfall Satellite Estimates over Continental South America. *Journal of Hydrometeorology*. https://doi.org/10.1175/2008JHM1048.1

Villarini, G., Mandapaka, P. V., Krajewski, W. F., & Moore, R. J. (2008). Rainfall and sampling uncertainties: A rain gauge perspective. *Journal of Geophysical Research Atmospheres*. https://doi.org/10.1029/2007JD009214

Vincent, P. (2008). *Saudi Arabia: an environmental overview*. CRC Press.

Vörösmarty, C. J., Green, P., Salisbury, J., & Lammers, R. B. (2000). Global water resources: Vulnerability from climate change and population growth. *Science*. https://doi.org/10.1126/science.289.5477.284

Wagener, T., Wheater, H. S., & Gupta, H. V. (2004). *Rainfall-runoff modelling in gauged and ungauged catchments*. World Scientific.

Wagner, P. D., Fiener, P., Wilken, F., Kumar, S., & Schneider, K. (2012). Comparison and evaluation of spatial interpolation schemes for daily rainfall in data scarce regions. *Journal of Hydrology*. https://doi.org/10.1016/j.jhydrol.2012.07.026

Waha, K., Krummenauer, L., Adams, S., Aich, V., Baarsch, F., Coumou, D., … Schleussner, C. F. (2017). Climate change impacts in the Middle East and Northern Africa (MENA) region and their implications for vulnerable population groups. *Regional Environmental Change*. https://doi.org/10.1007/s10113-017-1144-2

Wahl, T., Jain, S., Bender, J., Meyers, S. D., & Luther, M. E. (2015). Increasing risk of compound flooding from storm surge and rainfall for major US cities. *Nature Climate Change*. https://doi.org/10.1038/nclimate2736

Wilcke, R. A. I., Mendlik, T., & Gobiet, A. (2013). Multi-variable error correction of regional climate models. *Climatic Change*. https://doi.org/10.1007/s10584-013-0845-x

Wilks, D. S. (2006). *Statistical methods in the atmospheric sciences, second edition*. *International Geophysics Series, Academic Press*. https://doi.org/10.1098/rspa.2007.0277

Willems, P., Arnbjerg-Nielsen, K., Olsson, J., & Nguyen, V. T. V. (2012). Climate change impact assessment on urban rainfall extremes and urban drainage: Methods and shortcomings. *Atmospheric Research*. https://doi.org/10.1016/j.atmosres.2011.04.003

Woldemeskel, F. M., Sivakumar, B., & Sharma, A. (2013). Merging gauge and satellite rainfall with specification of associated uncertainty across Australia. *Journal of Hydrology*. https://doi.org/10.1016/j.jhydrol.2013.06.039

Wood, A. W., Leung, L. R., Sridhar, V., & Lettenmaier, D. P. (2004). Hydrologic implications of dynamical and statistical approaches to downscaling climate model outputs. *Climatic Change*. https://doi.org/10.1023/B:CLIM.0000013685.99609.9e

Wood, A. W., Maurer, E. P., Kumar, A., & Lettenmaier, D. P. (2002). Long-range experimental hydrologic forecasting for the eastern United States. *Journal of Geophysical Research D:*

Atmospheres. https://doi.org/10.1029/2001JD000659

World Meteorological Organization. (1989). *Calculation of monthly and annual 30-year standard normals*. *World Climate Programme*.

WWAP (United Nations World Water Assessment Programme). (2015). *The United Nations World Water Development Report 2015: Water for a Sustainable World; facts and figures. Paris, UNESCO*. https://doi.org/10.1016/S1366-7017(02)00004-1

WWAP (World Water Assessment Programme). (2012). *Managing Water under Uncertainty and Risk*. *The United Nations World Water Development Report 4 : Knowledge Base*. https://doi.org/10.1608/FRJ-3.1.2

Xie, P., Boyer, T., Bayler, E., Xue, Y., Byrne, D., Reagan, J., … Kumar, A. (2014). An in situ-satellite blended analysis of global sea surface salinity. *J. Geophys. Res. Oceans*. https://doi.org/10.1002/2014jc010046

Xie, P., & Xiong, A. Y. (2011). A conceptual model for constructing high-resolution gauge-satellite merged precipitation analyses. *Journal of Geophysical Research Atmospheres*. https://doi.org/10.1029/2011JD016118

Xu, H., Xu, C. Y., Chen, H., Zhang, Z., & Li, L. (2013). Assessing the influence of rain gauge density and distribution on hydrological model performance in a humid region of China. *Journal of Hydrology*. https://doi.org/10.1016/j.jhydrol.2013.09.004

Yang, Z., Hsu, K., Sorooshian, S., Xu, X., Braithwaite, D., & Verbist, K. M. J. (2016). Bias adjustment of satellite-based precipitation estimation using gauge observations: A case study in Chile. *Journal of Geophysical Research*. https://doi.org/10.1002/2015JD024540

Yang, Z., Hsu, K., Sorooshian, S., Xu, X., Braithwaite, D., Zhang, Y., & Verbist, K. M. J. (2017). Merging high-resolution satellite-based precipitation fields and point-scale rain gauge measurements-A case study in Chile. *Journal of Geophysical Research*. https://doi.org/10.1002/2016JD026177

Yatagai, A., Xie, P., & Alpert, P. (2007). Development of a daily gridded precipitation data set for the Middle East. *Advances in Geosciences*. https://doi.org/10.5194/adgeo-12-165-2008

Zeitoun, M. (2011). The Global Web of National Water Security. *Global Policy*. https://doi.org/10.1111/j.1758-5899.2011.00097.x

Zimmerman, J. B., Mihelcic, J. R., & Smith, J. (2008). Global stressors on water quality and quantity. *Environmental Science and Technology*. https://doi.org/10.1021/es0871457